University of Stavanger

Faculty of Science and Technology

MASTER'S THESIS

Study program/ Specialization: Master in Petroleum Geosciences Engineering	Spring semester, 2012 Restricted access
Writer: Nieve Ysmahan El Souki Poche	…… (Writer's signature)
Faculty supervisor: Karl Audun Lenhe, *University of Stavanger* External supervisor(s): Michael Erdmann , *Statoil ASA*	
Title of thesis: Recognition and Quantification of Petroleum Source Rocks from Well Log Data and its Applications.	
Credits (ECTS): 30	
Key words: Total Organic Carbon (TOC) Organic rich shales Source Rock Total Organic Carbon from Logs Rock Eval	Pages: …… + enclosure: …… Stavanger, …….. Date/year

Abstract

Petroleum source rocks constitute one of the main elements in petroleum systems. Several methods have been developed to characterize source rocks, mainly using geochemical and petrographical laboratory techniques to determine its effective potential of oil generation. Unfortunately laboratory methods are time consuming, costly and limited to a number of samples that vary in quality. Alternatively, geophysical well logs provide the most continuous record with depth of well data and several authors had demonstrated the effect that organic matter has in well logs.

In this study a log data set from two wells located in the North Sea and Barents Sea were evaluated using different tools and method with the purposed of predict source rocks richness. It was proven that the delta log R technique *(Passey et.al., 1990)* widely used, is an indirect empirical approximation able to quantify Total Organic Carbon only in the presence of calibration data and homogeneous shale package, otherwise can lead in misleading results. Additionally, it was found that using this method the best accuracy is achieved in source rocks with TOC in a range between 4 to 10 %. It was observed that the main source of uncertainty using this method corresponded to the arbitrary and subjective definition of baselines values used in the delta log R equation. An improvement was proposed using trend baselines for non-source rocks, instead of constant values with depth which allowed to recognize anomalous intervals (or source rock) making it a more reasonable practice.

Additionally, a new model to predict TOC from well logs was generated using multiple linear regressions and based on Gamma Ray, Resistivity and Transit time readings. This model is able to predict with a simplified procedure the Total Organic Carbon from well logs giving a better approach in heterogeneous intervals than the previous method. It may help to generate new models using statistical tools that allow a directly determination of TOC from logs with a better control of variables and avoiding biased procedures.

Acknowledgements

This thesis has been carried out at the Department of Petroleum Engineering, University of Stavanger, Norway and Statoil ASA, Stavanger, Norway under the supervision of Associate Professor in Formation Evaluation and Petrophisics Karl Audu Lehne and Dr. Michael Erdman at Statoil ASA.

I would like to express my gratitude to Karl Lehne for his support and invaluable suggestions that made this work successful. I owe my deepest gratitude to Michael Erdman, his knowledge and commitment to the highest standards inspired and motivated me.

I also wish to thank to Statoil ASA for giving me this opportunity providing the data and facilities. I offer my sincerest gratitude to the Statoil team for their support and collaboration, especially to Jorunn Johannesen, Ann Elin Gilje and Tor Magne Broks for helping me in any single issue.

I would like to thank to Professor Reidar Bratvold for his advice and insight throughout my work.

I would like to show my gratitude to my fellow students for the rewarding experience shared during these two years, particularly to Papi Ninga, Mihreteab Serekebirhan and Safa Gasimov for being not only excellent colleagues but also very good friends, for their understanding and advices during this period.

I am deeply and forever indebted to my parents and sisters for their love, support and encouragement throughout my entire life, despite the geographical distance.

I sincerely thank the support provided by Leonardo Duerto during my studies, his advice was consistently timely and useful.

I will like to express my thanks to my friends in Norway Annita Geppert and Mireya Leal and also to my colleagues and friends in Venezuela and elsewhere, especially to Peivy Holod, Josmat Rodriguez, Antenor Aleman, Juan Torres and Ramon Villarroel for their unconditional friendship and constant care about my progress during these two years.

Above all, I would like to thanks my son Samuel for being my wonderful source of inspiration; every step I take is to help you know the way in the journey of life.

Table of content

ABSTRACT **1**

ACKNOWLEDGEMENTS **2**

TABLE OF CONTENT **3**

LIST OF TABLES **4**

LIST OF ABBREVIATIONS **4**

TABLE OF FIGURES **5**

1. INTRODUCTION **10**

1.1 Previous Studies and Log Evaluation Techniques 12
1.1.1 Gamma Ray logs 12
1.1.2 Density Logs 16
1.1.3 Resistivity Logs 21
1.1.4 Sonic Log 23
1.1.5 Method of Meyer and Nederlof (1984) 24
1.1.6 Method of Passey et al. (1990) 27

2. METHODOLOGY **32**

2.1 Δ Log R Technique 32
2.2 Tools 36
2.2.1 BasinMod 1D (Platte River Associates, Inc.) *36*
2.2.2 Permedia MPath version 4.18.1 (Landmark Software and Services, Halliburton). *40*
2.2.3 In-house spreadsheet solution (Microsoft Excel, Microsoft Office Professional Plus 2010) *43*
2.2.4 New Trend Technique (Microsoft Excel, Microsoft Office Professional Plus 2010) *46*
2.3 Statistical Analysis 48
2.3.1 Multiple Linear Regression (MLR) 49

3. WELL DATA **51**

Well Data NO 34/8-6 52
Well Data NO 7120/12-1 55

4. RESULTS **58**

4. 1 BasinMod 1D (Platte River Associates, Inc.) *58*
4.2 Permedia MPath version 4.18.1 (Landmark Software and Services, Halliburton). *63*
4.3 New Trend Technique (Microsoft Excel, Microsoft Office Professional Plus 2010) *72*
Results Well NO 34/8-6 72
Results Well NO 7120/12-1 83
4.4 Multiple Linear Regression Model (MLR) *93*

5. DISCUSSION **97**

About Δ Log R method (Paseey, et. al., 1990) and tools 97
Trend Technique 100
Well data implications 103
About the Multiple Regression Model 105

6. CONCLUSION **106**

7. REFERENCES **107**

8. APPENDICES **112**

List of Tables

***Table 1**: Summary of baselines values at each horizontal break used in TOC estimation from logs, Well NO 34/6-8. ..... 63*
***Table 2**: Summary of baselines values at each horizontal break used in TOC estimation from logs, Well NO 7120/12-1..... 67*
***Table 3**: Summary of the intervals and parameter defined in TOC estimation for the well NO 34/8-6 using trend baselines..... 73*
***Table 4**: Summary of the intervals and parameter defined in TOC estimation for the well NO 7120/12-1 using trend baselines. 83*
***Table 5**: Determination coefficients of the Regression Model 93*
***Table 6**: Regression Model for dependence variable: TOC RE. Beta: partial regression coefficient; B: partial regression coefficient standardized; t: statistic test; p-level: level of significance of t-test. 93*
***Table A**: In-house spreadsheet tested in the Well NO 34/8-6. Summary of the intervals and parameters used in TOC estimation from logs (Fig)..... 112*

List of Abbreviations

TOC: Total Organic Carbon

Ro: Vitrinite Reflectance

RE: Rock Eval pyrolysis

LOM: Level of Organic Metamorphism

TOC ΔLogR (delta log R): TOC curve calculated from logs using the method of *Passey et. al*. (*1990*).

Table of figures

Fig. 1: A. *Gamma-ray log from Pike County, Ohio, showing features typical of Devonian shale in western part of Appalachian basin (adapted from Wallace et al, 1977).* ***B.*** *Comparison of volume percent of organic matter in Devonian shales calculated from gamma-ray logs and determined from core samples (Ideal agreement is shown by dashed line)* ***C.*** *Distribution of differences between volume percent of organic matter determined from core samples and calculated from gamma-ray logs. Data from Cleveland Member of Ohio Shale and lower part of Olentangy Shale are excluded. (Modify from Schmoker, 1981).* *13*

Fig 2: *Correlation between GR and TOC for the Lower Member of the Lewis Shale, Washakie Basin in Wyoming. The higher TOC values from the well Ch 276D#1 influence the correlation. The CSM Strat Test 61 well data points comprise the lower end of TOC values (Rigoris, 2005)* *14*

Fig 3*: Spectral gamma ray log showing elemental composition of the Barnett Formation in the Texas United Blakely #1 well. Wise County, Texas (Ruppel & Kane, 2006). A strong correlation exists in some shales with Uranium content from the spectral gamma ray log.* *15*

Fig 4*: Distribution and log response characteristics of oil source rocks (Ning 36 well), showing a positive uranium anomaly at the base of the Chang 7 member (Box in Orange). GA: gamma ray. SP: spontaneous potential. RILD: deep investigate induction log. The API, mv and Xm are units for GA, SP and RILD, respectively (Modify from Yang H. et al., 2010).* *15*

Fig. 5: *Density and resistivity of the Liassic Posidonien Schiefer in shallow well in south Germany. Resistivity is from Microlaterolog. High resistivity peaks in shale are thin limestone intercalations (from Meyer & Nederlof, 1984)* *17*

Fig 6*:* ***A.*** *Crossplot for Jackson County well showing strong linear relation between density and gamma-ray intensity. Wire-line data are averaged over intervals of 6.1 m.* ***B.*** *Distribution of differences between volume percent organic matters measured in core samples and calculated from density logs (Schmoker, 1979).* *18*

Fig 7*:* ***A.*** *Laboratory measurements of organic-carbon content of Bakken shales, Williston Basin (59 analyses representing 39 locations in North Dakota) versus log-derived formation density of comparable intervals.* ***B.*** *Comparison of organic-carbon content of Bakken shales calculated from density logs (TOC = (154.497/ ρ) - 57.261) and measured from core samples where ideal agreement is shown by dashed line (Schmoker & Hester, 1983).* *19*

Fig.8: *Calculated volumetric average response of density log to organic matter content, expressed in terms of total organic carbon (TOC). For each porosity (φ=0 % and φ=10 %) the effects of modeling with matrix densities of 2.65 and 2.70 g/cc is shown (Meldenson & Toksoz 1985).* *20*

Fig 9*: Effects of organic matter content in resistivity logs response: Gamma-ray and resistivity logs typical of upper (U) and lower (L) shale members of Bakken Formation.* ***A.*** *Low resistivity values reflect water-saturated, thermally immature shales (Union Oil Company of California Hanson #1-C-13, 13-153N-85W).* ***B.*** *High resistivity values reflect thermally mature shales that have generated oil (Smokey Oil Company Will #I 4-23, 23- 157N-94W)(Modified from Schmoker and Hester, 1990).* *22*

Fig 10*: Schematic of volumetric components in source and non-source rock, showing the differences in solid and fluid components and the maturity effects in source rocks (Modified from Passey et al., 1990).* *22*

Fig. 11: *Kimmeridge Shale, North Sea. Note high gamma-ray reading and the considerable lower sonic. Underlying Heather Formation is very silty. (Modify from Meyer & Nederlof, 1984)* *23*

Fig. 12: *The identification of source rocks intervals on a cross plot of bulk-density and resistivity. Oblique line is position of D = O (discriminant analysis). Points below this line (D = positive) = source rocks; points above this line (D = negative) = no source rocks. Misclassification occurs at low shale densities, borderline cases, and high limestone resistivities (Meyer & Nederlof, 1984).* *25*

Fig. 13: *The identification of source rocks intervals on a cross plot of sonic transit time and resistivity. Oblique line is the position of D = O (discriminant analysis). Points below this line (D = negative) = no source rock; points above this line (D = positive) = source rock. Note that most misclassifications occur at low interval velocities, borderline cases, and high limestone resistivities (Meyer & Nederlof, 1984).* *26*

Fig 14*:* ***A.*** *Input data for discriminant functions: sonic, resistivity, density, and gamma-ray logs for a portion of the Paris Basin well.* ***B.*** *Discriminant scores derived from combinations of sonic, resistivity, density, and gamma-ray logs. Positive values indicate the probable existence of source rocks, whereas negative values indicate barren rock. In three of the four cases, the technique fails to identify rocks with total organic carbon contents of 4-6 wt % (Herron, 1990).* *27*

Fig 15: **A.** *Diagram relating Δ logs R to TOC via maturity showing the possible upper and lower limit of LOM calibration (Passey et al., 2010).* **B.** *TOC to S_2 via maturity diagram for type I and II (oil-prone) kerogen.* **C.** *TOC to S_2 via maturity diagram for type III (gas prone) kerogen (Passey et al., 1990).* 29
Fig. 16: *Schematic guide for the interpretation of a wide variety of features observed on Δ log R overlays (Passey et al., 1990).* 31
Fig. 17: *Example of Log normalization, note the sonic scale adjusted to 50 µ/ft equivalents to 1 resistivity cycle.* 32
Fig. 18: *Illustration of sonic and resistivity logs overlain in a non-source rock to define the baseline (in light green) for $\Delta\log R$ calculations. Note the dash green line indicating the gamma ray cutoff.* 33
Fig. 19: *Sonic and resistivity logs separation in a source rock interval or $\Delta\log R$ separation.* 34
Fig. 20: *Correlation scale between level of organic metamorphism (LOM) and vitrinite reflectance (%Ro) (Modify from Hood et al., 1975).* 35
Fig. 21: *Illustration of the BasinMod tool "**TOC From Well Logs**" used to calculate organic rich shales. The well should be simulated to activate the tool. It displays the current stratigraphy in the well and the relevant logs to perform the calculation.* 36
Fig. 22: *Illustration of shifting curve procedure in a non-source interval (indicated by the red arrow).* 37
Fig. 23: *Definition of reference interval of non-source rock (indicated by red arrows and light green section) and the corresponding results of TOC calculations (third track, to the right, black curve)* 38
Fig. 24: *The baseline (indicated by and small red arrow in track 2) can be adjusted and TOC curve will be recalculated: Note that a background TOC can be included.* 38
Fig. 25: *Example of baseline interval and TOC calculation interval (indicated by the red arrow). The black curve corresponds to TOC calculated from logs and red points are values of TOC measure in core.* 39
Fig. 26: *Extraction of values of TOC calculated from well logs.* **A.** *In track 3 to the right the TOC curve calculated from logs, black points are manual values selected from the curve, red points are TOC values measure in core for calibration.* **B.** *Values selected from the TOC curve calculated saved in a table format.* 39
Fig. 27: *Loading data into Permedia MPath to perform TOC calculations.* **A.** *Main window showing the project directory and the list of tables and well log* **B.** *Table editor for discrete values (LOM, %TOC from core, etc.)* **C.** *Well viewer displaying well logs and data from tables to be used in the TOC from logs calculation.* 41
Fig. 28: *Main window of Delta Log R calculator showing the possible parameters that can be defined to perform the TOC calculator from logs. Red arrows indicated important parameters describe in the text above.* 42
Fig. 29: *Well viewer displaying the input data (logs, cutoff and baselines) and TOC calculation results (Delta log R and TOC curve). In Track 8 (from left to right, small red arrow), the green curve represent the TOC calculated from logs, the pink points are the TOC values measured in core for calibration. In this example the TOC curve does not fit the measured values and some adjustments have to be made. Modification can be done using In the Scene window to the left, for each input parameter.* 42
Fig. 30: *Example of adjustment the TOC curve to measure data using horizontal breaks to define logs baselines by intervals. Note the improvement of the TOC curve fitting the calibration data compared with the example shown in* **Fig 29**. 43
Fig. 31: *Input data in the Spreadsheet tool developed by Norsk Hydro. Three input spreadsheet: RE, for Rock Eval data measure in core and cuttings; Ro, for maturity data (vitrinate reflectance %Ro) for LOM estimations and Input for well log data.* 44
Fig. 32: *Calculation Norsk Hydro Spreadsheet showing the workflow of TOC estimation (steps in uppercase bold letters). After intervals (Step 1), Gamma Ray cutoff (Step 2), baselines (Step 3) and LOM values (Step 4) are defined the delta log R separation is calculated automatically (Step 5) and used in the TOC computation (Step 6).* 45
Fig. 33: *Output data in the Spreadsheet tool developed by Norsk Hydro, showing a summary table of intervals and parameters (upper left) and plots with relevant logs and TOC curve and calibration data (TOC meas).* 45
Fig. 34: *Example of Trend Technique for baselines calculation.* **A.** *Original Logs: Gamma Ray (GR), Transit time (DT) and Resistivity (RD).* **B.** *Gamma Ray filtered with a lower (80 API) and upper cutoff (90 API) for non-source shales. Transit time and Resistivity logs showing the values only in shale intervals according to the Gamma Ray cutoff and its respective trend lines (DT in Blue and RD in red) and equations used as baselines in TOC calculation using delta log R method (Passey et. al.,1990).* 47
Fig. 35: *Example of scatter plots showing linear correlation (blue line), correlation coefficient r and r^2.* **A.** *Ideal case of positive correlation where TOC values are predicted as expected.* **B.** *Good positive correlation indicated by r and r^2 close to 1, with some variability or noise.* 49
Fig. 36: *Map of offshore Norway showing the well location in this study (White circles), NO 7120/12-1 in the Barents Sea and NO 34/8-6 in the North Sea.* 51

Fig. 37: *Summary of Wireline log data used for TOC calculation, for the well NO 34/8-6. Red box indicated interval evaluated (CALI: caliper; GR: Gamma Ray; RHOB: Density; NPHI: Neutron Porosity; DT: Transit time; RD: Deep Resistivity).* 53
Fig. 38: *Rock Eval data used in this study for the well NO 34/8-6.* **A**. *TOC values measured in conventional core (COCH) and ditch cutting (DC) used for calibration in the main intervals of source rock.* **B**. *and* **C**. *Maturity values used for TOC log calculation: LOM values estimated from vitrinite reflectance data (%Ro).* 54
Fig. 39: *TOC data from wells NO 34/7-21 and 34/4-1, at Kyrre Formation used as a reference for calibrations at the Cretaceous interval.* 54
Fig. 40: *Summary of Wireline log data used for TOC calculation, for the well NO 7120/12-1. Red box indicated interval evaluated (CALI: caliper; GR: Gamma Ray; RHOB: Density; NPHI: Neutron Porosity; DT: Transit time; RD: Deep Resistivity).* 56
Fig. 41: *Rock Eval data used in this study for the well NO 7120/12-1.* **A**. *TOC values measured in conventional core (COCH), sidewall (SWC) and ditch cutting (DC) used for calibration.* **B**. *and* **C**. *Maturity values used for TOC log calculation: LOM values estimated from vitrinite reflectance data (%Ro).* 57
Fig. 42: *Result of TOC curve from logs obtained in case 1* **A**. *Well logs used in the estimation, TOC curve calculated (in black), calibration interval (orange box), TOC values for calibration (red circles) and baselines interval (green box), note the lack of organic matter in the lower part of the Cretaceous interval (values of TOC curve below zero)* **B**. *Zoom in of the interval calibration at the Jurassic section showing the TOC curve calculated and calibration values.* 59
Fig. 43: *Result of TOC curve from logs obtained in case 2. The best approach in the Jurassic section (Blue box) is achieved using a baseline in the lower Cretaceous interval. Note that in this case, an important estimation of organic content is obtained in the Upper Cretaceous section (Jorsalfare Formation and Upper Kyrre Formation).* 60
Fig. 44: *Point selection from the TOC log curve to obtain TOC numeric values at the Jurassic level. Track (1) Toc log curve (in black) and calibration point (red circles). Track (2) manual point selection (black diamonds). The magnification of the green box shows the difficulty to obtain values from the curve at the same depth in intervals with high density calibration data.* 61
Fig. 45: *Comparison between measured values of TOC (TOC RE) and values manually selected from TOC logs (TOC Logs) at the Jurassic Level. (A) A detail interval was choose to illustrating the mismatch regarding to different depths (B) plot of amplify scale of TOC against depth shows the dispersion of both set of data.* 62
Fig. 46: *Results of TOC from logs using horizontal breaks (HB) in Permedia, well data NO 34/8-6. Tracks from left to right: Measure depth (m), caliper (In), Gamma Ray (API, cutoff in green dash line) Transit time (DT µs/ft) and Resistivity (RD Ohm.m) with its baselines (dahs lines), LOM from %Ro, Delta Log R (*$\Delta \log R = \log 10(R/\text{Rbaseline}) + 0.02*\Delta t\text{-}\Delta t\text{baseline}$*), TOC log curve (%wt, in green) with calibration values (brown, orange and pink dots), and Formations. Note that the baselines were adjusted with and small increment for the case of the Resistivity and reduction for the case of the Transit time curve.* 64
Fig. 47: *Result of TOC curve from logs obtained in the Jurassic section of well NO 34/8-6, using horizontal breaks (HB) and different baselines values.* 65
Fig. 48: *Comparison of frequency distribution for TOC RE and TOC from logs in well NO 34/8-6, both showing bimodal distributions at the Jurassic level. At the bottom of each histogram are the results of exploratory data analysis.* 66
Fig. 49: *Results of TOC from logs using Permedia MPath software, well data NO 7120/12-1. Tracks from left to right: Measure depth, Gamma Ray (cutoff IN green dash line) Transit time (DT) and Resistivity (RD) (baselines in dash lines) non shifted and shifted, LOM from %Ro, TOC log curve (in green) with calibration values (pink dots), and Formations. Note that on the left, the DT and RD logs are scaled for estimations and on the right track both logs are shifted for each horizontal break (HB) to visualize the delta log separation, in consequence, the values of the baseline do not correspond to the upper scale in the track for Zone A.* 68
Fig. 50: *Results of TOC from logs using Permedia MPath software, well data NO 7120/12-1. Calculations of TOC log in Zone A using horizontal breaks (HB) with independent baselines values by interval. Note that the baselines were adjusted in such a way that for Resistivity it increments with depth and for Transit time decreases with depth.* 69
Fig. 51: *Results of TOC from logs using Permedia MPath software, well data NO 7120/12-1. Calculation of TOC log in Zone B using horizontal breaks (HB) with independent baselines values by interval. Note that the baselines were adjusted with an increment in Resistivity and reduction in Transit time with depth.* 70
Fig. 52: *Comparison of absolute frequency distribution for TOC RE and TOC from logs in the well NO 7120/12-1, showing different distributions. At the bottom of each histogram are the summary results of exploratory data analysis which also indicated differences in both set of data (max, mean, range, etc).* 71

Fig. 53: Trend line definition for interval study in the Well NO 34/8-6, showing Gamma Ray values filtering for shale in a range between 80-90 API and trend baselines for Resistivity and Transit time corresponding to shales defined by the GR. Last track show the calibration results in the Jurassic section using these baselines. 74
Fig. 54: Results of TOC Calculation using trend lines as baselines. Track 4 (from left to right) shows the result of Transit Time and Resistivity trend obtain from the mentioned logs only for shale values (representing by all the points in the plot) and delta log separation. Values in green indicated that the delta log R used in Passey equation was lower than zero hence TOC was not estimated (for R and DT), points in red are the values of Resistivity were the delta log R was over zero thus TOC values were estimated and the same for blue dots indicated values of Transit time relevant for the TOC estimation or delta log R more than zero. 75
Fig. 55: Results of TOC Calculation using trend lines as baselines. Detail from the previous figure (Fig. 54) to show the accuracy obtain at the Jurassic level in comparison with the calibration values. 76
Fig. 56: A. Results of linear correlation between TOC estimation and TOC measured from Rock Eval. B. Histogram of the absolute frequencies of the differences between TOC estimated and measured. C. Linear correlation of the differences (TOC RE and TOC measured)..... 78
Fig. 57: Calibration between TOC measured and estimated showing positions in which the differences were more than 2% of TOC (black triangles), in the well NO 34/8-6. 79
Fig. 58: Comparison of relative and cumulative frequency distribution for TOC RE and TOC from logs in the well NO 34/8-6, showing similar bimodal distribution. At the bottom to the left, the summary results of exploratory data analysis also indicate similarities in both set of data. At the right bottom, boxplots represents quartiles (Q1, Q2 and Q3), maximum and minimum values for visual comparison..... 80
Fig. 59: Comparison boxplots representing quartiles (Q1, Q2 and Q3), maximum and minimum values for subintervals in the Jurassic section, well NO 34/8-6. 81
Fig. 60: Comparison of relative and cumulative frequency distribution for TOC RE and TOC from logs in subintervals at the Jurassic level in the well NO 34/8-6. 82
Fig. 61: Quantile-Quantile plot of percentiles comparing the distribution of TOC measured and estimated in well 34/8-6. Departure of values from the y=x curve indicates different distributions. 83
Fig. 62: Trend line definition for interval 1 in the Well NO 7120/12-1, showing Gamma Ray values filtering for shale in a range between 60-90 API and trend baselines for Resistivity and Transit time corresponding to shales defined by the GR. Last track show the calibration results in the Cretaceous -Jurassic section using these baselines..... 85
Fig. 63: Trend line definition for interval 2 in the Well NO 7120/12-1, showing Gamma Ray values filtering for shale in a range between 60-90 API and trend baselines for Resistivity and Transit time corresponding to shales defined by the GR. Last track show the calibration results in the Triassic section using these baselines. 86
Fig. 64: Results of TOC Calculation using trend lines as baselines, well NO 7120/12-1. Result of Transit Time and Resistivity trend obtain from the mentioned logs only for shale values (representing by all the points in the plot) and delta log separation. Values in green indicated that the delta log R used in Passey et al. equation was lower than zero hence TOC was not estimated (for R and DT), points in red are the values of Resistivity were the delta log R was over zero thus TOC values were estimated and the same for blue dots indicated values of Transit time relevant for the TOC estimation or delta log R more than zero. ***A.*** *Interval 1 showing the estimation and calibration.* ***B.*** *Interval 2 with estimation and its respective calibration..... 87*
Fig. 65: Results of linear correlation between TOC estimation and TOC measured from Rock Eval, for the entire interval (A) and for Cretaceous (B), Jurassic (C) and Triassic (D) intervals, in the well NO 7120/12-1. 88
Fig. 66: Comparison of relative and cumulative frequencies distribution for TOC RE and TOC from logs in the well NO 34/8-6, showing similar distributions. At the bottom to the left, the summary results of exploratory data analysis. At the right bottom, boxplots representing quartiles (Q1, Q2 and Q3), maximum and minimum values for visual comparison. 89
Fig. 67: Comparison of boxplots representing quartiles (Q1, Q2 and Q3), maximum and minimum values for the Cretaceous, Jurassic and Triassic intervals, in the well NO 7120/12-1..... 90
Fig. 68: Comparison of relative and cumulative frequency distribution for TOC RE and TOC from logs for the Cretaceous, Jurassic and Triassic intervals, in the well NO 7120/12-1..... 91
Fig. 69: Quantile-Quantile plot of percentiles comparing the distribution of TOC measured and estimated in the well NO 7120/12-1. Departure of values from the y=x curve indicated different distributions. 92
Fig. 70: Scatter plot of linear regression for each independent variable (Gamma Ray, Resistivity and Transit Time) against TOC RE showing the confident interval and the correlation coefficient. 94
Fig. 71: Comparison of the results of Delta log R and Multiple Regression models as TOC predictors. In Green TOC curve from Delta Log R, in blue TOC values from Multiple Regression Model, in pink TOC measured values

from Rock Eval. ***A.*** *Data from the well NO 34/8-6, Visund area, North Sea.* ***B.*** *Data from well NO 7120/12/1, Troms I area, Barents Sea. 95*
Fig. 72*: Results of Multiple Regression models as TOC predictors. In blue TOC values from Multiple Regression Model, in pink TOC measured values from Rock Eval.* ***A.*** *Data from the well NO 34/8-6, Visund area, North Sea.* ***B.*** *and* ***C.*** *Data from well NO 7120/12/1, Troms I area, Barents Sea, for the Cretaceous-Jurassic and Triassic intervals respectively. 96*
Fig. 73: *Case 1 TOC calculations using a baseline in the upper Cretaceous using BasinMod.* ***A****. Well logs used in the estimation, interval of study (red box) and interval of baselines (green box)* ***B****. Zoom in of the interval baseline showing the constant baseline values taking by the software. Note that there is an uncertainty related to the location of the baselines since the log response has variations. 98*
Fig. 74*: TOC estimation in the well NO 34/8-6 at the level of the Jurassic section, showing that major differences (black triangles) with respect to calibration data were found in heterogeneous intervals from the lower part of Draupne Fm. and Heater Fm. The core present in this section describes this variation in lithology. 99*
Fig. 75*: On the right, comparison of 2 set of transit time and resistivity baselines used in the TOC estimation in the well NO 34/8-6. In black set of baseline 1 and in green set of baselines 2, values summarized in the table. The question that arise looking at this baselines is: will be the log response of a non-source rock (NSR) shale* ***A*** *located in the upper part of this interval similar to the same shale located in the lower part?. A more reasonable solution can be the use of a trend line such as is illustrated on the left of this figure. 101*
Fig. 76: A. *Shale travel time vs. Depth for Miocene and Oligocene shales, Upper Texas and Southern Louisiana Gulf Coast (Hottmann & Johnson, 1965).* ***B.*** *Average shale sonic transit time vs. depth in Beaufort-Mackenzie Basin, Northern Canada (Issler, 1992). 102*
Fig. 77: A. *Conductivity in clean shales in 26 wells in 5 offshore areas and 4 onshore fields from West Cameron to south Timbalier areas (Mcgregor, 1965)* ***B.*** *Shale travel time vs. Depth for Miocene and Oligocene shales, Upper Texas and Southern Louisiana Gulf Coast (Hottmann & Johnson, 1965). 103*
Fig. 78: *Possible depth mismatch between log data and calibration values due to cable tension and elasticity in wireline logging tools. On the right the initial results, on the left a fit after a shifting of 2,5 m between both set of data. 104*
Fig. A1*: TOC estimations using the In-house spreadsheet with data from the Well NO 34/8-6 in the interval 1, showing the results obtained using 2 different baselines intervals for Transit time (Dtb) and Resistivity (Rb) logs (values in yellow boxes). In the track of TOC from logs the two TOC estimation curves are compared. 113*
Fig. A2*: TOC estimations using the In-house spreadsheet with data from the Well NO 34/8-6 in interval 2, showing the results obtained using 3 different baselines for Transit time (Dtb) and Resistivity (Rb) logs (values in yellow boxes) and also comparing the thickness of the baselines intervals. In the track of TOC from logs the three TOC estimation curves are compared. 114*
Fig. A3*: TOC estimations using the In-house spreadsheet with data from the Well NO 34/8-6 in the interval 3, showing the results obtained using 3 different baselines for Transit time (Dtb) and Resistivity (Rb) logs (values in yellow boxes). In the track of TOC from logs the three TOC estimation curves are compared. 115*

1. Introduction

A source rock is a sedimentary rock that has generated or used to be able to generate petroleum (*Tissot and Welter, 1978*) and is the first requirement for hydrocarbon accumulation in a petroleum system. Source rocks are commonly shale and lime-mudstones that contain significant amounts of organic matter. Non-source rocks also contain organic matter, but the amount is general not significant (less than 1wt %). The study of source rocks is needed for and accurate understanding of petroleum resources potential in a sedimentary basin.

A crucial test in the recognition of a petroleum source bed is the determination of its content of organic matter (*Tissot and Welter, 1984*). Total organic carbon (TOC, wt %) describes the quantity of organic carbon in a rock sample and includes both kerogen and bitumen (*Magoon, L.B. and W.G. Dow, 1994*). In shales, the total organic carbon is a parameter that describes the richness of potential source rocks. The Rock Eval parameter, Hydrogen Index (HI) describes which portion of the TOC can be converted to petroleum. Values of TOC are used as an input in basin modeling of generation and accumulation of hydrocarbons.

Several methods have been developed to characterize source rocks, mainly using geochemical techniques to set the main features such as total organic carbon (TOC) content (as a quantitative indicator), maturity, type of kerogen or organic matter quality, among others to determine its effectives potential of oil generation.

Laboratory geochemical analysis can be done to determine mentioned properties on cuttings from well or plugs from cores, such us Rock Eval pyrolysis that is used to detect petroleum potential in sediments (TOC) and to identify the type and maturity of organic matter. This method regardless its great advantages, has some problems such as lack of analysis results in some intervals (cutting space between samples), probability of loss of rich intervals during the sampling, is costly and time consuming, and sometimes is not conclusive. Additionally, samples sometimes can be altered by drilling fluids, thus TOC and HI determination can lead in misleading results.

The effects of organic matter and free hydrocarbon in the pore space of source rocks have also and effect in well logs. Previous studies reveal that the value of TOC can be calculated by extracting especial relationships from logs which is advantageous because of the fact that well logs are the most complete and readily available well data and moreover when the data set is restricted to log data or few or no geochemical information is available. Apart from that, it allows a better understanding and description of effective source rock thickness.

Various methods for recognition and quantification of source rocks from well log data exist. Application within the petroleum industry focuses mainly on the so-called delta log R method described by *Passey et al.* (*1990*).

The method has some limitations and possibly wrong assumptions. There is a need to study this topic in detail by utilizing the method and reflecting on the uncertainty in outcomes, possibly comparing with alternative methods.

Moreover, the effect of the type of depositional environment of the source rock, in the estimation of total organic carbon using well logs is one point to be considered since is well known that marine

source rocks often have a more homogenous distribution of organic matter throughout the gross formation packages while lacustrine systems on the other hand are often lithologically very heterogeneous and the organic rich intervals are irregularly distributed both vertically and laterally which results in low net thickness values.

The purpose of this study is to estimate Total Organic Carbon from well logs and the main objectives of this Thesis are:

- To summarize and describe existing techniques and to test selected ones on individual well log data sets with special focus on advantages and drawbacks of the various methods.
- To test different tools for the purpose: in-house spreadsheet solutions (*Microsoft Excel, Microsoft Office Professional Plus 2010*), *BasinMod 1D* (*Platte River Associates, Inc.)* and *Permedia MPath* version *4.18.1*(*Halliburton*).
- Investigate and possibly assist in creation / implementation of new code.
- To apply petrophysical methods to provide source rocks richness estimations.

To accomplish these objectives, two wells provide by Statoil ASA, were evaluated: the well NO 34/8-6 located in the North Sea specifically at the North of the Visund Field, and the well NO 7120/12-1 in the Barents Sea, in Troms I area.

1.1 Previous Studies and Log Evaluation Techniques

There are several studies in which the identification and quantification of source rocks have been done using Gamma Ray, Density, Neutron, Sonic and Resistivity logs and combination of them.

1.1.1 Gamma Ray logs

Several authors (*Russel 1945*, *Swanson 1960*, *Hassan et al. 1976*, *Supernaw et al. 1978*) have observed a strong correlation between uranium and organic material. So after calibration with core data, it is possible to evaluate the organic carbon content of source rock from its uranium content and from that its hydrocarbon potential (*Serra, 2008*).

Russel (1945) found that certain types of organic matter were associated with abnormally high radioactivity, others with low or normal radioactivities, and that the results of the work were related to the nature of the organic content, the supply of radioactive matter in solution, the rate of deposition and the variations in conditions of sedimentation and types of life existing. *Russel* also discuss the variation of radioactivity in organic matter and conclude that the dominant type of organic life existing in the seas has varied with geologic time, and this in turn has influenced the distribution of radioactive matter among the different types of sedimentary deposits, although it could hardly have affected the total amount of radioactive matter deposited rather than by any direct effect of age.

It is postulated that the uranium in shales is concentrated from sea water within, on, or near the humic type of organic matter by one or all of the following ways: direct precipitation (by reduction of the hexavalent to the tetravalent form) of uranium, probably by hydrogen sulfide; removal of uranium ions from solution by adsorption and complexing on solid humic materials; and adsorption or complexing of uranium by humic acids while in solution (*Swanson, 1960*).

Schmoker (1981) found an equation to estimate the organic matter content of the Devonian shale of the Appalachian basin, using gamma ray logs to calculated the fractional volume of the organic matter content (ϕ_0) taking into account the gamma ray intensity in API units for both, in the presence of organic matter (Υ) and if no organic matter is present (Υ_B), and the slope (A) of the cross plot of gamma ray intensity and formation density (API units/(g/cm^3). The derived equation is given by:

$$\phi_0 = (\gamma_B - \gamma)/1.378A \qquad (1.1a)$$

Using this equation it was found that the distribution of the differences between organic matter content determine from core samples and estimated from gamma ray logs has a mean of 0.44% and a standard deviation of 1.98% which indicated an adequate accuracy of the method for the Devonian shales except for shale intervals with anomalous low gamma ray values in which the estimation was likely too low (***Fig 1***).

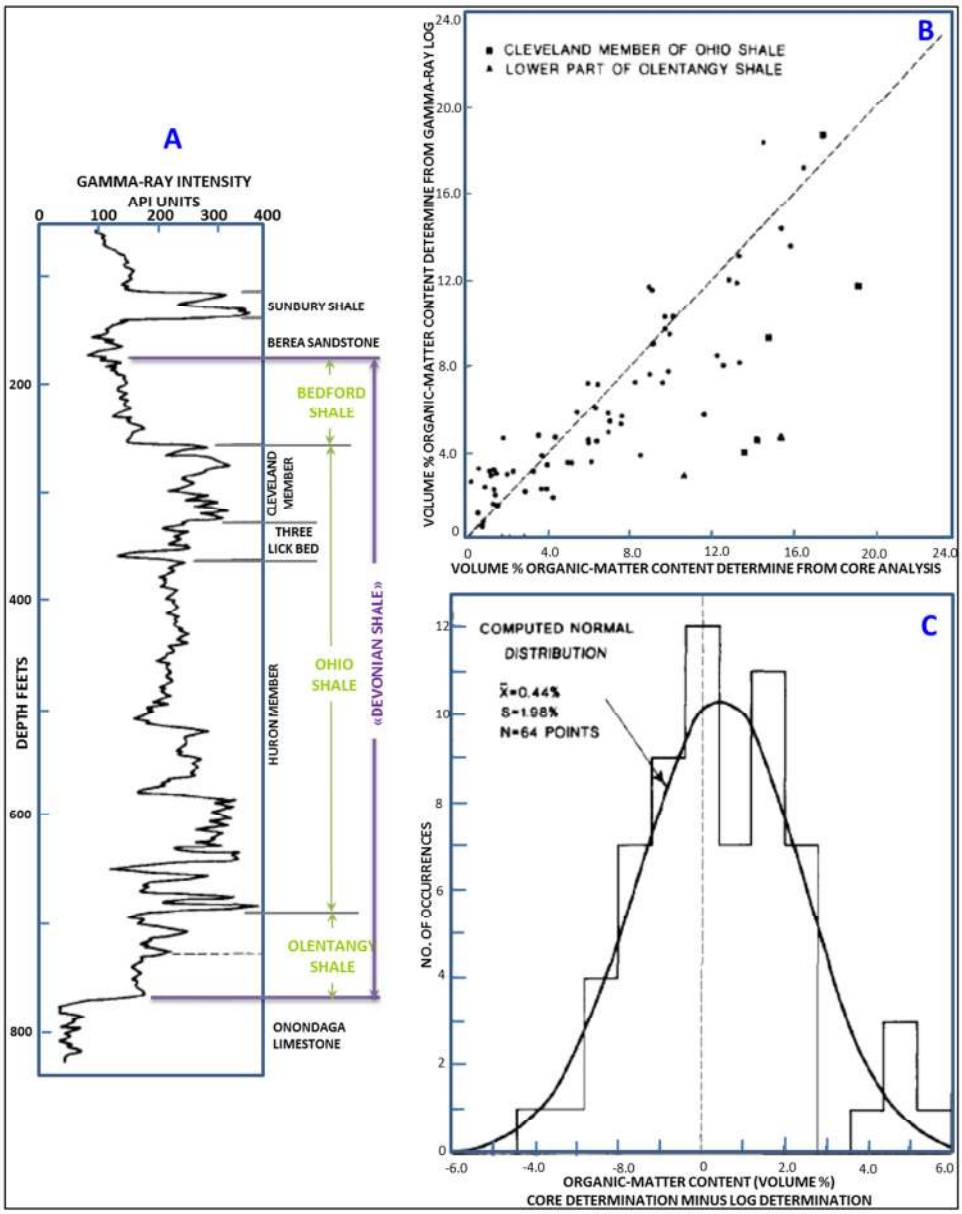

Fig. 1: **A.** Gamma-ray log from Pike County, Ohio, showing features typical of Devonian shale in western part of Appalachian basin (adapted from *Wallace et al, 1977*). **B.** Comparison of volume percent of organic matter in Devonian shales calculated from gamma-ray logs and determined from core samples (Ideal agreement is shown by dashed line) **C.** Distribution of differences between volume percent of organic matter determined from core samples and calculated from gamma-ray logs. Data from Cleveland Member of Ohio Shale and lower part of Olentangy Shale are excluded. (Modify from *Schmoker, 1981*).

Rigoris (2005) derive a predictive relationship using the gamma ray response at relatively low TOC values (0.45-2.5%) in the Lower Member of the Lewis Shale, Washakie Basin in Wyoming. Using the relationship between normalized TOC and GR curves *Rigoris (2005)*, found the following equation:

$$TOC = 0.0285 \times GR - 2.2939, \quad r2 = 0.7627 \qquad (1.1b)$$

The reasonable correlation coefficient suggests that TOC and GR are correlated (***Fig 2***).

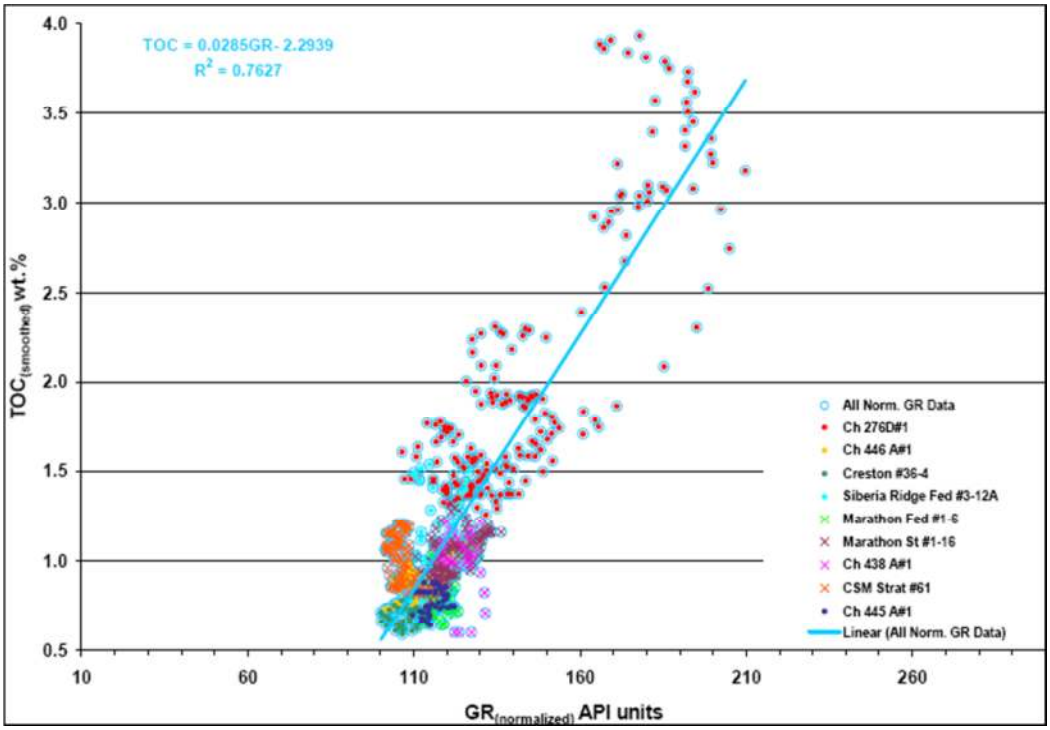

Fig 2: Correlation between GR and TOC for the Lower Member of the Lewis Shale, Washakie Basin in Wyoming. The higher TOC values from the well Ch 276D#1 influence the correlation. The CSM Strat Test 61 well data points comprise the lower end of TOC values (*Rigoris, 2005*)

Although marine source rock generally have high Uranium response (***Fig. 3***), in most of the cases lacustrine source rocks have not gamma ray signature and are not uranium enriched since lakes do not have reserves of dissolved uranium available to be adsorbed by organic matter while oceans do (*Rider, 2008*). Exceptions can be found such as the case of lacustrine source rocks characterized by remarkable positive radioactive gamma-ray values (***Fig. 4***), and showing extensive distribution areas and varying thicknesses, detected at the base of the Late Triassic Chang 7 member in the Erdos Basin (*Yang H. et al., 2010*). Possible uranium sources may be the extensive U-rich volcanic ash that resulted from contemporaneous volcanic eruption and uranium material transported by hydrothermal conduits into the basin. Uranium is enriched together with organic matter and elements such as Fe, S, Cu, V and Mo in the rocks.

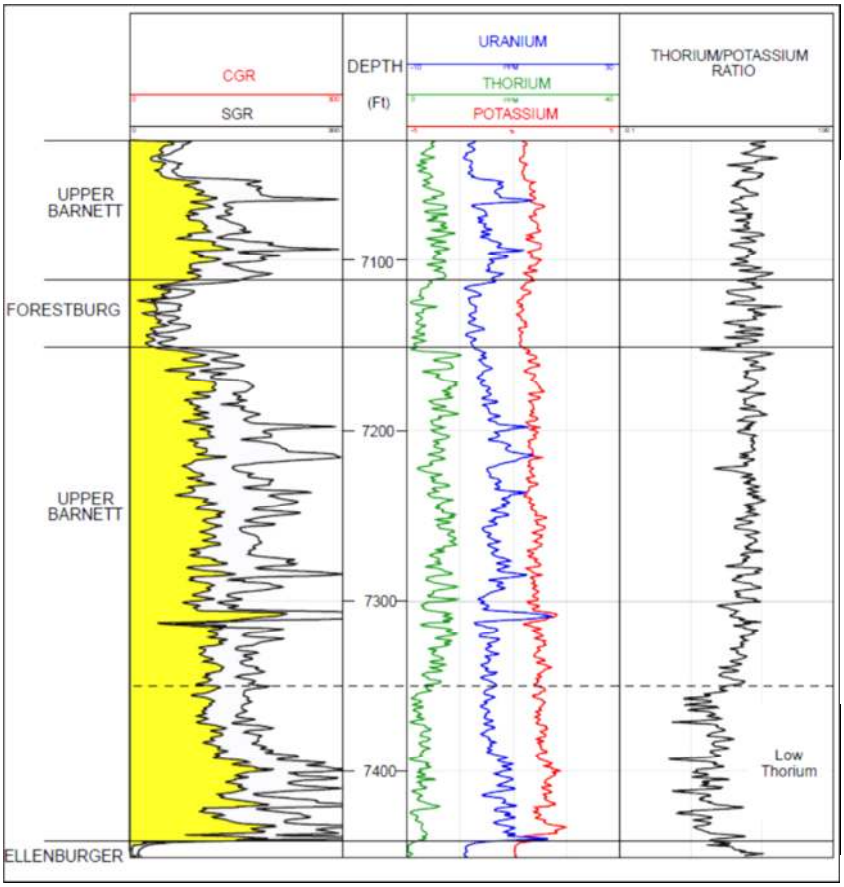

Fig 3: Spectral gamma ray log showing elemental composition of the Barnett Formation in the Texas United Blakely #1 well. Wise County, Texas (*Ruppel & Kane, 2006*). A strong correlation exists in some shales with Uranium content from the spectral gamma ray log.

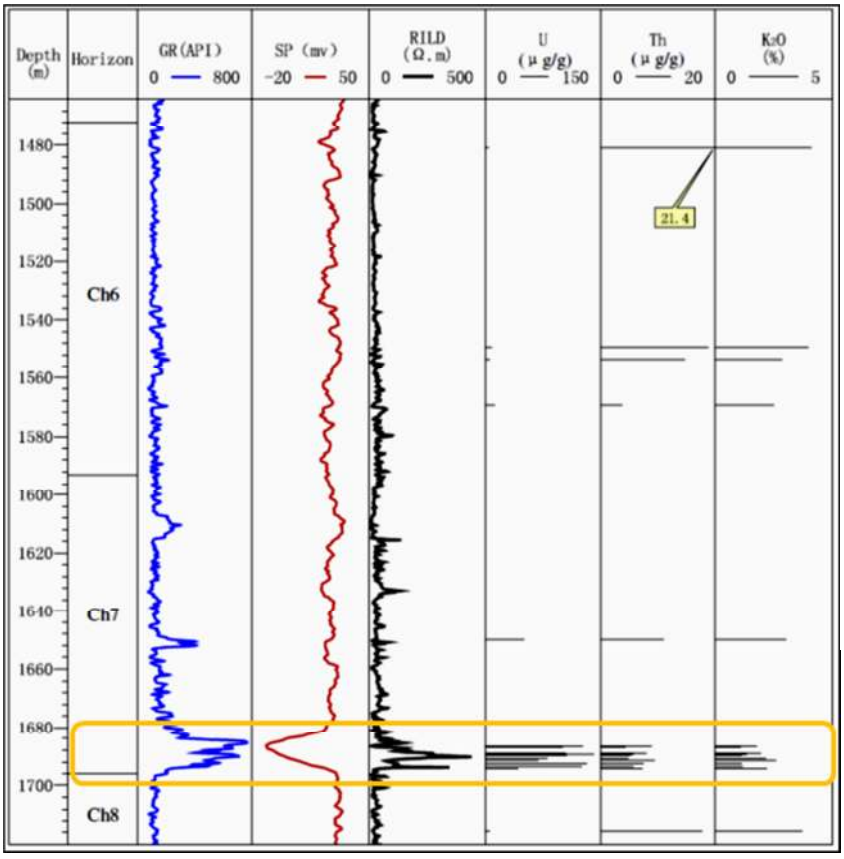

Fig 4: Distribution and log response characteristics of oil source rocks (Ning 36 well), showing a positive uranium anomaly at the base of the Chang 7 member (Box in Orange). GA: gamma ray. SP: spontaneous potential. RILD: deep investigate induction log. The API, mv and Xm are units for GA, SP and RILD, respectively (Modify from *Yang H. et al., 2010*).

Another example of lacustrine source rock with high uranium content is the Green River Formation; in which uranium anomalies were associated with localized organic matter and phosphate-rich beds in the Wilkins Peak Member (*Mott & Drever, 1983*). In this study it was also observed that the gamma ray tool shows high intensity readings related to the uranium, both in organic matter and also in the phosphatic beds which may result in misleading information to study source rock TOC abundance.

Coals also have a low gamma ray values due the fact that uranium is not adsorbed by organic matter in terrestrial swamps where not clay is presence. Thus pure coals have the typical low gamma ray response while shaly coal has a value which depends on the shale content (*Kayal and Christoffel, 1989*). The contrast in this response between pure coals and organic shales is remarkable, especially when, in typical cyclic deltaic sequences, a low gamma ray coal is immediately overlain by a high gamma ray, organic rich shale.

1.1.2 Density Logs

Presence of organic matter in shales lowers their density (***Fig. 5***). The normal average matrix density of a mixture of clay minerals is about 2.7 g/cm^3, while organic matter has densities between 0.50 g/cm^3- 1.80 g/cm^3. The presence of organic matter therefore has a marked effect on the overall shale bulk density (*Rider, 2008*).

Changes in organic content produce significant changes in formation density, and the organic content of the shales can be computed directly from formation density if variations from other causes are considered (*Schmoker, 1979*). *Schmoker* determined the organic content of the Appalachian Devonian shales from density logs, in which the formation density of the shales were treated as a four-component system consisting of rock matrix (m), interstitial pores (i), pyrite(p), and organic matter (0), define by the densities and fractional volumes of these four components:

$$\rho = \varphi_0\rho_0 + \varphi_p\rho_p + \left(1 - \varphi_0 - \varphi_p - \varphi_i\right)\rho_m \qquad (1.2b)$$

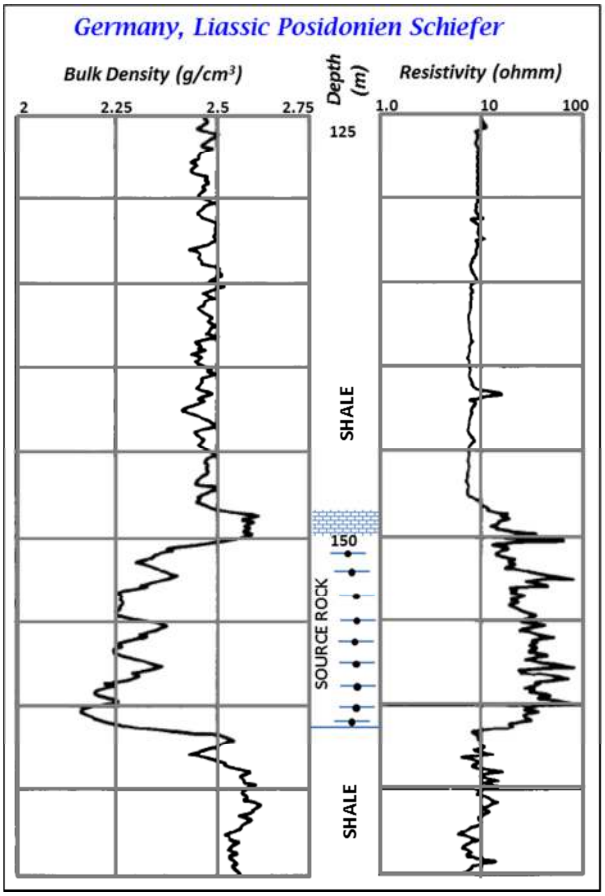

Fig. 5: Density and resistivity of the Liassic Posidonien Schiefer in shallow well in south Germany. Resistivity is from Microlaterolog. High resistivity peaks in shale are thin limestone intercalations (*from Meyer & Nederlof, 1984*)

To compute organic content from density logs, *Schmoker (1979)* reduced this equation to an expression relating formation density (ρ) to organic content (φ_0) using a relation of fractional volume of pyrite and organic matter φ_p = 0.135 φ_0 + 0.0078, setting ρ_p = 5.0 g/cc, ρ_0 = 1.0 g/cc, and ρ_m = 2.69 g/cc, and taking into account the formation density with not organic matter content by ρ_b= $\varphi_i(\rho_i$-2.690)+2.708, which allow to calculated the volume-percent organic content by a basic equation:

$$\varphi_0 = \rho_B - \rho/1{,}378 \qquad (1.2c)$$

Schmoker (1979) used this equation to calculate the organic content in 5 wells with an overall agreement between the method and laboratory analyses of core samples; however the resulting distribution has a mean of 0.4% and a standard deviation of 1.5% which can be related to the simplifications and assumptions in deriving the equation an according to the author uncertainties of this magnitude may be present in the laboratory data (***Fig. 6***). *Schmoker (1979)* also consider the use of density and gamma ray crossplots to determine the regional applicability of this method, based on the linear relation between this measurements which demonstrates that density variations are caused by variations in organic content (confirming the fundamental assumption of the method), because other factors such as porosity or mineralogic variations that might change the density would not affect the gamma-ray intensity (***Fig. 6***). However, because the density log is pad-type tool and therefore sensitive to borehole rugosity, the usefulness of this tool is decreased in many wells in which the shales are washed out (*Passey, 1990*).

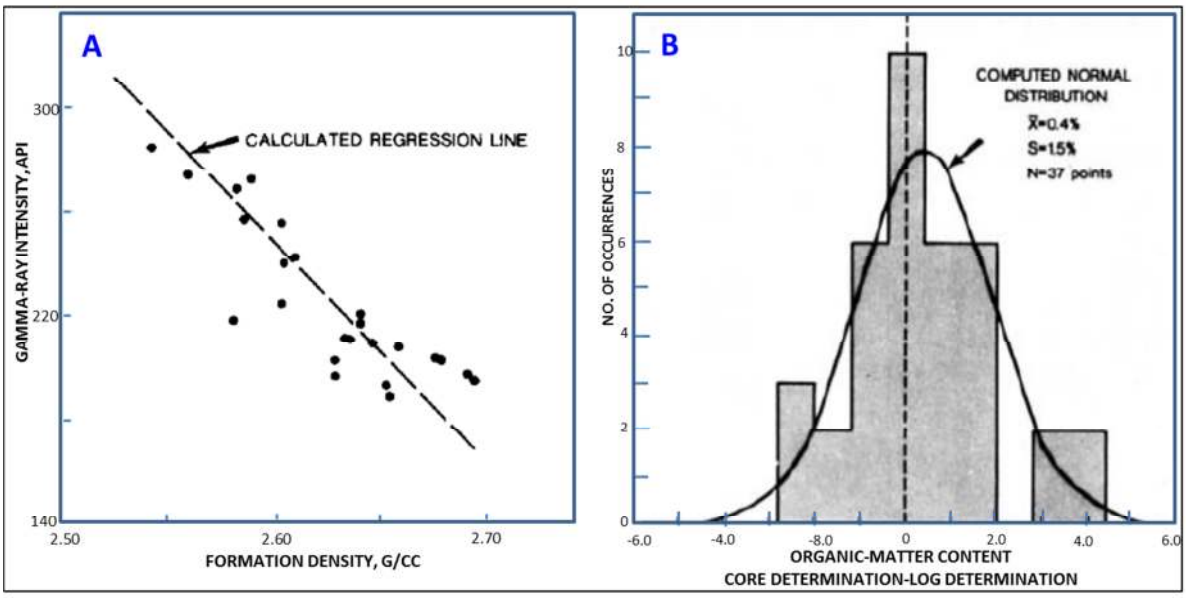

Fig 6: **A.** Crossplot for Jackson County well showing strong linear relation between density and gamma-ray intensity. Wire-line data are averaged over intervals of 6.1 m. **B.** Distribution of differences between volume percent organic matters measured in core samples and calculated from density logs (*Schmoker, 1979*).

Using a similar approach *Schmoker & Hester (1983)* calculated organic carbon content from density logs in the upper and lower members of the Mississippian and Devonian Bakken Formation in the United States portion of the Williston basin. The organic content was estimated using the following equation where TOC is organic-carbon content (wt. %) and ρ is formation density (g/cm^3):

$$TOC = (154.497/\rho) - 57.261 \qquad (1.2d)$$

Schmoker & Hester (1983) found a significant negative correlation between density and organic-carbon content, substantiating the basic premise of the density-log method that density varies primarily in response to changes in organic-matter content (***Fig. 7A***). Using this equation resulted in an overall agreement between organic-carbon contents calculated from density logs and the laboratory analyses (***Fig. 7B***). *Schmoker & Hester (1983)* considered that because comparisons are not based on identical samples and because experimental errors are present in laboratory procedures, differences between laboratory and density-log determinations of organic-carbon content should not be attributed solely to inaccuracies in the density-log method and that the method is sufficiently accurate and reliable for Bakken shale applications. In shales with lower organic-carbon content, the error in the density-log method would probably decrease in an absolute sense, but would increase as a percentage of organic carbon content. They also noted that because the density log can be significantly affected by the presence of heavy minerals, such a pyrite, a correction for pyrite was necessary based on a linear relationship between pyrite and organic matter.

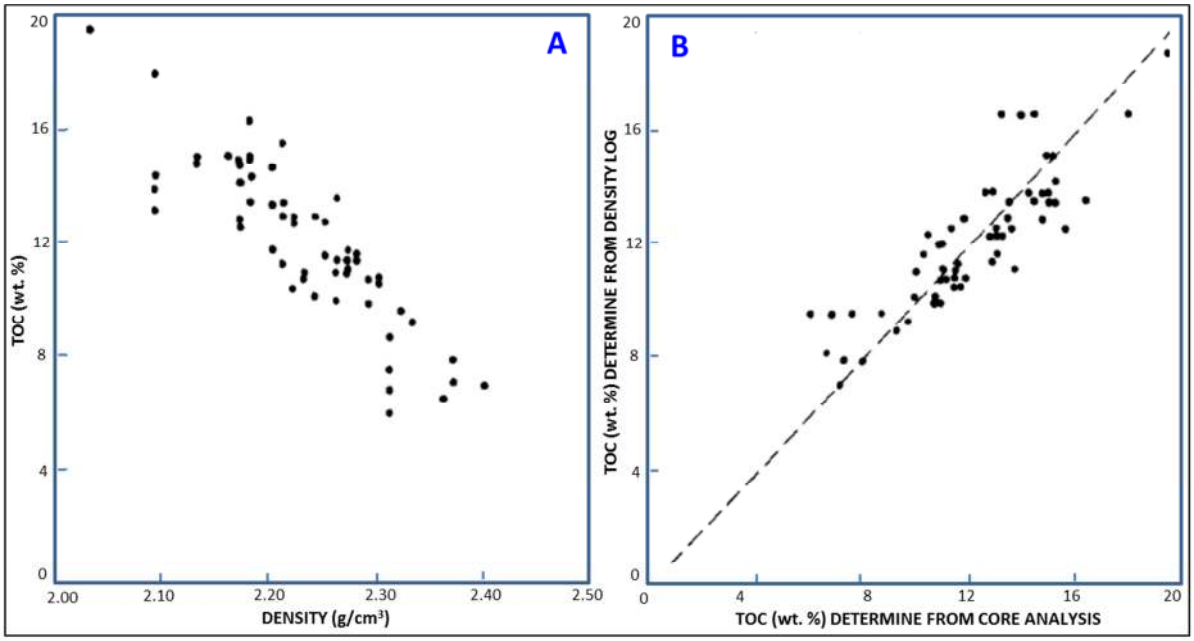

Fig 7: **A.** Laboratory measurements of organic-carbon content of Bakken shales, Williston Basin (59 analyses representing 39 locations in North Dakota) versus log-derived formation density of comparable intervals. **B.** Comparison of organic-carbon content of Bakken shales calculated from density logs (TOC = (154.497/ ρ) - 57.261) and measured from core samples where ideal agreement is shown by dashed line (*Schmoker & Hester, 1983*).

Meyer & Nederlof (1984) considered that in shales with a similar degree of compaction, all other factors being equal, water saturation also should be equal. It follows, therefore, that if $\rho_{source\ rock}$ is smaller than ρ_{shale}, it must be a function of the amount of organic matter present:

$$Vol.\%\ organic\ matter = \frac{\rho_{shale} - \rho_{source\ rock}}{\rho_{shale} - \rho_{organic\ matter}} \qquad (1.2e)$$

The value of $\rho_{\text{organic matter}}$ is approximately the same as ρ_{water} (i.e., + 1 g/cm^3). They also found that at shale densities of 2.25 g/cm^3 or greater, the minimum concentration of organic matter for the density log to respond is about 1%. As previous mentioned in the work of *Schmoker and Hester (1983)*, they discuss the fact that bulk density readings may not be a reliable indication of organic matter in the presence of larger concentrations of heavy minerals (pyrite). Rugose boreholes also render density readings unreliable *Meyer & Nederlof (1984)*.

Using a similar approximation as *Schmoker & Hester, (1983)* with a three component system (matrix, kerogen, and pore fluid), *Meldenson & Toksoz (1985)* calculated TOC in terms of weight percentage with an inverse linear relationship (i.e. hyperbolic) in density:

$$TOC = \alpha \left[\frac{1}{1 - \frac{\rho_k \left[\frac{\rho_m \rho_b}{\rho_k} + \rho_m V_{w-} V_{w-} \rho_m \right]}{\left[\rho_b + \rho_m V_{w-} V_{w-} \rho_m \right]}} \right] \qquad (1.2f)$$

Where α is a constant relating TOC (%wt.) to kerogen (%wt.), usually taken as 0.7-0.8, ρ_b, ρ_m and ρ_k are bulk, matrix and kerogen densities respectively and V_w is pore-volume fraction. According to this equation bulk density is very sensitive to TOC, an increase of 10% TOC should cause a density decrease of almost 0.50 g/cc and replacing part of the matrix by water-filled pores shifts these curves to the right (lower densities)(***Fig. 8***).

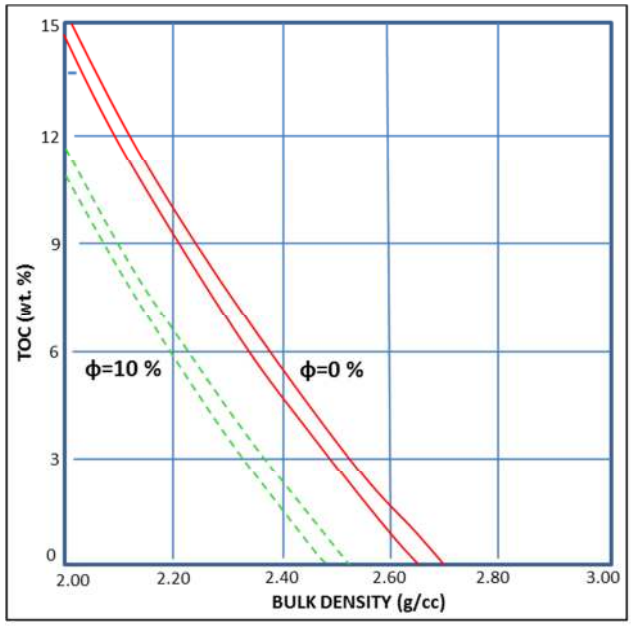

Fig.8: Calculated volumetric average response of density log to organic matter content, expressed in terms of total organic carbon (TOC). For each porosity (ϕ=0 % and ϕ=10 %) the effects of modeling with matrix densities of 2.65 and 2.70 g/cc is shown *(Meldenson & Toksoz 1985)*.

Myers & Jenkys (1992) modified the *Schmoker (1979)* method using conventional density logs, modeling the source rock as a three component system (matrix, kerogen and porosity) using equations adapted from *Meldenson & Toksoz (1985)*. The potential source-rock is modeled in terms of a volume of matrix (assumed mudrock matrix density $\boldsymbol{\rho_{ma}}$= 2.70 g/cm^3), a water-filled porosity ($\boldsymbol{\varphi_{fl}}$ with density $\boldsymbol{\rho_{fl}}$=1.05 g/cm^3) and a volume of kerogen ($\boldsymbol{\varphi_{ker}}$ with density $\boldsymbol{\rho_{ker}}$=1.1 or 1.2 g/cm^3). Knowing the true porosity and matrix density of the organic-rich rock, the method calculates the weight% of organic matter (of an assumed density) required to affect the observed decrease in bulk density. The true porosity of the mudrock is assumed to be independent of increasing organic carbon content and can therefore be calculated from the bulk density in an adjacent organic-poor interval or from a porosity-depth curve. Assuming that the non-source interval has the same mineral matrix, water density and water-filled porosity as the source interval, the following equations were derive:

Density of non-source interval (taken from logs):

$$\rho_{ns} = \rho_{ma} * (1 - \varphi_{fl}) + \rho_{fl} * \varphi_{fl} \qquad (1.2g)$$

then, the Water filled porosity of the non-source interval is given by:

$$\varphi_{fl} = \frac{\rho_{ns} - \rho_{ma}}{\rho_{fl} - \rho_{ma}} \qquad (1.2h)$$

Density of source interval:

$$\rho_s = \rho_{ma} * (1 - \varphi_{fl} - \varphi_{ker}) + \rho_{fl} * \varphi_{fl} + \rho_{ker} * \varphi_{ker} \quad (1.2i)$$

The volume (porosity) filled with kerogen of a given density is determined by:

$$\varphi_{ker} = \frac{\rho_s - \rho_{ns}}{\rho_{ker} - \rho_{ma}} \quad (1.2j)$$

The total organic content is calculated using the mass of kerogen (M_{ker}) by:

$$TOC\% = 0.85 * M_{ker} \quad (1.2k)$$

From the previous set of equations, the conversion of kerogen volume to weight and the TOC% using a weight % kerogen equivalence to weight % carbon of 0.85, is given by:

$$\boldsymbol{TOC\% = \frac{0.85 * \rho_{ker} * \varphi_{ker}}{\rho_{ker} * \varphi_{ker} - \rho_{ma} * (1 - \varphi_{fl} - \varphi_{ker})}} \quad (1.2m)$$

1.1.3 Resistivity Logs

The resistivity log may be used both qualitatively and quantitatively to investigate source rocks (*Rider, 2008*). The effect a source rock has on the resistivity log depends on the maturity of organic matter: it has little effects when immature, but causes a large increased when it is mature (*Nixon, 1973; Meissner, 1978; Schmoker & Hester, 1989*); which can be related to the pore fluid content that causes the increase and not the solid matter since non-conducting hydrocarbons are generated in mature source rocks (***Fig. 9***).

In other words, a typical shale which is not a source rock consist of clay mineral matrix and a certain water filled porosity, while a source shale also contains both matrix and porosity but typically 4%-12% of the matrix is organic matter (*Rider, 2008*)(***Fig.10***). If the source is immature the pore space is filled with water, but if the source is mature, the pores contain both, water and free hydrocarbons in voids and fractures (*Du Rochet, 1981; Rider, 2008*). The resistivity logs responds to the free hydrocarbon fluids, the high resistivity is an indication that hydrocarbon fluids are present in the pores and not that a solid organic matter source is present (*Rider, 2008*).

With maturity, the resistivity of a source rock increases by a factor of 10 or more. Thus resistivity can be used as a maturity indicator for a given source rock formation *(Meyer & Nederlof, 1984).* However a high resistivity in a shale interval may be cause by other textural and compositional effects such a carbonate rich zone or lack of porosity, and not just a mature source rock implying that the resistivity log cannot be used alone, but by comparing the resistivity log to another log which is principally affected by texture and composition and not by pore fluid (*Rider, 2008*).

Meissner (1978) noted that overpressuring often affects the electrical resistivity of rocks (although the overpressuring was not the cause of the high resistivity anomalies), and that the high resistivities observed are opposite to the low resistivities generally associated with high fluid pressures.

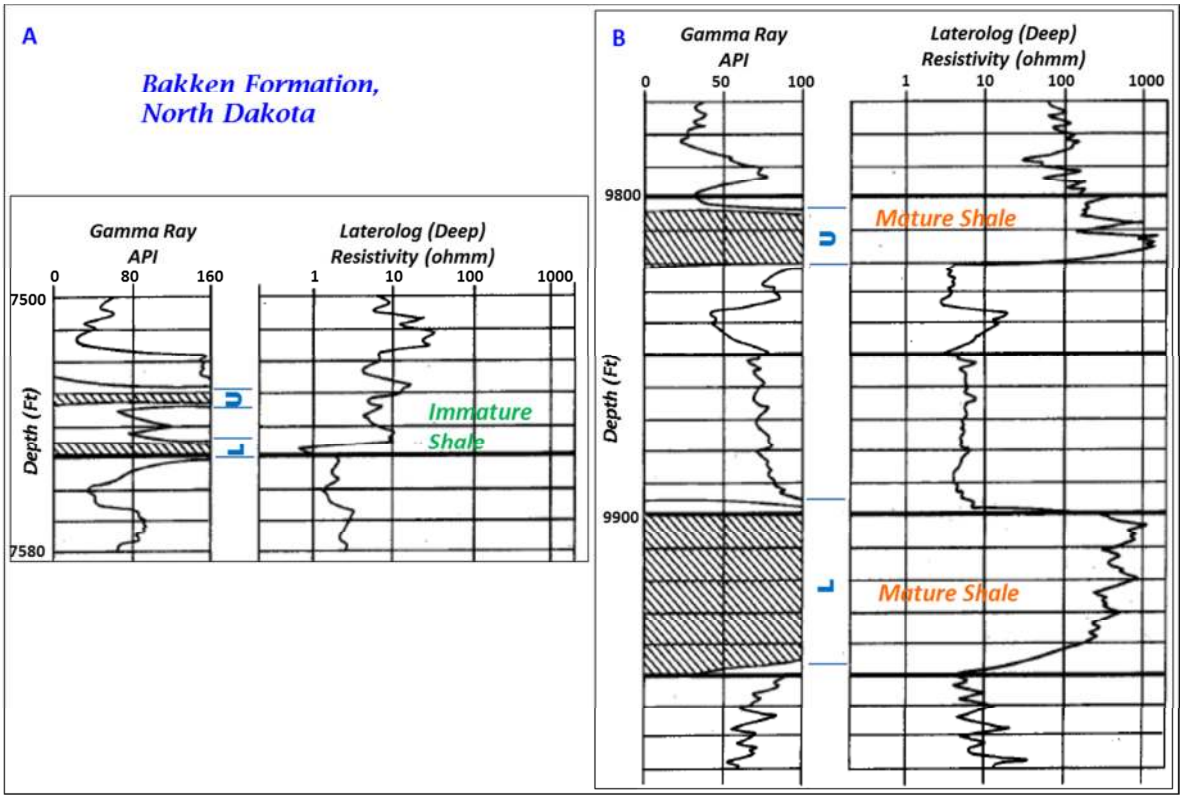

Fig 9: Effects of organic matter content in resistivity logs response: Gamma-ray and resistivity logs typical of upper (U) and lower (L) shale members of Bakken Formation. **A.** Low resistivity values reflect water-saturated, thermally immature shales (Union Oil Company of California Hanson #1-C-13, 13-153N-85W). **B.** High resistivity values reflect thermally mature shales that have generated oil (Smokey Oil Company Will #I 4-23, 23- 157N-94W)*(Modified from Schmoker and Hester, 1990).*

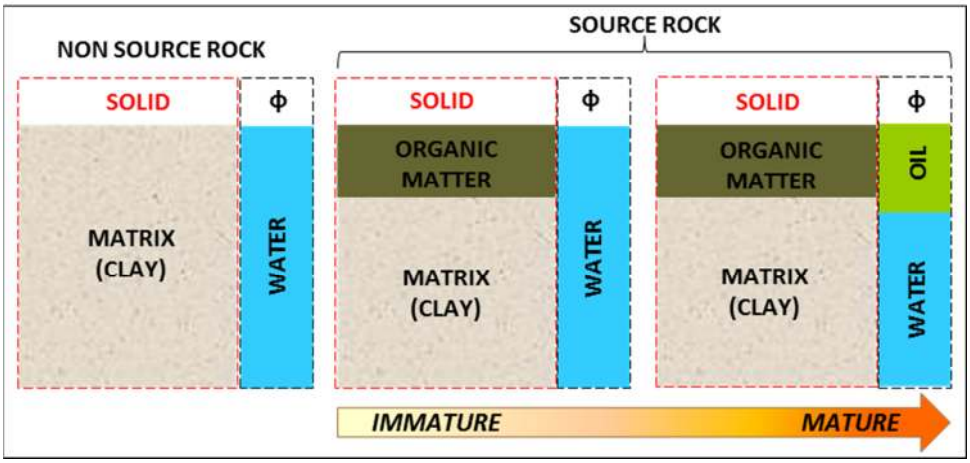

Fig 10: Schematic of volumetric components in source and non-source rock, showing the differences in solid and fluid components and the maturity effects in source rocks *(Modified from Passey et al., 1990).*

1.1.4 Sonic Log

The presence of organic matter, especially in shales, lower sonic velocities, apparently in direct relation to abundance and when combine with resistivity log values the velocity is a good qualitative and possible quantitative source rock indicator (*Rider, 2000*).

Because of the presence of organic material, source rocks retain a greater amount of the formation fluid than organic-lean sediments, and thus appear on sonic and density logs to be somewhat less compacted (*Meyer & Nederlof, 1984*).

Like density logs, sonic logs also show the difference in compaction between organic-lean sediments and source rocks (***Fig. 11***). Sonic logs, therefore, can be used to determine source rocks qualitatively: a relative decrease in sonic transit time and an increase in resistivity indicate an organic-rich layer in non-permeable sediments. Where density logs are affected by rugosity of the borehole wall or by the presence of pyrite, sonic logs may prove more reliable than density logs. Therefore, it is always useful to make both sonic/resistivity and density/resistivity crossplots for source rock identification (*Meyer & Nederlof, 1984*).

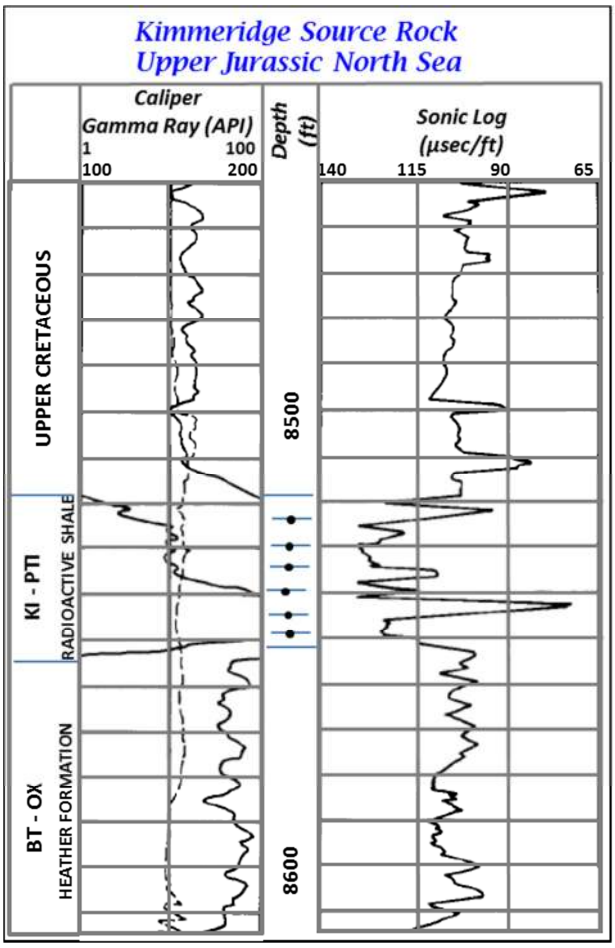

Fig. 11: Kimmeridge Shale, North Sea. Note high gamma-ray reading and the considerable lower sonic. Underlying Heather Formation is very silty. (*Modify from Meyer & Nederlof, 1984*)

Because the interval transit time is affected by the water/ organic matter ratio, mineral composition, carbonate/clay content, and grain-to-grain pressure, sonic logs cannot be used alone to estimate the

organic content of source rocks. They can be used, however, if correlated with density logs or, even better, if calibrated with cores (*Meyer & Nederlof, 1984*).

Dellenbach et al. (1983) develop a method using the transit-time and gamma ray curves to provide a parameter, I-x that relates linearly to organic richness. In their method, a source rock is defined by a relatively long transit time (slow velocity) and high gamma ray intensity. Even though the derived I-x parameter has been shown in some wells to correlate roughly linearly with organic richness, calibration with sample data from specific wells is required in order to determine organic richness quantitatively *(Passey et al., 1990)*.

Another method employing the gamma ray and transit-time curves was introduce by *Autric & Dumesnil (1984, 1985)* in which a resistivity parameter is added to the I-x method of *Dellenbach et al. (1983)*. This method involves the selection of a variable which relates to the resistivity in non-sources shales. The resistivity curve is used only to help qualitatively discriminate potential source rock from non-source rocks; the organic richness then is determine using the I-x method (after calibration to sample data) *(Passey et al., 1990)*.

1.1.5 Method of Meyer and Nederlof (1984)

A more generally applicable model and one that does not require calibration with core data, was proposed by *Meyer and Nederlof (1984)* which provide a family of four functions, based on sonic, resistivity, density and gamma ray logs, designed to discriminate between organic rich sediments with greater than 1.5% organic carbon and organic poor sediments. Each of the four discriminant functions was derived twice: once for shales only and once for all lithologies. When applied to data, if the function produces a positive value, the formation should not have significant organic value. Although this technique is semi-quantitative in nature, it has been shown to work in many environments, and it offers the significant advantages over other published techniques of not requiring core data and not demanding complex, subjective interpretive input (*Herron, 1990*).

Some considerations are the bases of this method. During compaction, water is expelled; consequently, the density increases and the sonic transit time decreases. Because of the presence of organic material, source rocks retain a greater amount of the fluid formation than organic-lean sediments, and thus appear on sonic and density logs to be somewhat less compacted. Organic matter, like the mineral matrix, is normally not electrically conductive. Organic-rich sediments, therefore, have a higher resistivity than organic-lean sediments.

This method based on the statistical analysis of source rock from around the world, showed that if resistivity log values were cross-plotted with either sonic or density log values, then a sample could be reliably identify as either source or not source (*Meyer & Nederlof, 1984*).

Since resistivity measurements are dependent on temperature, and standardization was done to apply this method, using the Arps formula (Schlumberges, 1972):

$$R_t = R_{75} * \frac{82}{T + 7} \quad (1.5a)$$

or

$$R_{75} = R_t * \frac{T+7}{82} \quad (1.5b)$$

Where T is the formation temperature (in ˚F) at the depth concerned which are derive from a gradient calculated.

Using various combinations of log parameters, a discriminant analysis was performed using the scheme of pseudo-regression (Kendall, 1961). The data points were subdivided into two classes on the basis of geochemical sample analyses: Class 1: source rocks and Class 2: non-source rocks which were plotted on a graph (***Fig. 12, 13***), the log parameters (density, resistivity) are the coordinates used to locate the observations. For classification, the best possible line separating class 1 from class 2 was established using discriminant function. Therefore, a typical equation for the sonic/resistivity combination for shales is:

$$D = -6.906 + 3.186 \log_{10} \Delta t + 0.487 \log_{10} R_{75} \quad (1.5c)$$

Where Δt is in µsec/ft and R_{75} is the resistivity corrected to a standard temperature of 75˚F (24˚C). If D is positive, the rock is a probable source rock; if D is negative, the rock is probably barren; and if D is zero, the case remains undecided. For the two-variable cases of sonic/resistivity and density/resistivity, crossplots were made showing the classification boundary based on the discriminant formula, which roughly separates the source rocks from the non-source rocks (***Fig. 12, 13***).

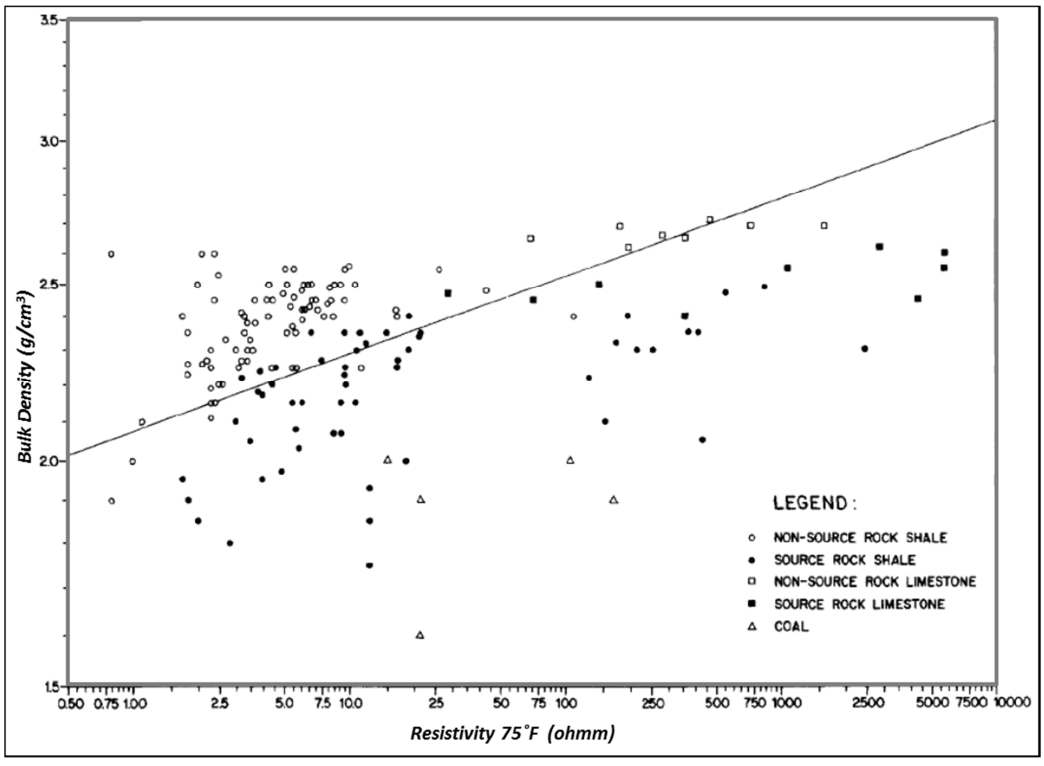

Fig. 12: The identification of source rocks intervals on a cross plot of bulk-density and resistivity. Oblique line is position of D = O (discriminant analysis). Points below this line (D = positive) = source rocks; points above this line (D = negative) = no source rocks. Misclassification occurs at low shale densities, borderline cases, and high limestone resistivities (*Meyer & Nederlof, 1984*).

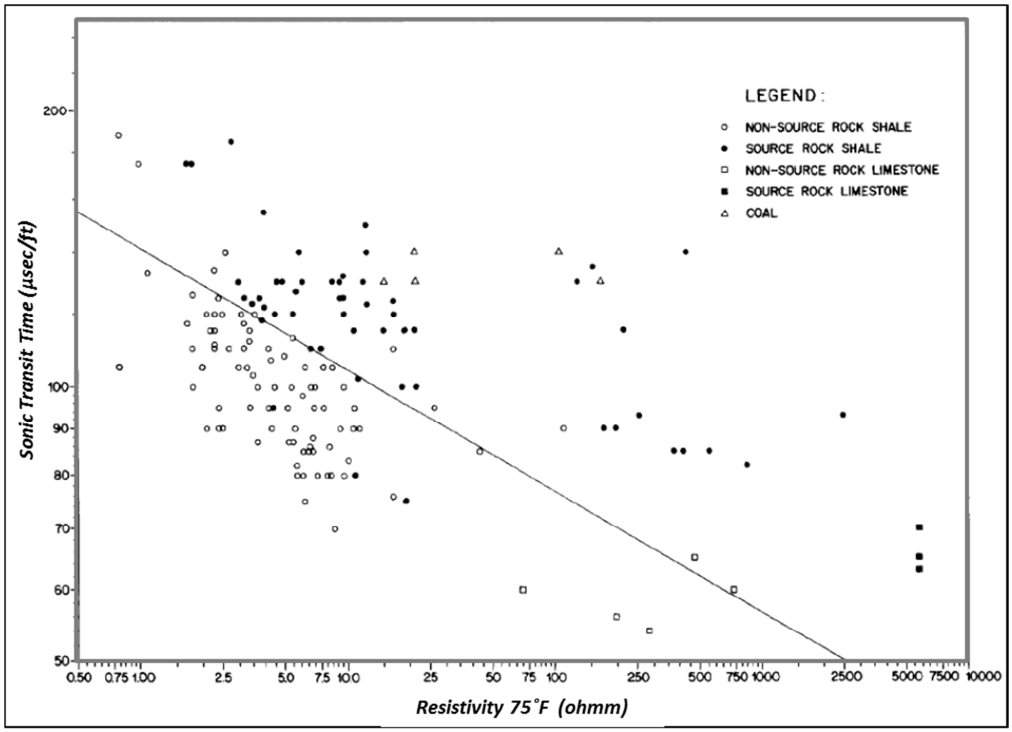

Fig. 13: The identification of source rocks intervals on a cross plot of sonic transit time and resistivity. Oblique line is the position of D = O (discriminant analysis). Points below this line (D = negative) = no source rock; points above this line (D = positive) = source rock. Note that most misclassifications occur at low interval velocities, borderline cases, and high limestone resistivities (*Meyer & Nederlof, 1984*).

The results of the analysis show that there was a 91 % confidence in the ability to correctly classify and about 9% misclassifications. Thus the results have to be considered in a probabilistic sense. The D scores calculated for the learning set result in two approximately normal distributions for class 1 and class 2 (each of which has its own mean and standard deviation), but which overlap to some extent. Such distributions can be employed to obtain the probability of having a source rock (*Meyer & Nederlof, 1984*).

Misclassifications was assumed to be related to several facts such as: a miscorrelation between chemical and petrophysical data because of thin-layer effect; heavy minerals such as pyrite which produce high density readings if sufficiently concentrated; in under-compacted soft formations, the physical contrast between layers that are rich or lean in organic matter becomes minimal, particularly when organic concentrations are low and in high density/high velocity formations such as certain limestones and dolomites, the resistivity correction may be exaggerated (*Meyer & Nederlof, 1984*).

The *Meyer & Nederlof* discriminant functions were applied to the Paris Basin log data using the input data presented in ***Fig. 14 A***, and the results are presented in ***Fig. 14 B***. The solid lines represent the functions derived for shales, and the dashed lines represent those derived for all lithologies. In spite of the fact that this is a very rich organic interval, only the gamma ray-sonic-resistivity combination correctly identifies the presence of organic matter. The sonic-resistivity and gamma ray-density-resistivity combinations identify only the sections where TOC is greater than 6 wt. % as being potential source rocks, and the density-resistivity combination fails over the entire interval (*Herron, 1990*)

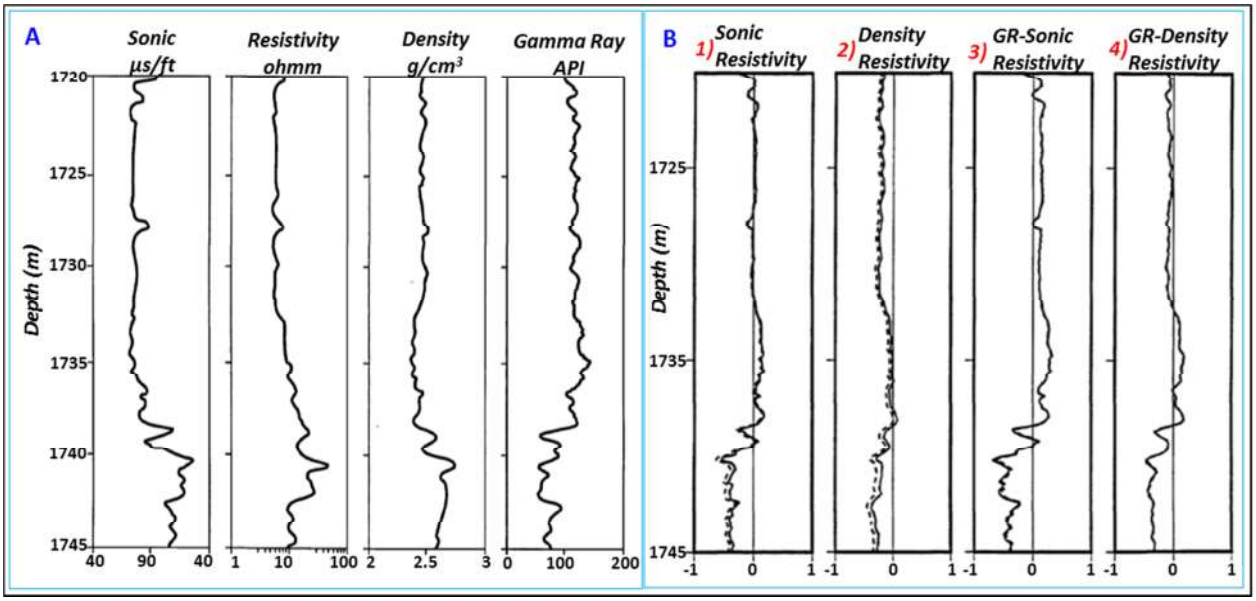

Fig 14: **A.** Input data for discriminant functions: sonic, resistivity, density, and gamma-ray logs for a portion of the Paris Basin well. **B.** Discriminant scores derived from combinations of sonic, resistivity, density, and gamma-ray logs. Positive values indicate the probable existence of source rocks, whereas negative values indicate barren rock. In three of the four cases, the technique fails to identify rocks with total organic carbon contents of 4-6 wt % (*Herron, 1990*).

A similar approximation using discriminant analysis using a combination of logs proved to be useful qualitative technique to identify Cretaceous lacustrine source rocks in the Campos Basin, offshore Basil (*Abrahao, 1989*).

The crossplots are a useful tool in the evaluation of frontier exploration wells as well as in basin evaluation. Only a low possibility exists for error. Even so, it is suggested that, wherever possible, the log interpretation method should be corroborated by geochemical sample analysis (*Meyer & Nederlof, 1984*).

1.1.6 Method of Passey et al. (1990)

Passey et al. (1990) invented a new technique called $\Delta \, Log \, R$. This technique employs the overlaying a properly scaled porosity logs on a resistivity curve for identifying and calculating total organic carbon. In organic-lean rocks, the two curves parallel each other and can be overlain. In organic-rich rocks or reservoir rocks, a separation between the curves occurs. By using the gamma ray log, reservoir rocks can be identified. Therefore, the separation in organic-rich intervals is measured and called $\Delta \, log \, R$ parameter. Such a parameter is used to calculate the total organic carbon content. This method is applied in a wide variety of lithologies showing a good agreement with core data in estimating TOC content (*Rider, 2000*).

The sonic and resistivity logs are used in a standard depth plot format but the method requires two essential steps to make them compatible, before they can be interpreted. First, both logs are scale normalize by plotting the sonic log on a scale were 50 µsec/ft =1 logarithmic cycle on the resistivity log. Second a non-source shale interval is located (in the stratigraphic interval being considered) and the two logs made to plot one on the other over that interval, which is call $\Delta \, log \, R$ plot. When two

logs are plotted like this, they will track each other over all non-source shale, regardless compaction and compositional changes. In source intervals, there will be a marked separation. There will also be a separation in hydrocarbon reservoirs and in coals but this can be eliminated on lithological grounds. The level of maturity must be known for the quantification since the resistivity log responds to the amount of liquid hydrocarbon in the shale pores (*Rider, 2000*).

In applications, the transit-time curve and the resistivity curves are overlain and base-lined in a fine-grained, "non-source" rock. A baseline condition exists when the two curves "track" or directly overlie each other over a significant depth range. With the baseline established, organic-rich intervals can be recognized by separation and non-parallelism of the two curves. The separation between them, designated as $\Delta \log R$, can be measured at each depth increment *(Passey et al., 1990)*.

The $\Delta \log R$ separation is linearly related to TOC and is a function of maturity. Using the delta log R diagram (***Fig. 15***), the delta log R separation can be transformed directly to TOC if the maturity (in level of organic metamorphism units, LOM; *Hood et al., 1975*) can be determined or estimated. In practice, LOM is obtained from a variety of sample analyses (vitrinite reflectance, thermal alteration index, or Tmax), or from estimates of burial and thermal history *(Passey et al., 1990)*.

If the maturity (LOM) is incorrectly estimated, the absolute TOC values will be somewhat in error, but the vertical variability in TOC will be correctly represented. If OMT (organic matter type) is known, then pyrolysis S2 values, as defined by Rock Eval, can be predicted using the transformations of TOC to S2, as illustrated in ***Fig. 15 B*** and ***C*** *(Passey et al., 1990)*.

The algebraic expression for the calculation of delta log R from the sonic/resistivity overlay is:

$$\Delta \log R = \log_{10}(R/R_{baseline}) + 0.02 * (\Delta t - \Delta t_{baseline}) \quad (1.6a)$$

where $\Delta \log R$ is the curve separation measured in logarithmic resistivity cycles, R is the resistivity measured in ohm-m by the logging tool (LLD or ILD), Δt is the measured transit time (DT) in µsec/ft, $R_{baseline}$ is the resistivity corresponding to the $\Delta t_{baseline}$ value when the curves are base-lined in non-source, clay-rich rocks, and 0.02 is based on the ratio of 50 µsec/ft per one resistivity cycle *(Passey et al., 1990)*.

The empirical equation for calculating TOC in clay-rich rocks from Δ log R (***Fig 15A***) is:

$$TOC = (\Delta \log R) * 10^{(2.297 - 0.1688 * LOM)} \quad (1.6b)$$

where TOC is the total organic carbon content measured in weight percent, and LOM is the maturity *(Passey et al., 1990)*.

An LOM of 7 corresponds to the onset of maturity for oil-prone kerogen, and an LOM of 12 corresponds to the onset of over-maturity for oil-prone kerogen.

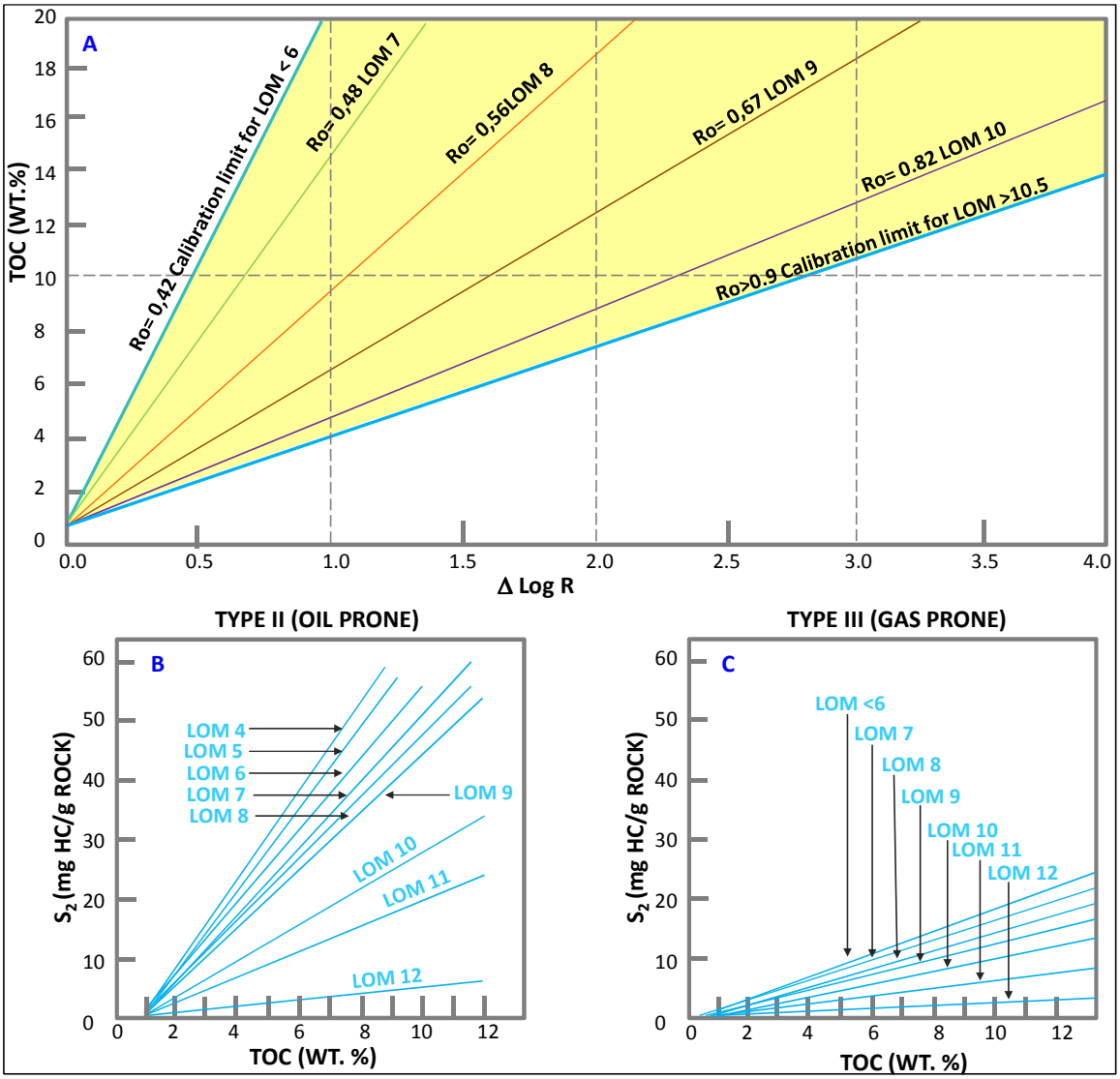

Fig 15: **A.** Diagram relating $\Delta \ logs \ R$ to TOC via maturity showing the possible upper and lower limit of LOM calibration *(Passey et al., 2010)*. **B.** TOC to S_2 via maturity diagram for type I and II (oil-prone) kerogen. **C.** TOC to S_2 via maturity diagram for type III (gas prone) kerogen *(Passey et al., 1990)*.

Base-lining the transit-time and resistivity curves in non-source, clay-rich rocks implies that the base-lined interval is essentially "zero TOC"; in fact, this interval may have approximately 0.5-0.8 weight percent (global shale average TOC). Because of this background TOC, in practice 0.8 wt.% is added to the TOC calculated by the equation for all intervals in which positive delta log R separation occurs, regardless of the magnitude of the delta log R separation *(Passey et al., 1990)*.

A $\Delta \log R$ separation occurs in both organic-rich source rocks and hydrocarbon-bearing reservoir intervals; thus, a gamma-ray or SP cutoff can be used to eliminate the reservoir intervals when a TOC profile is calculated *(Passey et al., 1990)*.

According to *Passey et al., (1990),* if a transit- time curve is not available, the density or neutron curve can be substituted using empirically derived equations:

$$\Delta\, logR_{Neu} = log_{10}\left(\frac{R}{R_{baseline}}\right) + 4.0 * (\phi N - \phi N_{baseline}) \quad (1.6c)$$

And

$$\Delta\, logR_{Den} = log_{10}\left(\frac{R}{R_{baseline}}\right) - 2.50 * (\rho_b - \rho_{baseline}) \quad (1.6d)$$

Where $\Delta\, logR_{Neu}$ and $\Delta\, logR_{Den}$ are the separation based on the neutron and the density logs respectively, ϕN is the neutron porosity reading from the well log in the interval of interest, $\phi N_{baseline}$ is the neutron porosity baseline value (scale in fractional porosity) and $\rho_b\ and\ \rho_{baseline}$ are the density values for the source rock and the baseline intervals, respectively.

Passey et al., (1990), also observed that no significant dependence on organic matter type were shown when predicting TOC from $\Delta \log R$ in clay rich rocks where TOC values are less than 15 wt.%, moreover the technique worked well in both oil-prone and gas-prone source rock. However thin organic rocks (less than 0.5 m thick) can be detected but the calculated TOC values are likely to be lower than measure values.

Figure 16 show schematically possible interpretations of $\Delta \log R$ separation in which organic-rich intervals are represented by zones C, F, H and I. The $\Delta \log R$ separation in the immature zone C is due entirely from the sonic curve response, whereas, in the mature zone F, the $\Delta \log R$ separation has both sonic and resistivity curve components. In the coaly sections (zones H and I), the gamma ray intensity is low. Where coal or coaly sediments are present, they are likely to be thinner and more interbedded than marine organic rich intervals. Typical responses in hydrocarbon reservoirs show a $\Delta \log R$ separation primarily because and increased in resistivity due to the non-conductive oil or gas (zones B, D and G). Hydrocarbon/water contacts often are readily apparent (zone G).

Intervals of low porosity have high resistivities because of an absence of electrically conducting fluid, as shown in zone K. These intervals can be recognized by relatively short transit time (generally less than 180 µsec/m or 55 µsec/ft). Intervals of non-source or non-reservoir generally have porosity and resistivity curves overlying (i.e., baselined) as shown in zones A, E, and J.

Anomalous $\Delta \log R$ separation not associated with source intervals generally can be attribute to hydrocarbon reservoirs, pore borehole conditions, un-compacted sediments, low porosity (tight) intervals, volcanics rocks or evaporites.

Passey et al., (1990), conclude that for rocks with low thermal maturity, the relationship between $\Delta \log R$ and TOC exist primarily because of the porosity curve component. As maturity increases, the resistivity curve component becomes increasingly important. For maturities below LOM 6 or above LOM 12, the relationship generally is applied, but the calibration is not rigorous at these extremes.

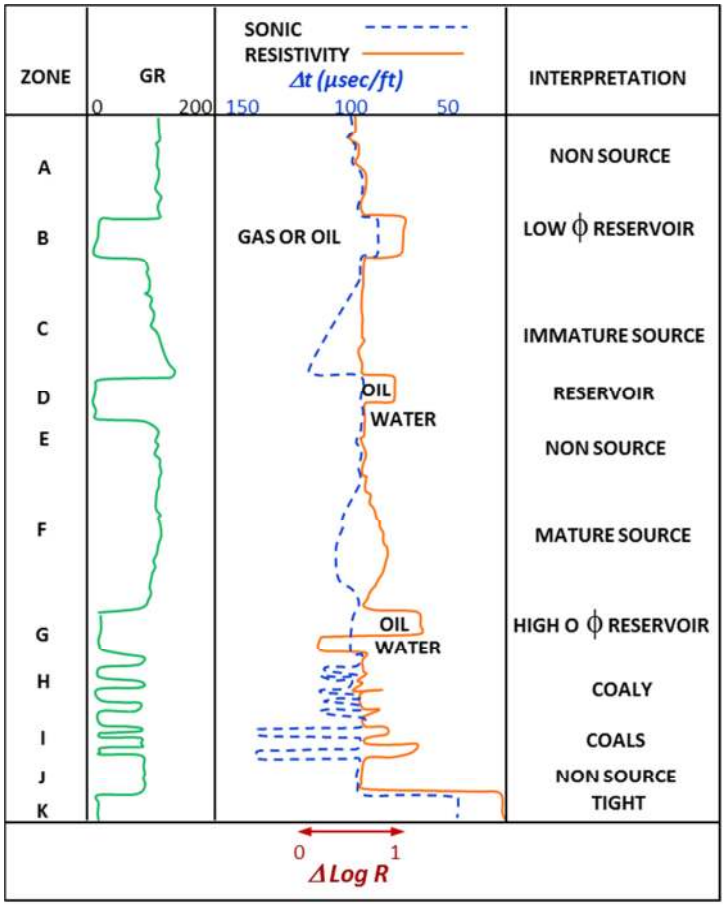

Fig. 16: Schematic guide for the interpretation of a wide variety of features observed on Δ log R overlays *(Passey et al., 1990)*.

This method seems to be useful qualitatively but quantitatively cumbersome and doubtful. Moreover with just the sonic log, it is impossible to separated low sonic values due to organic matter and low sonic values due porosity changes (such as overpressure). This is a frequent dilemma in much log interpretation: separating the compositional effects from the textural effects (*Rider, 2000)*. However, it is a widely use method and most of the computing tools are based on this technique, because of the fact that it claims to be able to quantify TOC content.

2. Methodology

2.1 Δ Log R Technique

All the tools that were tested in this study used $\Delta \ Log \ R$ technique develop by *Passey et al.*, (*1990*) explain previously. Basically three well logs are key to evaluate this technique:

Gamma Ray: to recognize shale intervals and to define a cutoff value that allow to calculated values of TOC only in the shale intervals. High gamma ray values were also used as early indicator or organic matter in the case of marine shales.

Transit time (Sonic): is the porosity curve that responds to the presence of low-density, low-velocity kerogen.

Resistivity: (preferably deep resistivity) responds to the formation fluid and is an indicator of level of maturity of rich source rocks intervals.

The caliper log is also an important curve since it allows determining the presence of cave in the hole that can affect the logs respond and as a consequence the TOC calculations. As it was mention previously, Bulk Density or Neutron Porosity can also be used as a porosity curves, but transit time is more accurate due its sensitivity to rock texture.

After the validation of the well logs in terms of cave problems and deep correction, the procedure was as follows:

1. Logs Normalization: In order to calculate the $\Delta \log R$ separation both logs (transit time and resistivity curve were normalize to a relative scaling to 50 µsec/ft of transit time was equivalent to 1 logarithmic cycle on the resistivity log (***Fig. 17***).

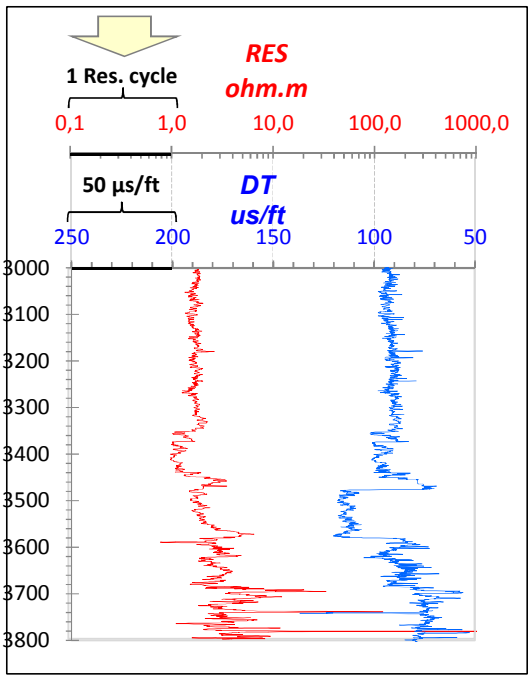

Fig. 17: Example of Log normalization, note the sonic scale adjusted to 50 µ/ft equivalents to 1 resistivity cycle.

2. A non-source shale interval is located (in the stratigraphic interval being considered) and the two curves are overlain and baselined in the non-source rock interval (***Fig. 18***).

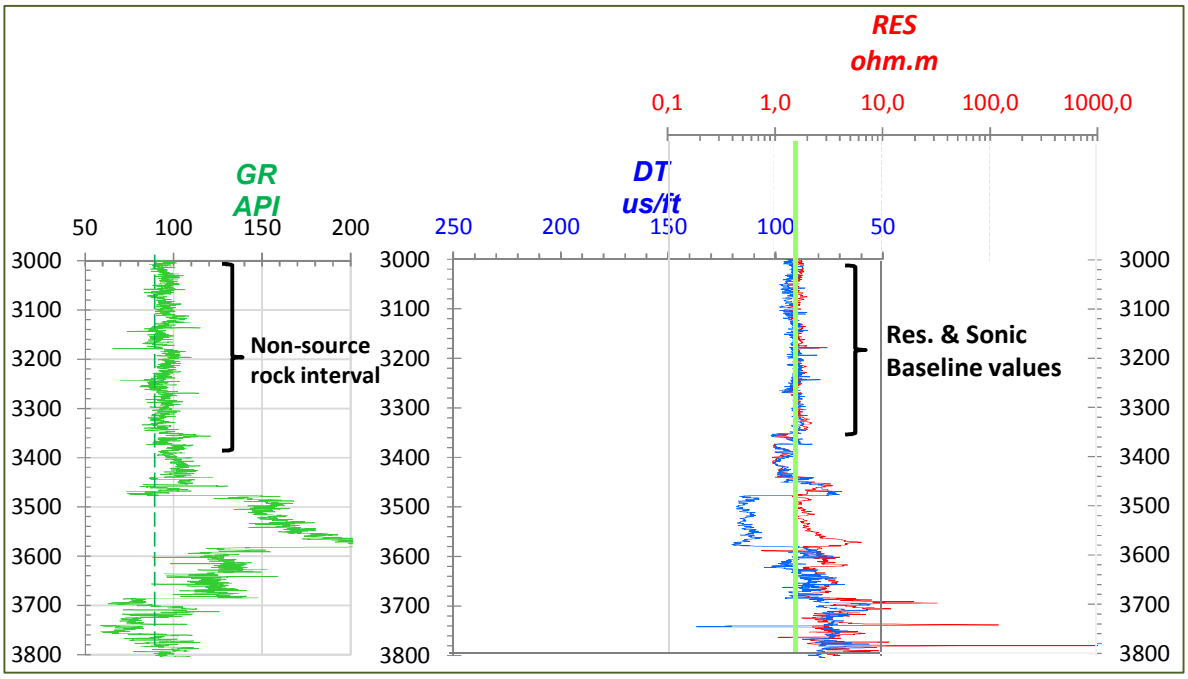

Fig. 18: Illustration of sonic and resistivity logs overlain in a non-source rock to define the baseline (in light green) for $\Delta \log R$ calculations. Note the dash green line indicating the gamma ray cutoff.

3. Organic rich shale intervals were recognized by the separation of the two curves (***Fig. 19***), designated as $\Delta \log R$ separation which is given by the equation ($1.6a$):

$$\Delta \log R = \log_{10}(R/R_{baseline}) + 0.02 * (\Delta t - \Delta t_{baseline}) \quad (1.6a)$$

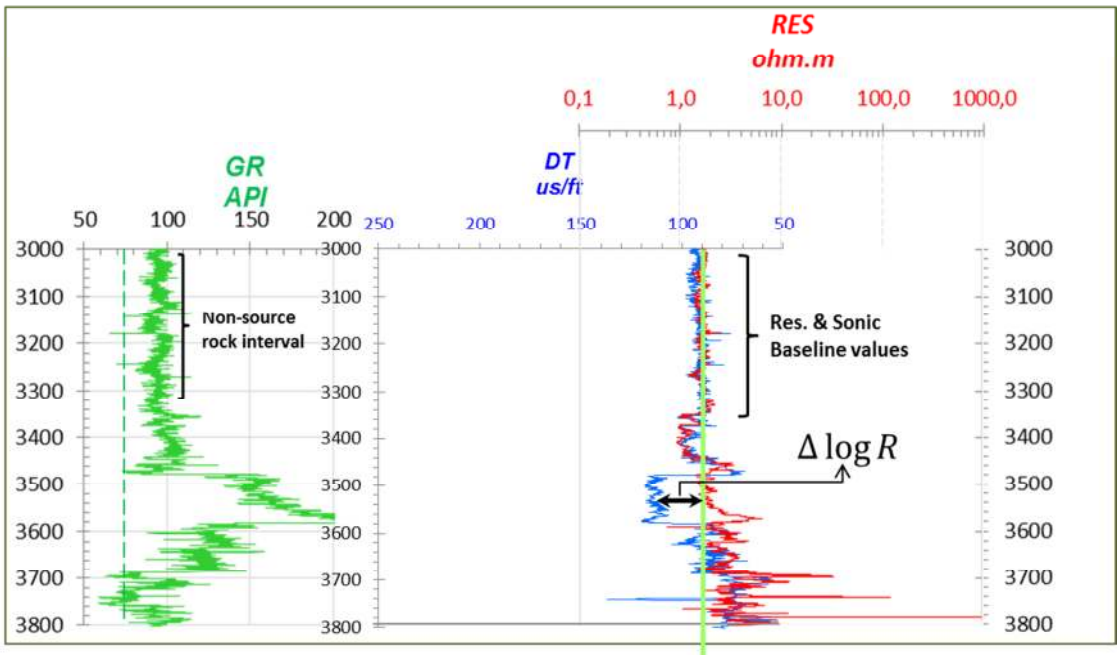

Fig. 19: Sonic and resistivity logs separation in a source rock interval or $\Delta \log R$ separation.

4. $\Delta \log R$ separation is linearly related to TOC and is a function of maturity (***Fig. 15A***). Using the equation $(1.6b)$, values of TOC were estimated:

$$TOC = (\Delta \log R) * 10^{(2.297 - 0.1688 * LOM)} \qquad (1.6b)$$

The level of organic metamorphism (LOM) was determined using values of vitrinite reflectance (%Ro) according to the scale correlation documented by *Hood et al.* (*1975*) (***Fig. 20).*** Vitrinite values are obtained from Rock Eval determination in rock samples (cuttings, core plugs, etc).

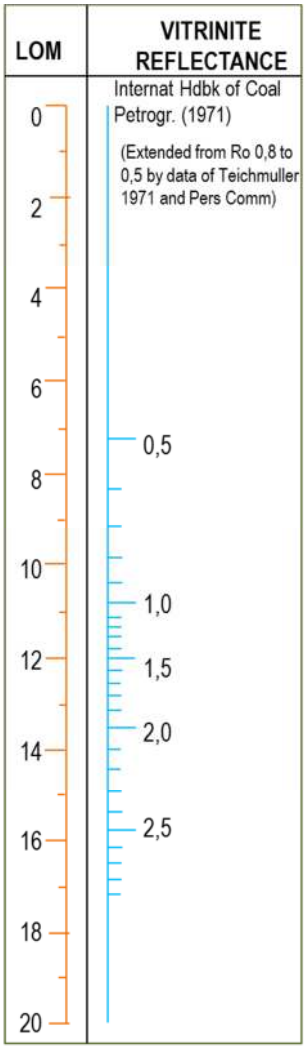

Fig. 20: Correlation scale between level of organic metamorphism (LOM) and vitrinite reflectance (%Ro) (Modify from ***Hood et al.***, ***1975***)

5. Finally, TOC values measured in conventional core (COCH), sidewall (SWC) and ditch cutting (DC, DCS) were used to calibrate the results obtained by this technique.

2.2 Tools

Three main tools were used to evaluate this technique in order to compared accuracy, efficiency and possible limitations in the TOC calculations. Base on analysis and results a new technique base in Passey equation is proposed.

2.2.1 BasinMod 1D (Platte River Associates, Inc.)

BasinMod 1D (2110) is a tool used for basin modeling to evaluated hydrocarbon potential (generation and expulsion) and petroleum system analysis. It has a module called *TOC From Logs* that allows to calculate present day TOC using well logs according to the Δ Log R method published by *Passey, et. al. (1990).*

To performed a TOC calculation using this tool it was necessary that the well were simulated previously, meaning that geohistory/burial history, thermal history, maturation, and timing of hydrocarbon generation and expulsion should be settled and calculated in advance (***Fig. 21***). It means that values such as maturity (%Ro) and TOC from core were already loaded.

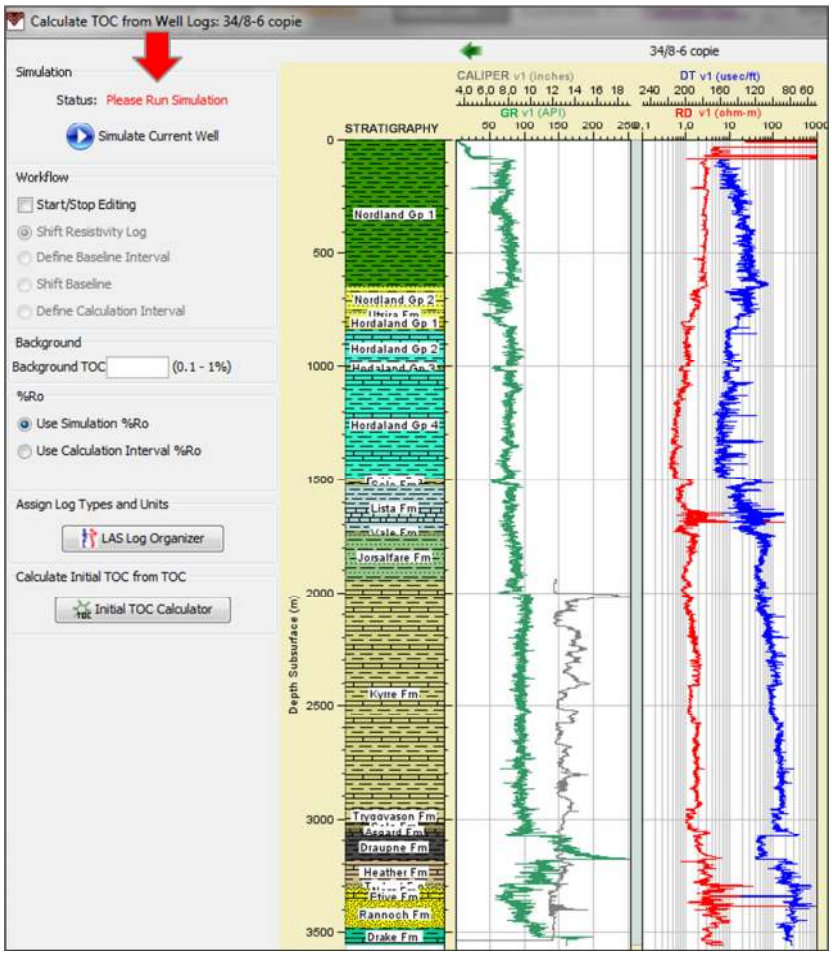

Fig. 21: Illustration of the BasinMod tool "**TOC From Well Logs**" used to calculate organic rich shales. The well should be simulated to activate the tool. It displays the current stratigraphy in the well and the relevant logs to perform the calculation.

After the well was simulated and the relevant logs were loaded the procedure was as follows:

1. After activation of the workflow (Start/Stop Editing) it allowed shifting the Resistivity curve in such a way that both curve overlie in the interval that was considered as a non-source rock shale (***Fig. 22***). It is necessary to have a previous knowledge of possible source and non-source intervals before decide the appropriated curve shifting.

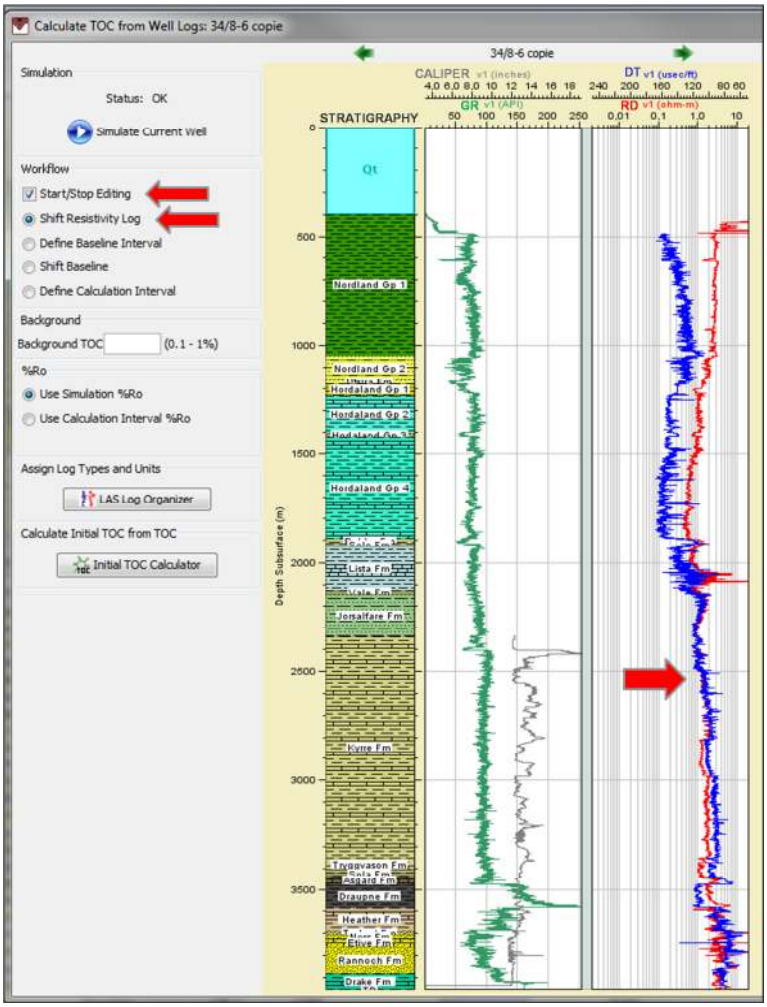

Fig. 22: Illustration of shifting curve procedure in a non-source interval (indicated by the red arrow).

2. The curve shifting was follow by the definition of the interval in which the baselines were allocated. Immediately after this selection the calculation was accomplished and the result values of TOC were displayed in a new track (***Fig. 23***). LOM values were calculated from measured values of vitrinite used in the model (%Ro), it was not possible to know the exact values of LOM apply by the tool.
3. As is illustrated in ***Fig. 24*** the baseline was adjusted until obtain a TOC curve that best fit with measured values (TOC values measure in core, for example).
4. Since baselines should be defined near the interval in which the possible source rock will be evaluated (one baseline for each interval to be evaluated) it was possible to select a calculation interval for TOC as is shown in ***Fig. 25***.

5. To obtain values from the TOC curve calculated, a manual selection, point by point was required, it is not possible to obtain all the values from the curve automatically using this tool (***Fig. 26***). The selected points were saved in a table format but it was not possible to save the curve neither the baseline values using this tool. To updated or evaluated new intervals it is necessary re-start the whole procedure.

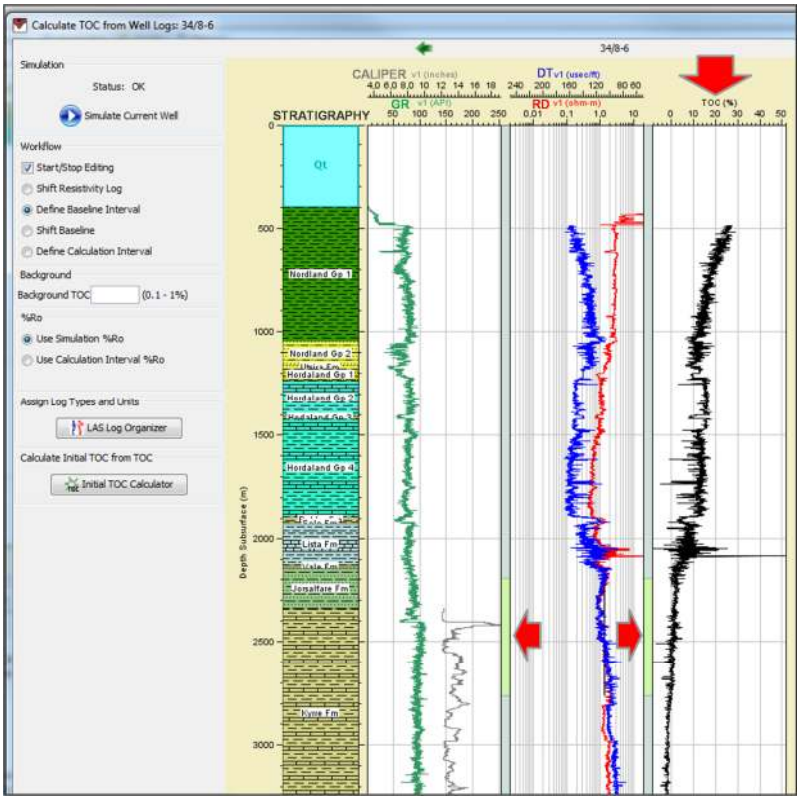

Fig. 23: Definition of reference interval of non-source rock (indicated by red arrows and light green section) and the corresponding results of TOC calculations (third track, to the right, black curve)

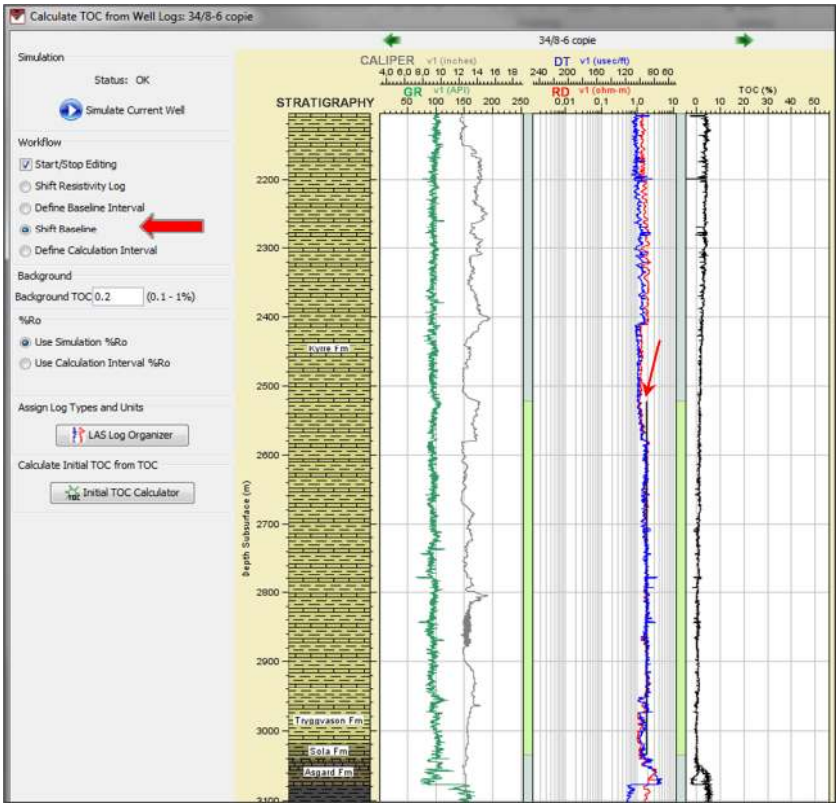

Fig. 24: The baseline (indicated by and small red arrow in track 2) can be adjusted and TOC curve will be recalculated: Note that a background TOC can be included.

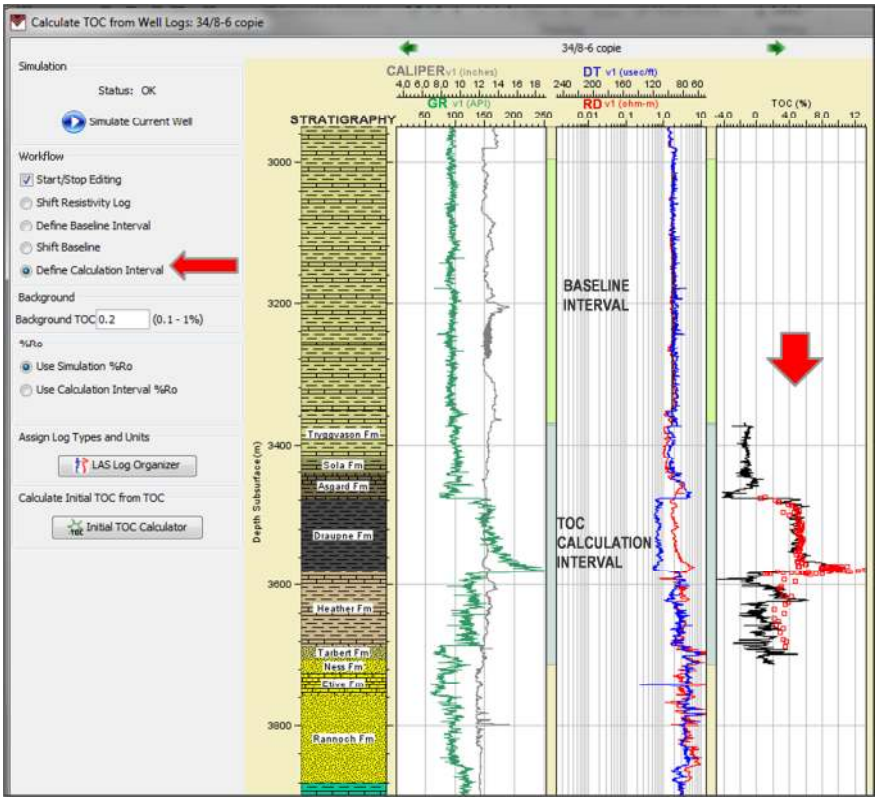

Fig. 25: Example of baseline interval and TOC calculation interval (indicated by the red arrow). The black curve corresponds to TOC calculated from logs and red points are values of TOC measure in core.

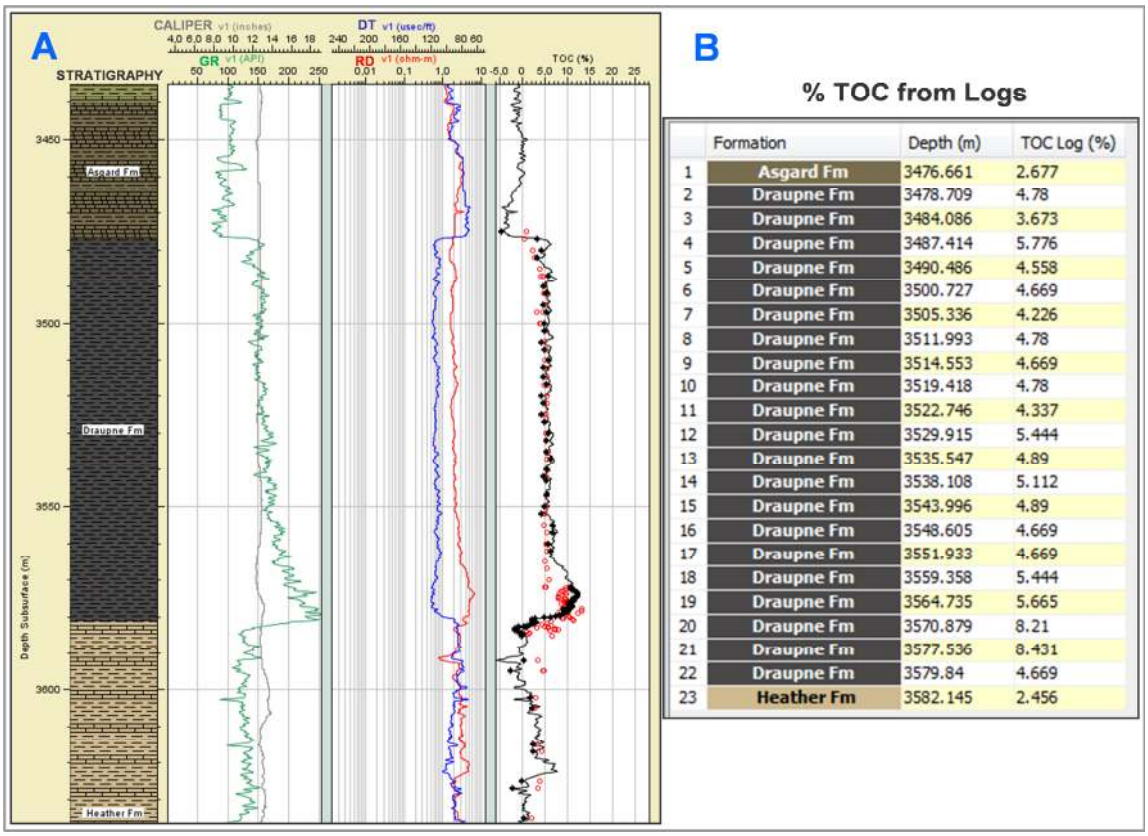

	Formation	Depth (m)	TOC Log (%)
1	Asgard Fm	3476.661	2.677
2	Draupne Fm	3478.709	4.78
3	Draupne Fm	3484.086	3.673
4	Draupne Fm	3487.414	5.776
5	Draupne Fm	3490.486	4.558
6	Draupne Fm	3500.727	4.669
7	Draupne Fm	3505.336	4.226
8	Draupne Fm	3511.993	4.78
9	Draupne Fm	3514.553	4.669
10	Draupne Fm	3519.418	4.78
11	Draupne Fm	3522.746	4.337
12	Draupne Fm	3529.915	5.444
13	Draupne Fm	3535.547	4.89
14	Draupne Fm	3538.108	5.112
15	Draupne Fm	3543.996	4.89
16	Draupne Fm	3548.605	4.669
17	Draupne Fm	3551.933	4.669
18	Draupne Fm	3559.358	5.444
19	Draupne Fm	3564.735	5.665
20	Draupne Fm	3570.879	8.21
21	Draupne Fm	3577.536	8.431
22	Draupne Fm	3579.84	4.669
23	Heather Fm	3582.145	2.456

Fig. 26: Extraction of values of TOC calculated from well logs. **A.** In track 3 to the right the TOC curve calculated from logs, black points are manual values selected from the curve, red points are TOC values measure in core for calibration. **B.** Values selected from the TOC curve calculated saved in a table format.

2.2.2 Permedia MPath version 4.18.1 (Landmark Software and Services, Halliburton).

Permedia MPath is a integrate petroleum systems modeling tool with different modules. *Permedia Petroleum Systems 1D* includes specialized modules for evaluating well and wireline data using the *Well Viewer* tool. The Delta log R module in *Well Viewer* calculates present-day TOC from a new variable – dlogr – and a level of maturity (LOM) based on *Passey, et. al.(1990).*

A difference of *BasinMod*, the module does not require of previous well simulation, the well data was analysed by an independent procedure as follows:

1. The log data was visualized directly in LAS format from a settled project directory. Values of TOC from core and LOM were loaded as tables to be displayed and used in the calculations in the well viewer as it is illustrated in ***Fig. 27***.
2. Initially the Delta Log R Calculator allows to define several parameters that are relevant to obtain more accurate results (***Fig. 28***), such as:
    - Gamma ray cutoff: all values bellow the cutoff will be excluded of the TOC calculations. It allows calculating TOC values only in shales.
    - Porosity Log Baseline: after choosing the porosity log it is possible to enter the value of the baseline.
    - Resistivity Log Baseline: it is also possible to adjust the value of the resistivity log separately from the porosity log.
    - LOM: values can be introduced directly into the calculation using a trace built from a data table.

    After those values were defined, TOC values were calculated and displayed in new tracks in the well viewer (***Fig. 29***).

3. As is shown in ***Fig. 29***, if values do not calibrated or if some adjustments were desired it was possible to change baseline and cutoff values and recalculate the TOC curve. Moreover it was possible to assign different baseline values for each interval defined by adding horizontal breaks throughout the well, as is illustrated in ***Fig. 30***.
4. The TOC curve from logs were able to be saved as a table format and the tool also allows to save all parameters and results by well.

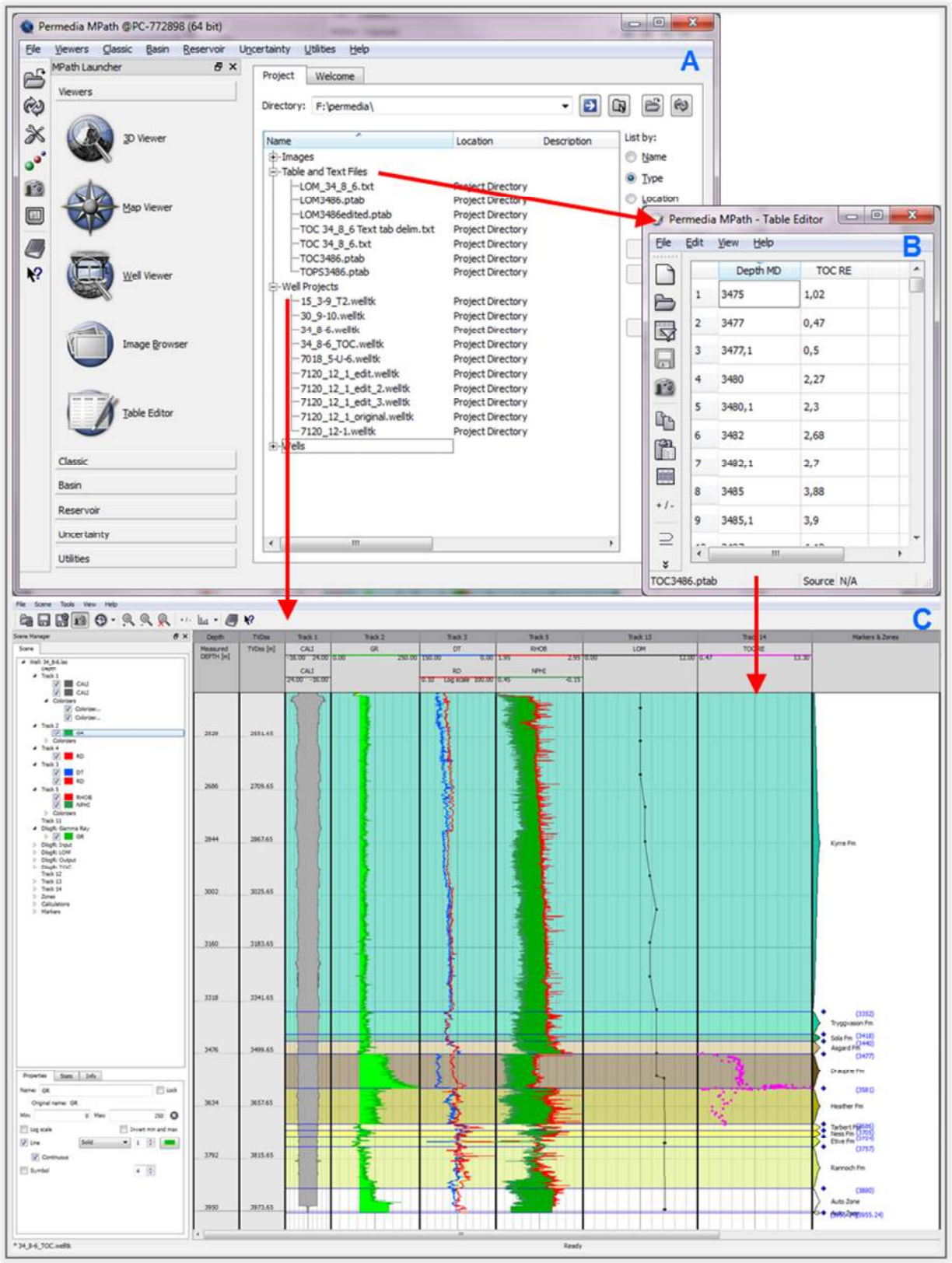

Fig. 27: Loading data into Permedia MPath to perform TOC calculations. **A.** Main window showing the project directory and the list of tables and well log **B.** Table editor for discrete values (LOM, %TOC from core, etc.) **C.** Well viewer displaying well logs and data from tables to be used in the TOC from logs calculation.

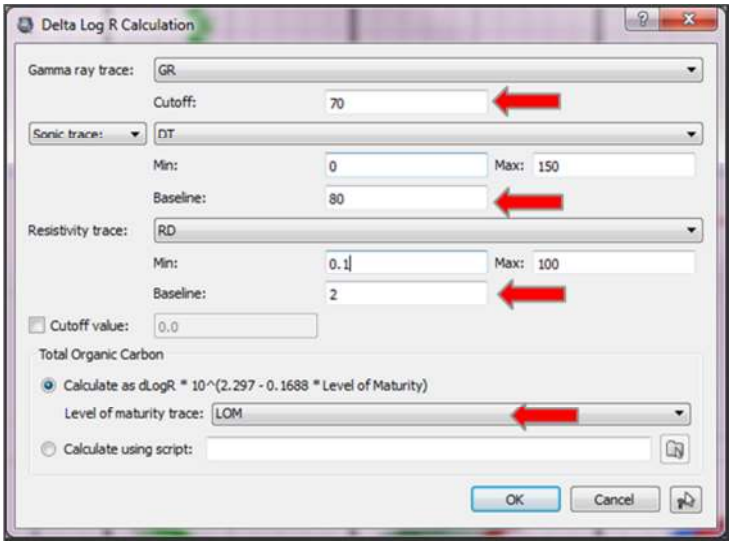

Fig. 28: Main window of Delta Log R calculator showing the possible parameters that can be defined to perform the TOC calculator from logs. Red arrows indicated important parameters describe in the text above.

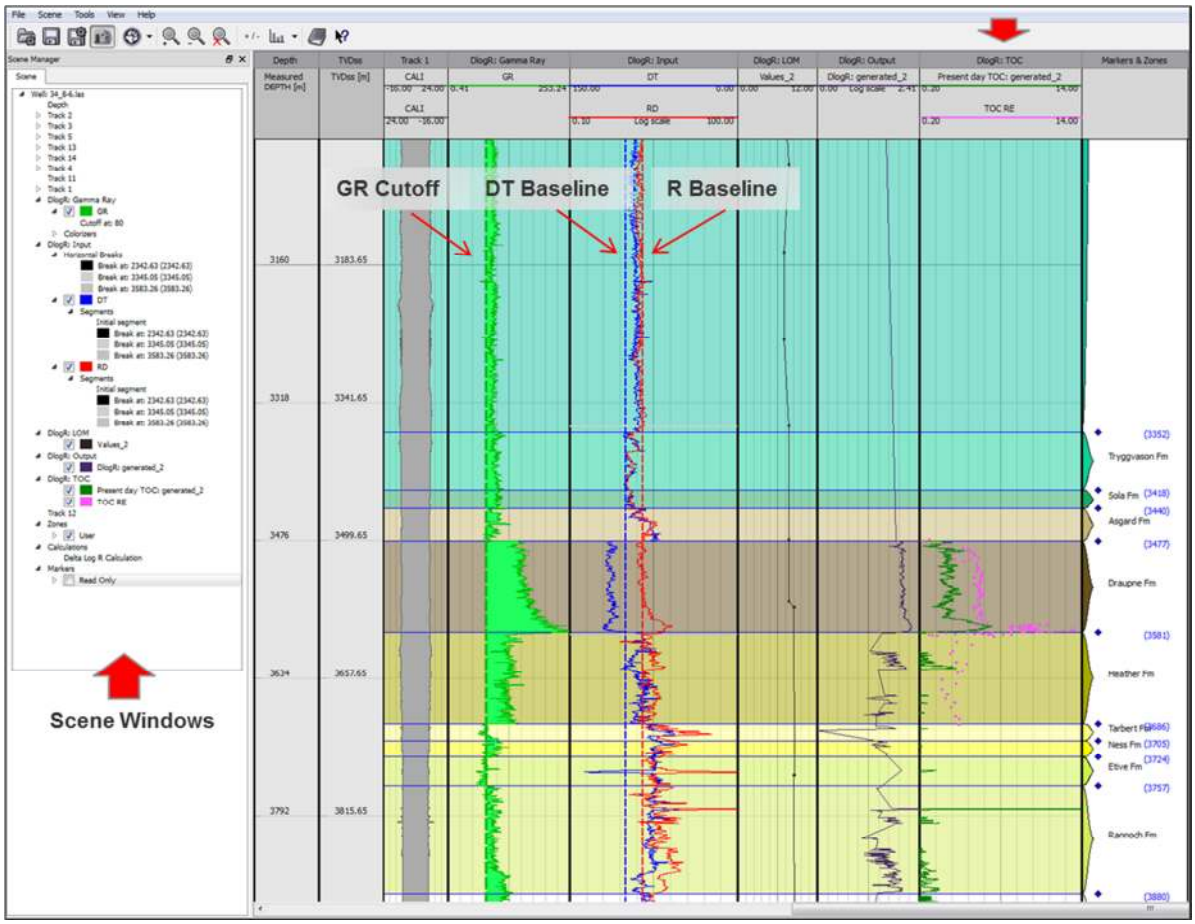

Fig. 29: Well viewer displaying the input data (logs, cutoff and baselines) and TOC calculation results (Delta log R and TOC curve). In Track 8 (from left to right, small red arrow), the green curve represent the TOC calculated from logs, the pink points are the TOC values measured in core for calibration. In

this example the TOC curve does not fit the measured values and some adjustments have to be made. Modification can be done using In the Scene window to the left, for each input parameter.

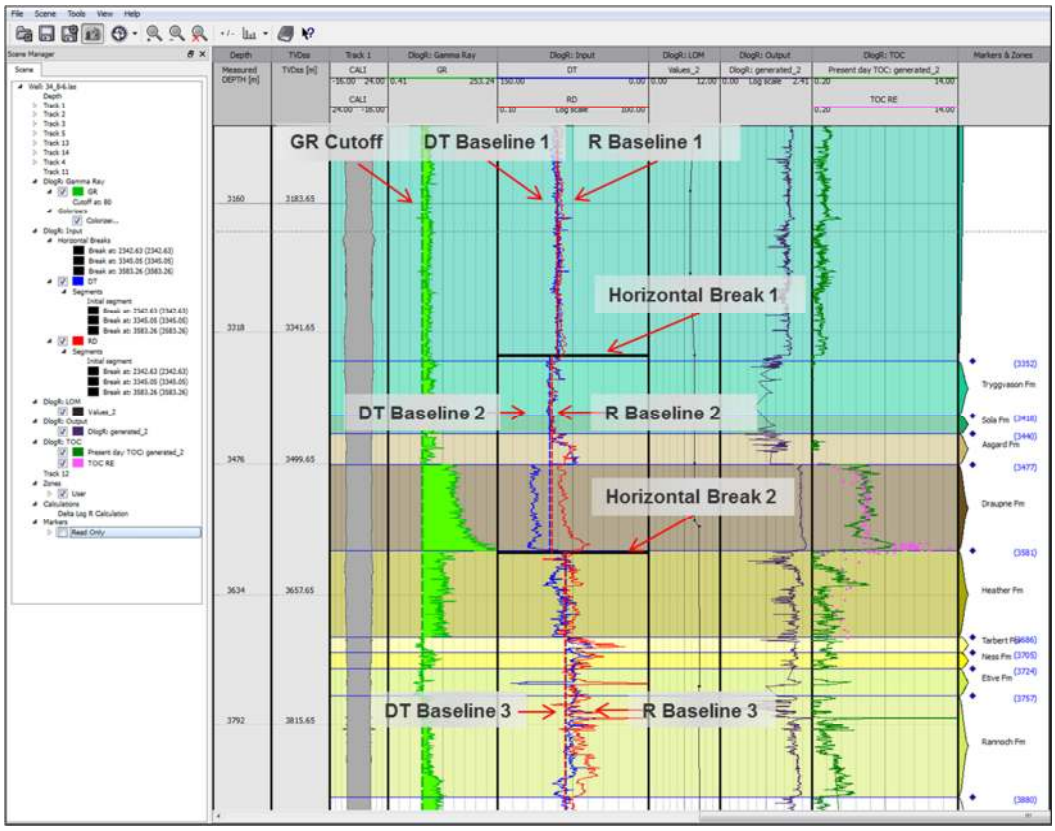

Fig. 30: Example of adjustment the TOC curve to measure data using horizontal breaks to define logs baselines by intervals. Note the improvement of the TOC curve fitting the calibration data compared with the example shown in ***Fig 29***.

2.2.3 In-house spreadsheet solution (Microsoft Excel, Microsoft Office Professional Plus 2010)

Norsk Hydro created an in-house Spreadsheet built in *Microsoft Excel* to calculated TOC from well logs base also in *Passey et. al. (1990)* technique. In this study this spreadsheet was used as a first attempt to test the Passey method because of the flexibility in the manipulation of the data which implied a complete manual procedure that allowed a deeply evaluation of the methodology and to test new insights that were not possible in the previous tool described.

This tool consist of five Spreadsheets linked to each other, consequently as soon as the data is loaded the calculation are performance automatically using long and sophisticated equations. Basically the procedure in this case can be divided in three main points:

→ *Input Data:* the logs, maturity and TOC from Rock Eval data is storage in three main spreadsheets in text format, in special labeled columns (***Fig. 31***).

→ *Calculations:* After the input data is loaded, the intervals to be evaluated should be defined, follow by the GR cutoff, baselines and LOM for each interval, the last one is calculated from vitrinite reflectance (%Ro) average by interval, given a suggested LOM that can be modified.

The values are entering manually and the delta log R and TOC curve are calculated from the logs, for each depth in the well in a fourth spreadsheet (***Fig. 32***).

→ *Output:* automatically all logs and calculated curve are displayed in specials plots in two last spreadsheet. The new TOC curve from logs is plotted against TOC values from Rock Eval to calibration purpose (***Fig. 33***).

The Spreadsheet was built is such a way that computations can be performed from different porosity curves and intervals. Intervals, baselines, cutoff and LOM values can be modify freely and results are visualized immediately allowing testing the data very fast and easy.

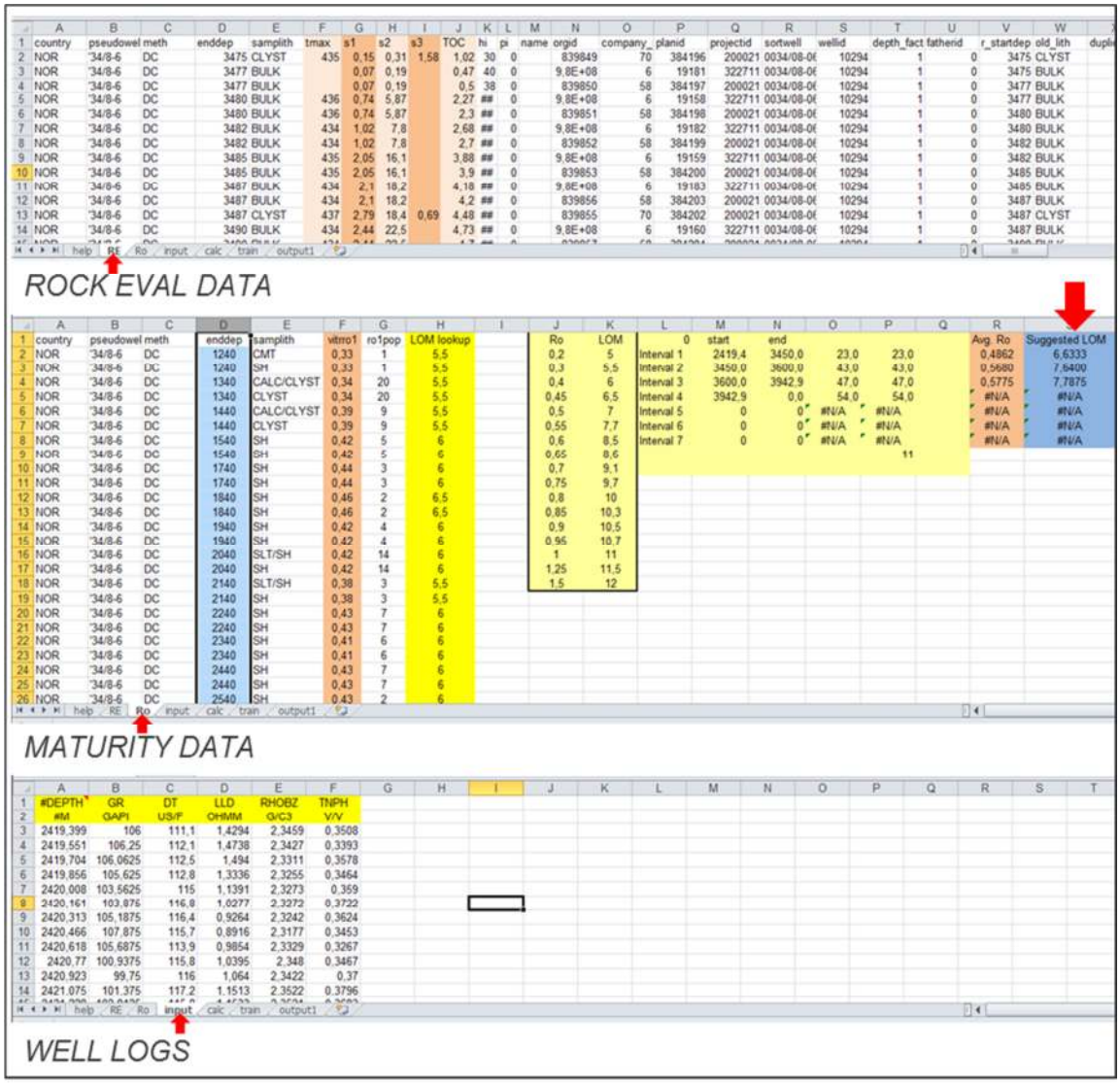

Fig. 31: Input data in the Spreadsheet tool developed by Norsk Hydro. Three input spreadsheet: RE, for Rock Eval data measure in core and cuttings; Ro, for maturity data (vitrinate reflectance %Ro) for LOM estimations and Input for well log data.

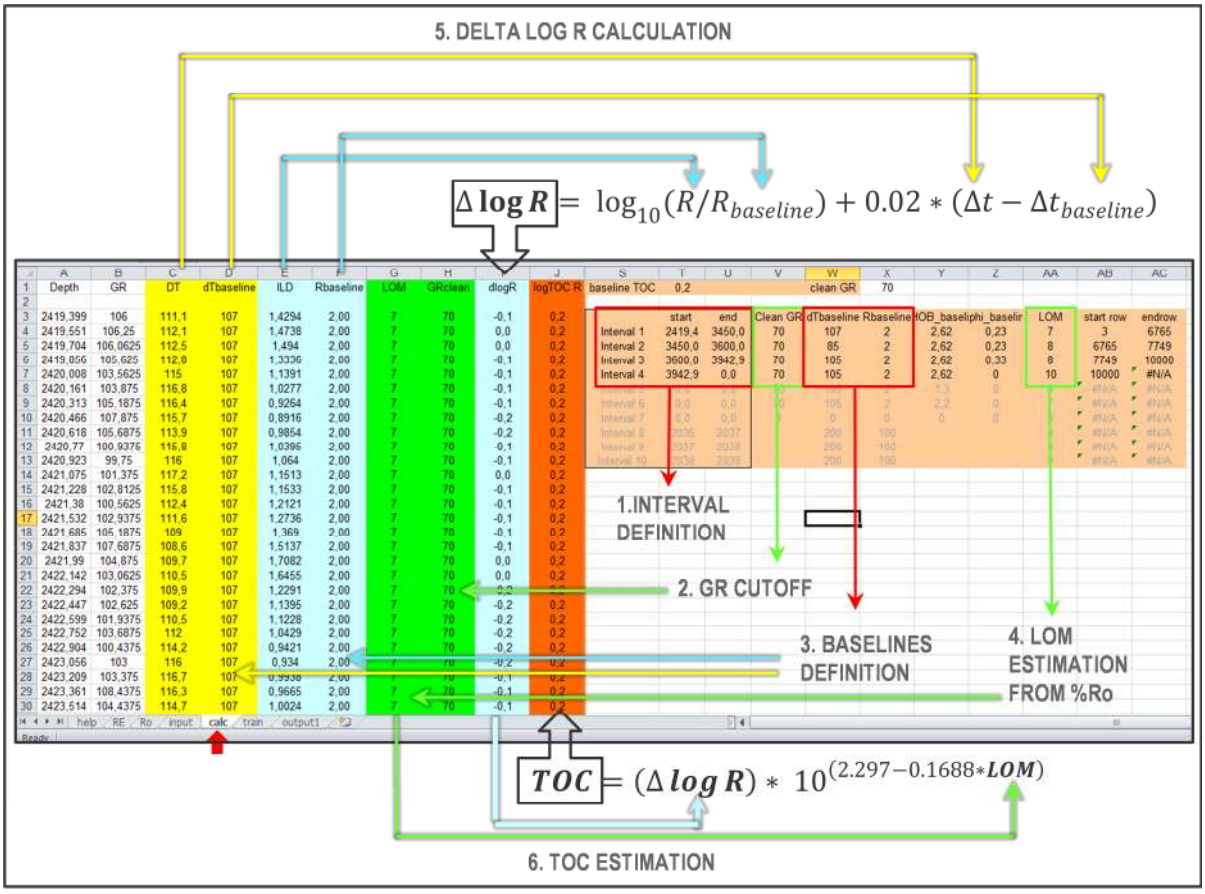

Fig. 32: Calculation *Norsk Hydro* Spreadsheet showing the workflow of TOC estimation (steps in uppercase bold letters). After intervals (Step 1), Gamma Ray cutoff (Step 2), baselines (Step 3) and LOM values (Step 4) are defined the delta log R separation is calculated automatically (Step 5) and used in the TOC computation (Step 6).

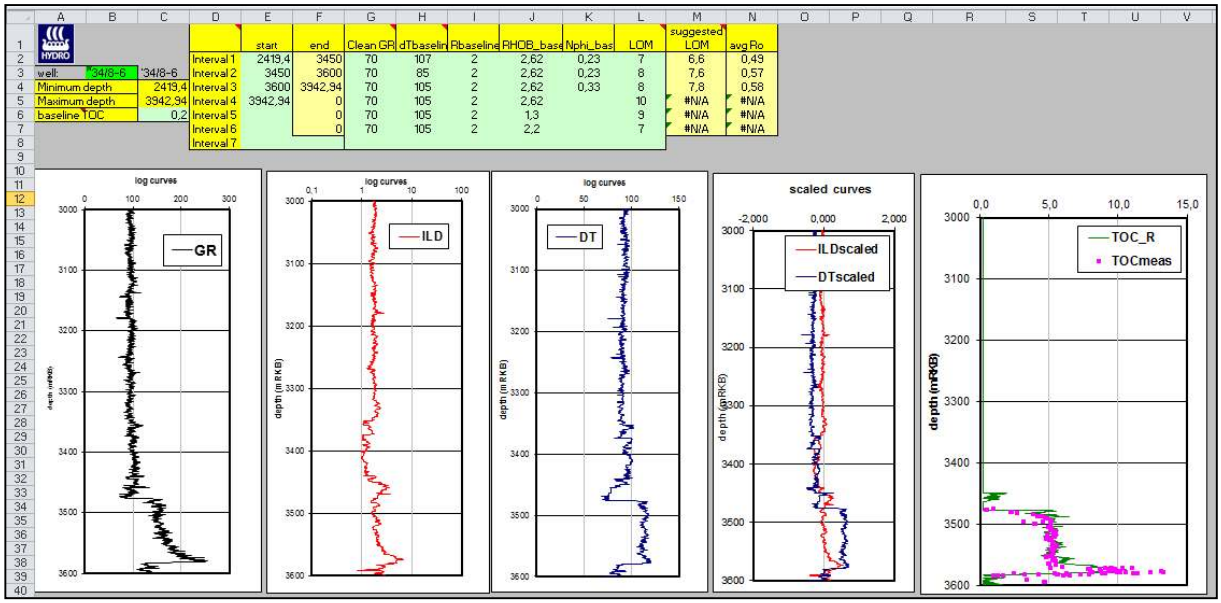

Fig. 33: Output data in the Spreadsheet tool developed by Norsk Hydro, showing a summary table of intervals and parameters (upper left) and plots with relevant logs and TOC curve and calibration data (TOC meas).

2.2.4 New Trend Technique (Microsoft Excel, Microsoft Office Professional Plus 2010)

After evaluating the previous tools, a new approach was implemented based in the use of trends of log response as a baselines instead a constant values by interval. The use of this technique was only possible in a Spreadsheet tool since the other tools that have been evaluated were limited to constants baselines.

The base and theoretical reason of this approach is explained in detail in the Results and Discussions section. Basically the baseline trends were defined using the values of the logs (transit time and resistivity) in non-source shales. To do that first non-source shales were filtering using Gamma Ray cut offs: a lower cutoff to avoid sandstones and an upper cutoff to avoid high values of Gamma Ray related to a rich organic interval. After this filtering, the same depths in which the Gamma Ray indicated non-source shales were used to filter the transit time curve and the resistivity curve, in other words the Gamma Ray was used as an aid to obtain the values of Transit time and resistivity in non-source rocks.

Using this results it was possible to create a trend line of non-source shale for Resistivity and Transit time which were used to calculated trend baselines (***Fig. 34***). Using the respective equation of each trend line it was possible to calculate the baseline for each value in the log, making it more accurate in terms of variation of logs response with depth. Using the baselines values the TOC from logs was calculated also for each value of the log with its own baseline and comparing with calibration data. Those trends act as non-source rocks predictors helping to recognize possible organic rich intervals using *Passey, et al. (1990)* equation.

The calculation of the baseline were done in a separated spreadsheet and the TOC computations were estimated using the *Norsk Hydro Spreadsheet* with some variations in the formulas and links to make possible the use of trend lines instead of constant baselines.

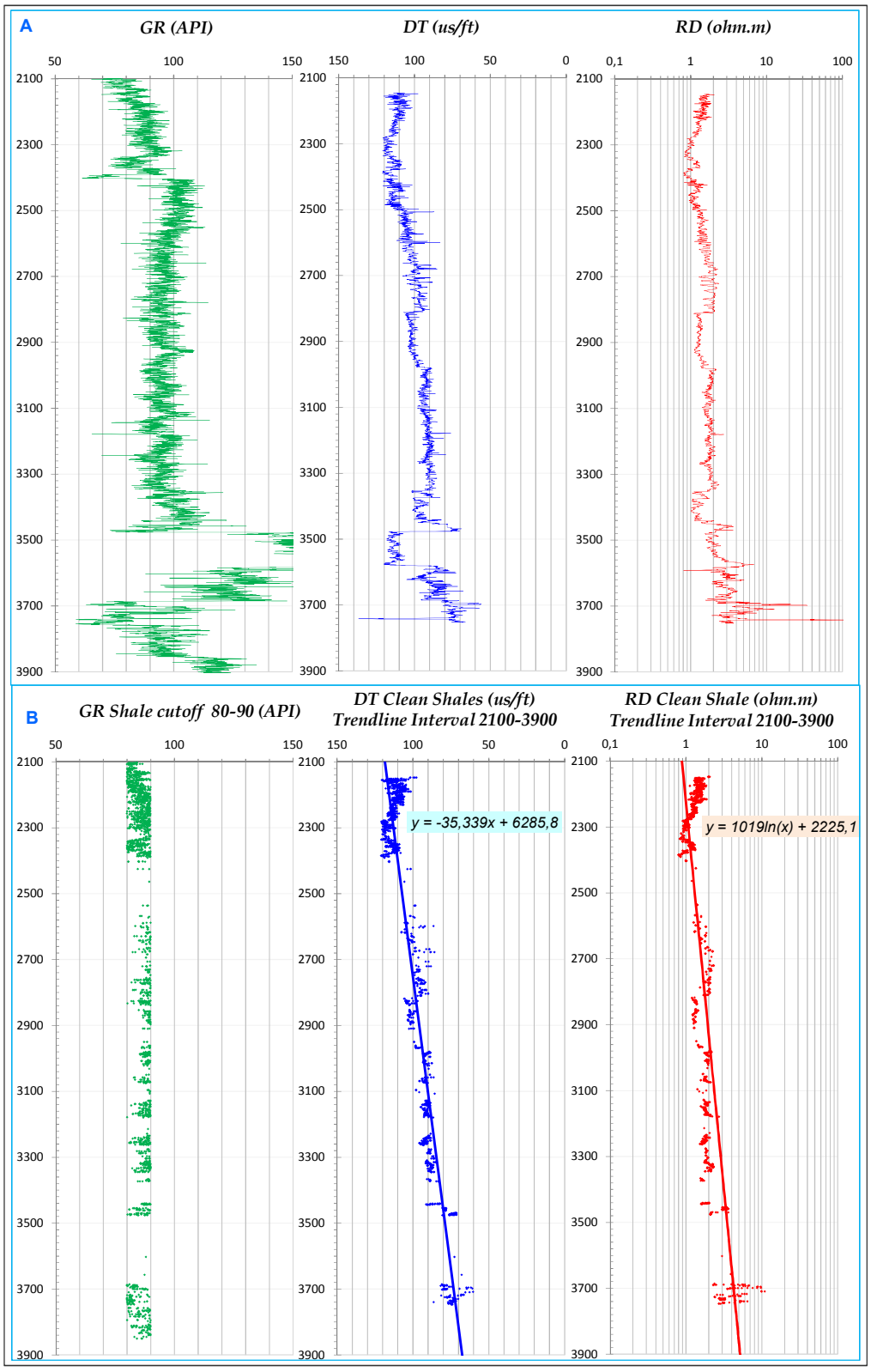

Fig. 34: Example of *Trend Technique* for baselines calculation. **A.** Original Logs: Gamma Ray (GR), Transit time (DT) and Resistivity (RD). **B.** Gamma Ray filtered with a lower (80 API) and upper cutoff (90 API) for non-source shales. Transit time and Resistivity logs showing the values only in shale intervals according to the Gamma Ray cutoff and its respective trend lines (DT in Blue and RD in red) and equations used as baselines in TOC calculation using delta log R method (*Passey et. al.,1990*).

2.3 Statistical Analysis

In order to describe and determine the grade of accuracy of the values of TOC obtain by the Trend Baseline Technique against the TOC values measured in rock, an exploratory data analysis was carried out. Descriptive statistic of both set of data was used to compare using boxplots. Quantiles were also used to study the grade of similarity between both distributions using quantile-quantile plots (Q-Q), basically to compare distributions.

The linear correlation between both set of data was also calculated to determine whether there was a relationship between two sets of variables using scatter plots. A useful visualization of prediction quality is to plot model data against measured results (***Fig. 35***). The data should fall on the diagonal in this plot. Deviations from the diagonal correspond to measurement noise or natural variability, but should not be systematic.

To measure the strength (linear dependence) and the direction of a linear relationship between the two variables the linear correlation coefficient (r) or Pearson's product-moment correlation coefficient was calculated. The correlation coefficient between two variables is defined as the covariance of the two variables divided by the product of their standard deviations:

$$r = \frac{\sum(x - \overline{x})(y - \overline{y})}{\sqrt{\sum(x - \overline{x})^2 \sum(y - \overline{y})^2}} \qquad (2.3a)$$

The value of a correlation coefficient can vary from minus one to plus one. A minus one indicates a perfect negative correlation, while a plus one indicates a perfect positive correlation. A correlation of zero means absence of a linear relationship between the two variables. When there is a negative correlation between two variables, as the value of one variable increases, the value of the other variable decreases, and vice versa.

The square of the correlation coefficient, r^2, is a useful value in linear regression. This value represents the fraction of the variation in one variable that may be explained by the other variable in other words it is a measure of how well a variable is likely to be predicted by the model. Given a data set with observed values x_i (TOC measured) with an associated modeled or predicted value y_i (TOC from log) and mean $\overline{x}$, the r^2 is given by:

$$r^2 = 1 - \frac{\sum(x_i - y_i)^2}{\sum(x_i - \overline{x})^2} \qquad (2.4b)$$

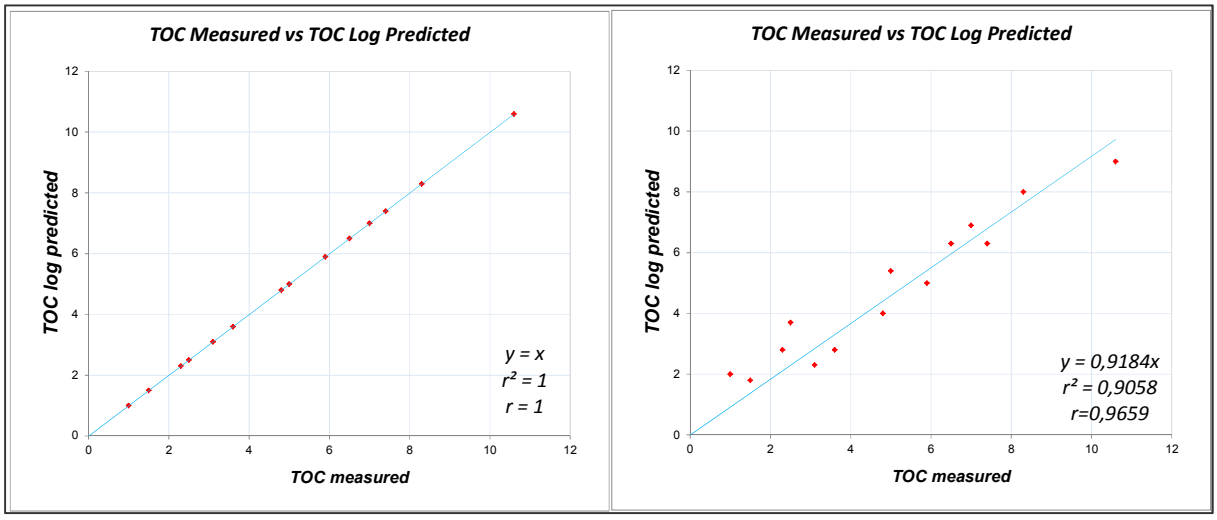

Fig. 35: Example of scatter plots showing linear correlation (blue line), correlation coefficient *r* and r^2. **A.** Ideal case of positive correlation where TOC values are predicted as expected**. B.** Good positive correlation indicated by *r* and r^2 close to 1, with some variability or noise.

The comparison of distributions of both sets of data was done using the frequencies distribution. The probability distribution function (PDF) and cumulative distribution function (CDF) helped graphically to assess the differences and similarities of the two population data.

A comparison of the absolute values of the difference between TOC from well logs (TOC ΔLogR) and TOC measured in rock (from Rock Eval or TOC RE) was done using the frequency distribution of the difference. It allows to evaluate the amount of values with short and large differences and possible reasons for this phenomenon. Additionally using these distributions helped to localize the large differences that were affecting the linear correlation.

2.3.1 Multiple Linear Regression (MLR)

With the purpose of knowing the relationship or the best predictor between the TOC values and the log response (GR, DT and R) a Multiple Linear Regression (MLR) was run. Multiple linear regression attempts to model the relationship between two or more explanatory variables and a response variable by fitting a linear equation to observed data.

A MLR model is an extension of the simple linear regression model for data with multiple predictor variables and one outcome ($x_{i1}, x_{i2}, \ldots, x_{ip-1}, y_i$) for i=1,2…,n units of observation (*Lynn E. Eberly, 2007*). It formalizes a simultaneous statistical relation between the single continuous outcome Y and the predictor variables X_k (K=1,2,…,p-1):

$$y_i = \beta_0 + \beta_1 x_{i1} + \beta_2 x_{i2} + \ldots + \beta_{p-1} x_{i,p-1} + \varepsilon_i \quad (2.3.1a)$$

$$\varepsilon_i \overset{indep}{\sim} N(0, \sigma^2)$$

Where β_0 represents the intercept (the mean of *Y* when all X_k=0), and each β_k represents a slope with respect to X_k (the magnitude of change in the mean of *Y* when X_k is larger by one unit and all other predictors are held constant) and ε_i is the model deviation.

In other words, the model is expressed as Dependent Variable = FIT + RESIDUAL, where the "FIT" term represents the expression $\beta_0 + \beta_1 x_{i1} + \beta_2 x_{i2} + \ldots + \beta_{p-1} x_{i,p-1}$. The "RESIDUAL" term represents the deviations of the observed values from their means, which are normally distributed with mean 0 and variance σ. The notation for the model deviations is ε_i.

The β_k are thus sometimes called partial regression coefficients. As for simple linear regression, this model can be equivalently written as:

$$y_i \overset{indep}{\sim} N\left(\beta_0 + \beta_1 x_{i1} + \beta_2 x_{i2} + \ldots + \beta_{p-1} x_{i,p-1} + \sigma^2\right)$$

The assumptions are thus the same as for simple linear regression:

- → The y_i are independent of each other.
- → The y_i each follows a normal distribution.
- → The mean of that distribution is a linear function of each x_{ik}.
- → The variance of that distribution is the same for all y_i (constant variance).

The general procedure for carrying out a regression analysis is as follows:

- → For each predictor, verify through a data plot that a linear relation is likely to be appropriated.
- → Estimate the linear relation model.
  Assess through diagnostics whether the model provides an appropriate fit to the data.
- → If so, use the model to draw inferences about the regression coefficients.
- → Reduce the model by removing non-significant predictors, if appropriate for the study goals.
- → Reassess through diagnostics whether the model provides an appropriate fit to the data.

There are several criteria to find a subset of potential independent variables *X's* that best predict a dependent variable *Y* (e.g., adjusted r2, likelihood ratio test, etc.) for model selection and many algorithms for including or excluding *X's* in the model (forward selection, backward elimination). In this study a Stepwise Regression was undertaken, which consists in a semi-automated process of building a model by successively adding or removing variables based on the F-statistics. Properly used, the stepwise regression puts more power and information than does the ordinary multiple regression, and it is especially useful for sifting through large numbers of potential independent variables and/or fine-tuning a model by poking variables in or out.

The stepwise option lets either begin with no variables in the model and proceed forward (adding one variable at a time), or start with all potential variables in the model and proceed backward (removing one variable at a time), the first one was used to select the variables in this work.

Statistica 6 (StatSoft Inc. 2001) was used to compute the Multiple Regression. At each step, the program performs the following calculations: for each variable currently in the model, it computes the t-statistic for its estimated coefficient, squares it, and reports this as its "F-to-remove" statistic; for each variable not in the model, it computes the t-statistic that its coefficient would have if it were

the next variable added, squares it, and reports this as its "F-to-enter" statistic. At the next step, the program automatically enters the variable with the highest F-to-enter statistic, or removes the variable with the lowest F-to-remove statistic, in accordance with certain control parameters specified.

3. Well Data

Two wells provide by Statoil ASA, were evaluated: the well NO 34/8-6 located in the North Sea specifically at the North of the Visund Field, and the well NO 7120/12-1 in the Barents Sea, in Troms I area, as it was mention in the Introduction Section (***Fig. 36***)

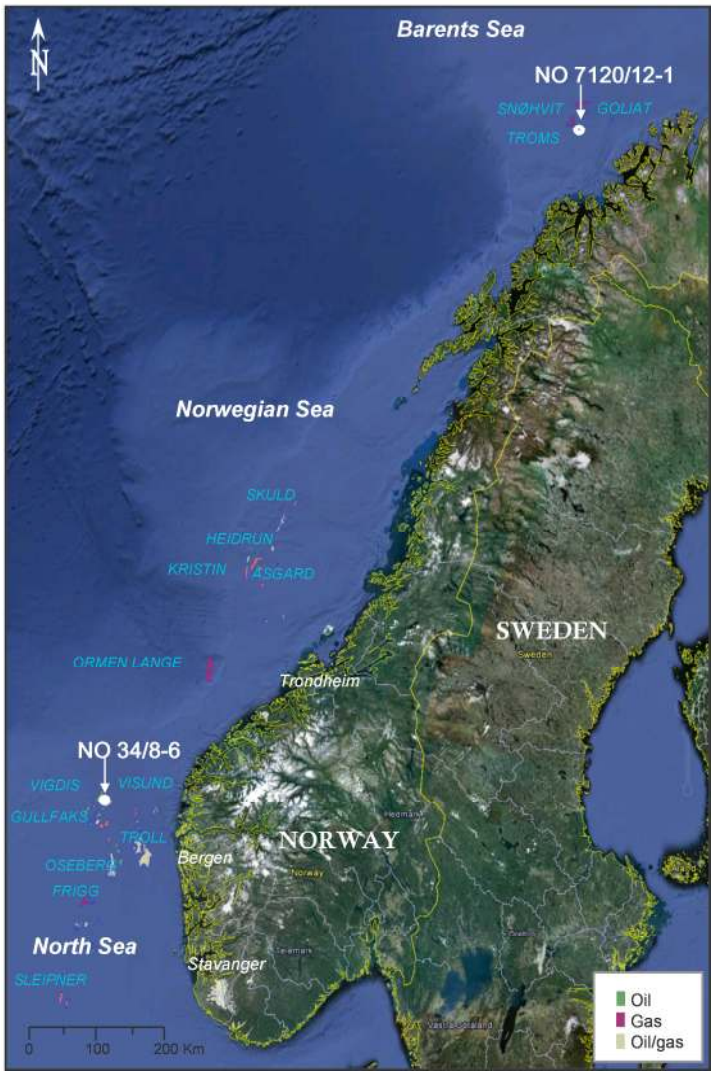

Fig. 36: Map of offshore Norway showing the well location in this study (White circles), NO 7120/12-1 in the Barents Sea and NO 34/8-6 in the North Sea.

Well Data NO 34/8-6

The well 34/8-6 is located at the north of the Visund area in the North Sea was evaluated in the Cretaceous-Jurassic section (***Fig. 37***). In this well, the Cretaceous consist in a 1332 m section, divided into two main formational groups: *Shetland Group* that comprises alternating sequence of non-calcareous and calcareous claystones and minor interbedded calcareous sandstones, dolomite and limestone; and *Cromer Knoll Group* that consist in grey and brown claystones and limestones. The Jurassic section is composed by the Viking Group with organic rich claystones and minor interbedded limestones and dolomite; Brent Group represented by a predominantly sandstone sequence with minor interbedded claystones and coals and Dunlin Group conformed by claystones with trace of limestones.

The interval encompassing Late Jurassic to earliest Cretaceous referred to as Kimmeridgian shales, is known to have been the source of oil and gas at various time and places in the North Sea (*Gautier L., 2005*). The Kimmeridge Clay Formation varies in its kerogen composition from organically-rich, highly-sapropelic, and oil-prone to organically-lean, inertinitic without hydrocarbon-generating potential (*B.S. Cooper & P.C. Barnard, 1984*). It have been reported that anoxic bottom water conditions persisted through much of the time of deposition of the Kimmeridge Clay Formation, resulting in accumulation of very thick intervals of sapropelic source rocks in some areas. Potentially oil-generating organic matter preserved in the Kimmeridge Clay Formation is derived from both waxy plant detritus and algal material originating in the marine environment (*B.S. Cooper & P.C. Barnard, 1984*).

The primary objective for well 34/8-6 was to test the presence of hydrocarbon-bearing sands within the Upper Jurassic Draupne Formation, but no sandstones developed were present (NPD, 2012). The well was permanently abandoned as a dry hole with hydrocarbon shows of shallow gas at 1235 and oil in the mud at 3180 m in the Kyrre Formation. The well was drilled with water base mud. The log data in this well was acquired using Wireline tools (***Fig. 37***).

Data from Rock Eval pyrolysis used for calibration (%TOC) and maturity (%Ro) to calculated level of organic metamorphism (LOM) were provided by Statoil and is show in ***Fig. 38***. Data for TOC calibration was only present in the Jurassic section at the level of Heather and Draupne formations in this well. In order to have references values of TOC at the Cretaceous sequence, data for two well close to this area was used for Kyrre Formation (***Fig. 39***). According to this data, the Cretaceous section presents a moderate organic content that do not exceed 2% and low thermal maturity. Important organic enrichment is found at Jurassic level with TOC average of 6% and thermal maturity in the onset of the oil window (Ro 0,6%).

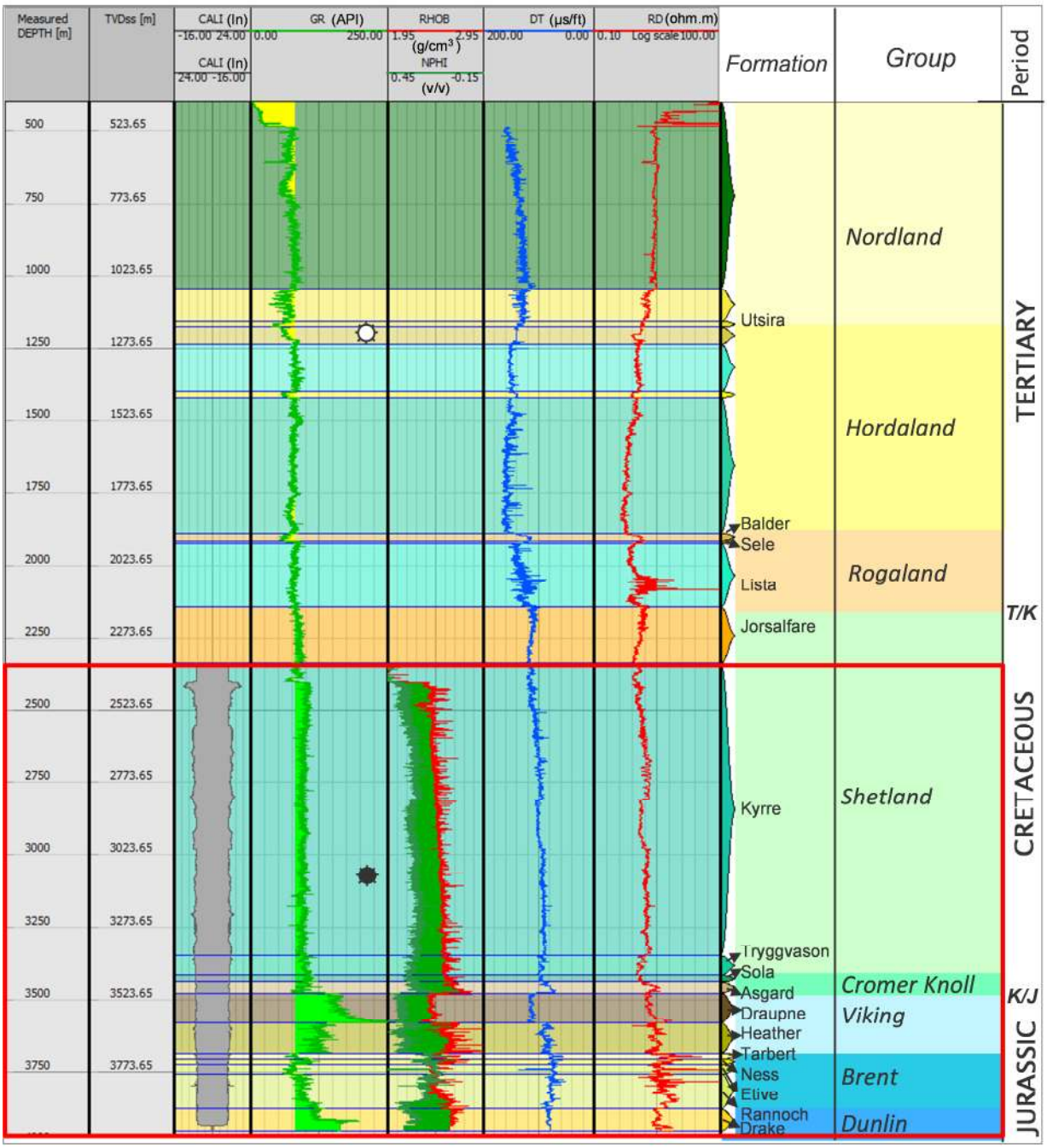

Fig. 37: Summary of Wireline log data used for TOC calculation, for the well NO 34/8-6. Red box indicated interval evaluated (CALI: caliper; GR: Gamma Ray; RHOB: Density; NPHI: Neutron Porosity; DT: Transit time; RD: Deep Resistivity).

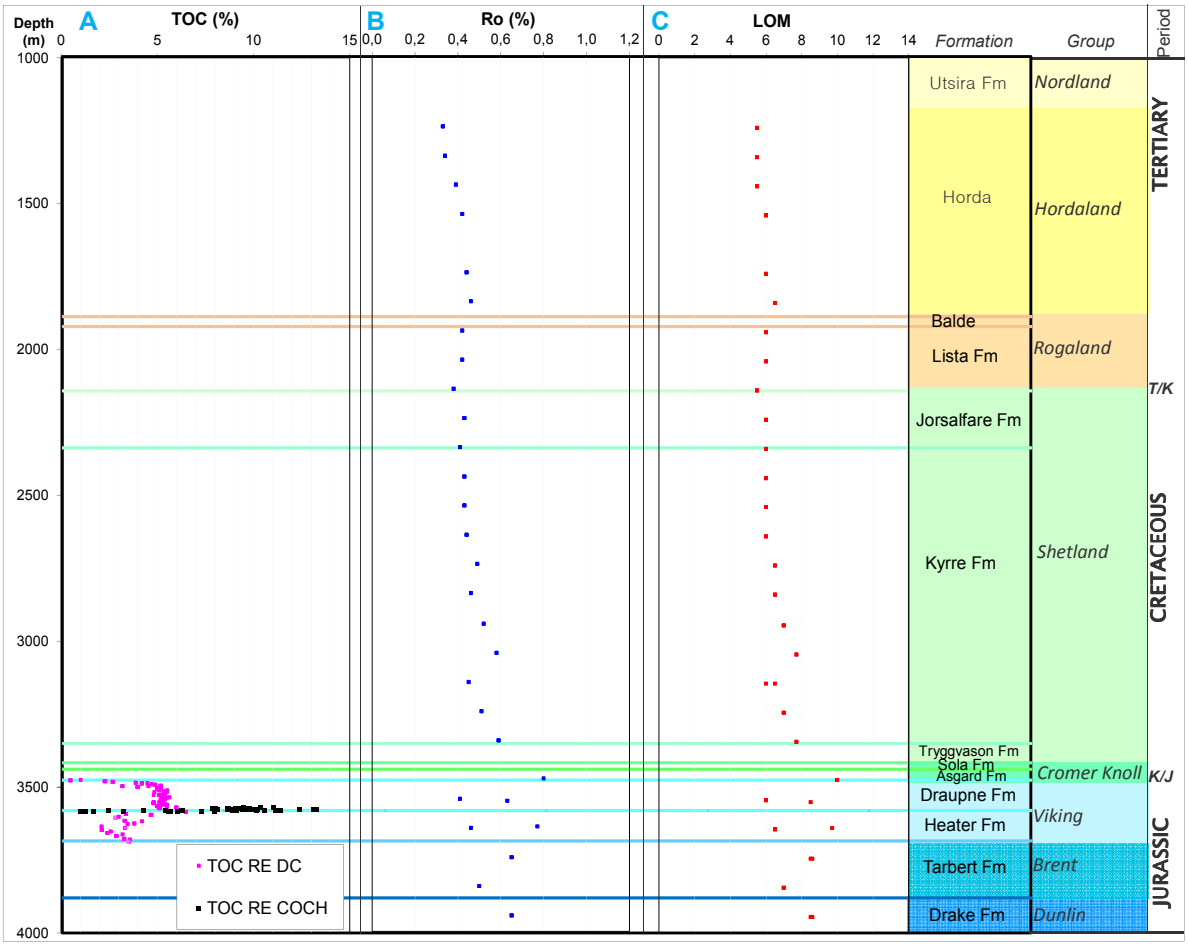

Fig. 38: Rock Eval data used in this study for the well NO 34/8-6. **A**. TOC values measured in conventional core (COCH) and ditch cutting (DC) used for calibration in the main intervals of source rock. **B**. and **C**. Maturity values used for TOC log calculation: LOM values estimated from vitrinite reflectance data (%Ro).

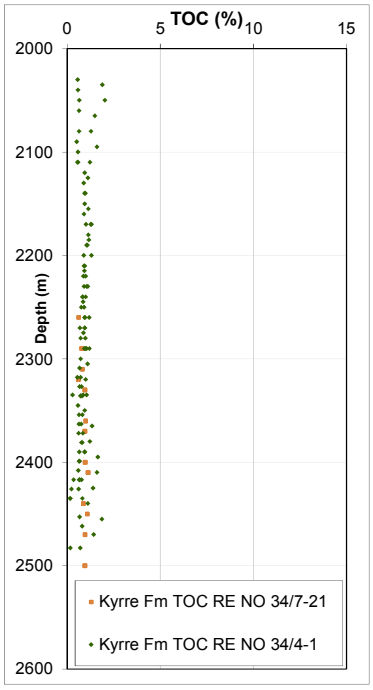

Fig. 39: TOC data from wells NO 34/7-21 and 34/4-1, at Kyrre Formation used as a reference for calibrations at the Cretaceous interval.

Well Data NO 7120/12-1

The well NO 7120/12-1 was the first well to be drilled offshore northern Norway in the Norwegian Sea, and comprised a Cretaceous-Jurassic-Triassic section with good coverage of geochemical data. The stratigraphic column can be summarized as follow (***Fig. 40***):

- The *Nygrunnen Group* in this well consist of interbedded calcareous claystones and sandstones condensed sequences deposited in open marine, deep shelf environments in the west passed into shallower starved shelf regimes. The claystones are assigned to the *Kveite Formation*, the condensed sequences to the *Kviting Formation*.
- The *Adventdalen Group* comprises shales, siltstones and sandstones of Late Jurassic to Early Cretaceous age. The group is dominated by dark marine mudstones, but includes also deltaic and shelf sandstones as well as thin, condensed carbonate beds. Important hydrocarbon source rocks occur in the Upper Jurassic succession (*Hekkingen, Fuglen* formations). *Hekkingen* formation consists of brownish-grey to very dark grey shale and claystone with occasional thin interbeds of limestone, dolomite, siltstone and sandstone, deposited Marine, deep water with anoxic conditions in open to restricted shelf environment. Lower parts of the formation show especially high gamma ray readings. This is used to differentiate the lower *Alge* (black shales rich in organic material deposited in restricted shelf environments) from the upper *Krill Member* (very dark grey shale and mudstone with occasional thin interbeds of limestone, dolomite, siltstone and sandstone) (*Dalland A. et al, 1988*).
- The *Kapp Toscana Group* comprises shales, siltstones and sandstones of Late Triassic to Middle Jurassic age deposited in a generally nearshore, deltaic environment and is characterized by shallow marine and coastal reworking of deltaic and fluviodeltaic sediments.

The well was planned to test possible sandstone reservoirs of Middle Jurassic, Early Jurassic, and Late Triassic age resulting in a dry hole with traces of hydrocarbons in thin sandstone reservoirs of Early Cretaceous and Late Triassic age (NPD, 2012). The well log data containing a uniform and good resolution log readings acquired using Wireline tools (***Fig. 40***).

The detail geochemical data set present in this well provided by Statoil allowed a good calibration and calculations for this well. TOC from Rock Eval indicated different levels of organic content: low in the Cretaceous interval, moderated within the Triassic section and high in the Jurassic shales. The whole section is. The Cretaceous section is thermally immature while the Jurassic and Triassic sections are moderated mature near the oil window (***Fig. 41***).

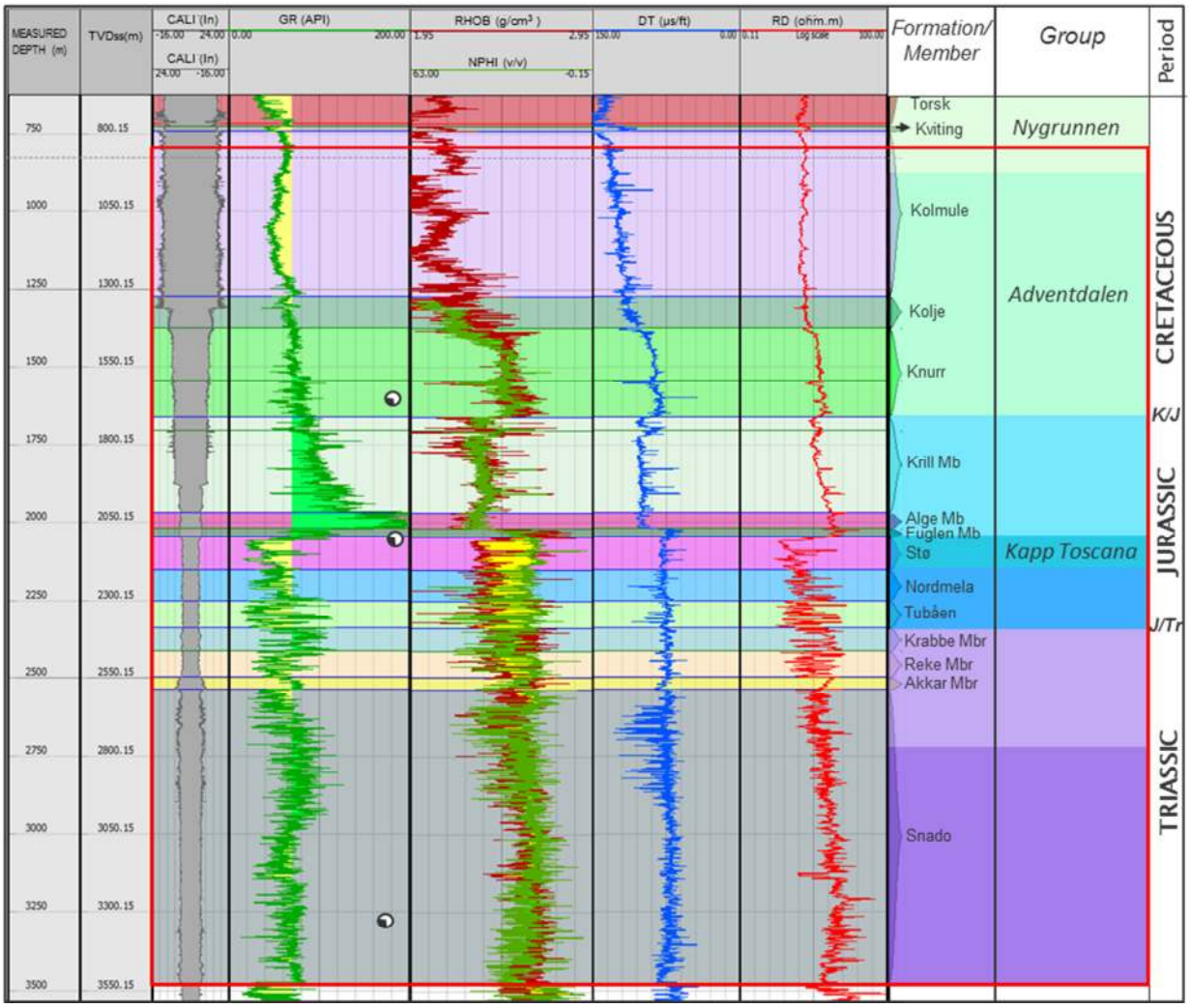

Fig. 40: Summary of Wireline log data used for TOC calculation, for the well NO 7120/12-1. Red box indicated interval evaluated (CALI: caliper; GR: Gamma Ray; RHOB: Density; NPHI: Neutron Porosity; DT: Transit time; RD: Deep Resistivity).

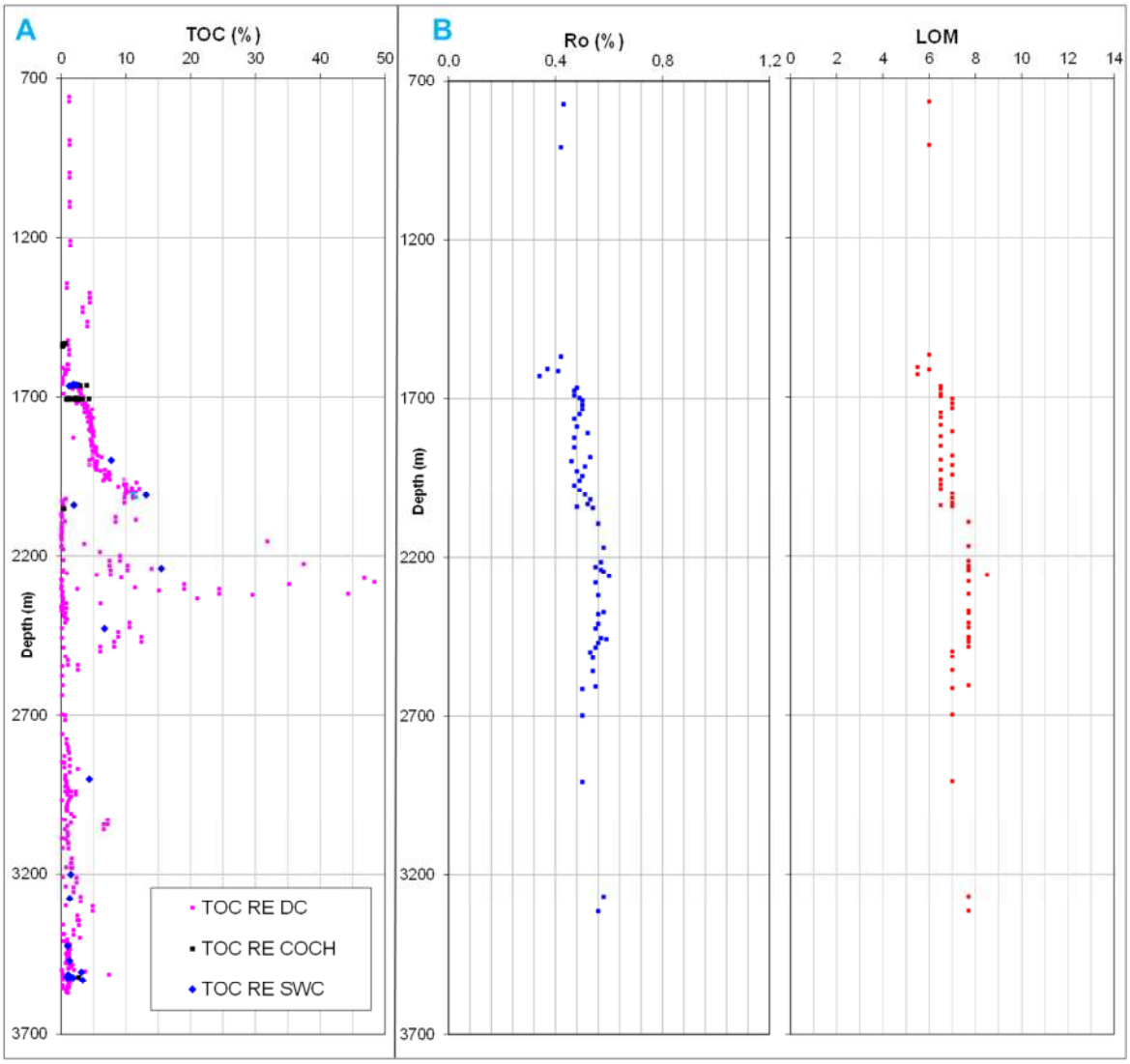

Fig. 41: Rock Eval data used in this study for the well NO 7120/12-1. **A**. TOC values measured in conventional core (COCH), sidewall (SWC) and ditch cutting (DC) used for calibration. **B**. and **C**. Maturity values used for TOC log calculation: LOM values estimated from vitrinite reflectance data (%Ro).

4. Results

This section compiles the results of all the tools and methods tested in this study. In each section different cases are shown to describe and compare the results obtained. Two different tools based on delta log R method were compared. Additionally and improvement of delta log R technique is shown in section 4.3 and a new model based on statistics (multiple linear regression) is proposed in section 4.4.

The background level of TOC in shales was established at 0,2 wt % for all the cases using Delta log R technique.

The well NO 34/8-6 was evaluated in the *Cretaceous- Jurassic* interval from 2200m to 3800m and the well NO 7120/12-1 from 700 to 3600m that includes a *Cretaceous-Jurassic-Triassic* section.

Limitations and advantages of the tool are also discussed in this section.

4. 1 BasinMod 1D (Platte River Associates, Inc.)

In order to compare estimations of TOC using different intervals of baseline, two cases where considered in the well NO 34/8-6:

Case 1:

A first case is shown in ***Fig 42*** in which the definition of the baseline for transit time and resistivity logs was taken in the upper Cretaceous interval where, according to the stratigraphy, shales with low organic content were expected. Transit time and Resistivity logs were shifted for this interval which is consider a no source rock in order to calculate the TOC curve for the rest of the section. Shifting Transit time and resistivity logs at that interval generated a delta log R separation within *Draupne Formation*. According to these baselines (for Resistivity and Transit time), the resulting TOC curve (***Fig 42***) showed the entire Cretaceous section with total absence of organic content (values below zero). However a good approximation is obtained in the *Jurassic* section, despite the fact that some values were underestimated especially in the interval of the *Heather Formation.*

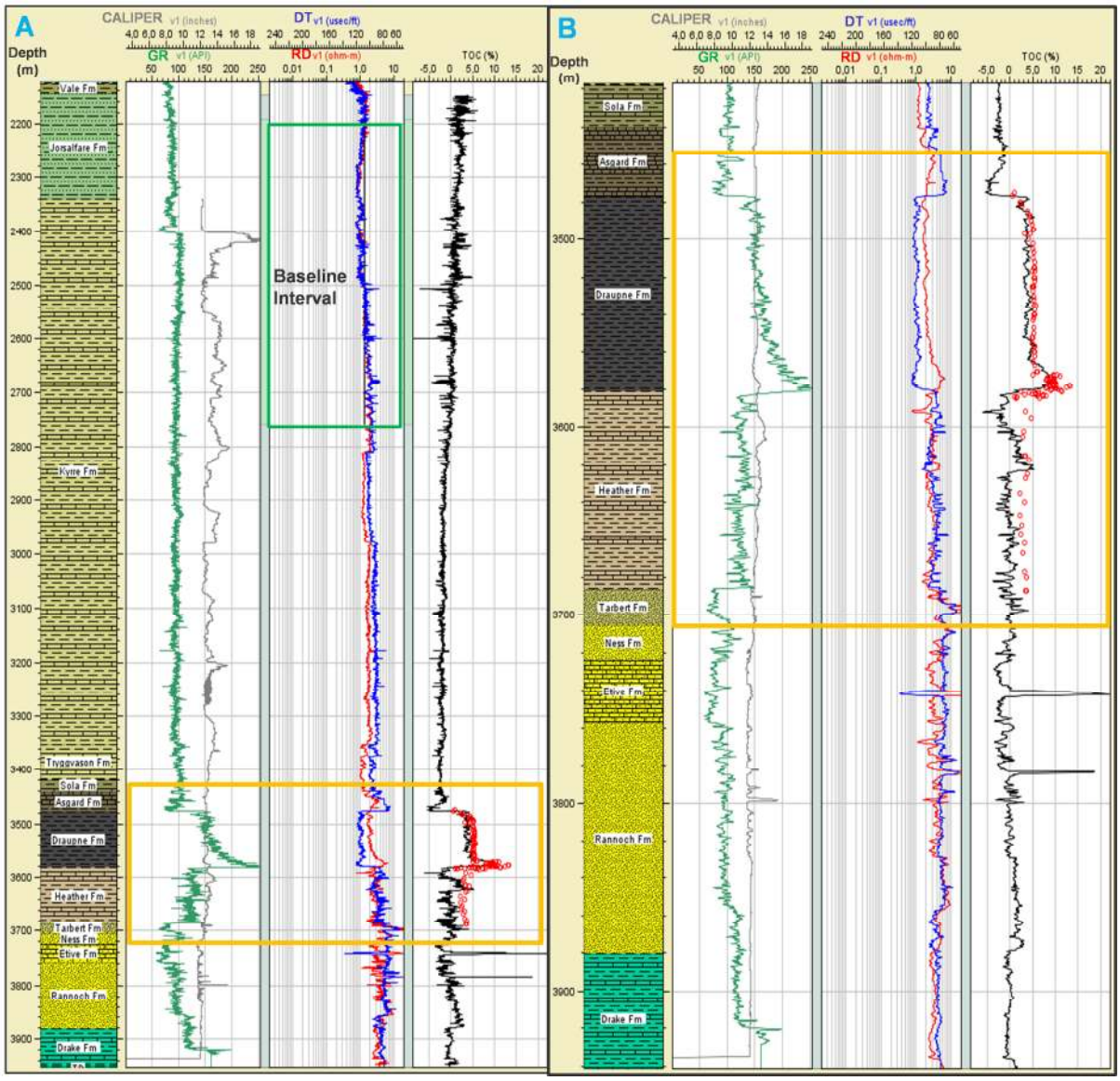

Fig. 42: Result of TOC curve from logs obtained in case 1 **A**. Well logs used in the estimation, TOC curve calculated (in black), calibration interval (orange box), TOC values for calibration (red circles) and baselines interval (green box), note the lack of organic matter in the lower part of the *Cretaceous* interval (values of TOC curve below zero) **B**. Zoom in of the interval calibration at the *Jurassic* section showing the TOC curve calculated and calibration values.

Case 2:

A second attempt was done, in this case, defining the lower *Cretaceous* section close to the *Jurassic* sequence as a baseline interval (***Fig 43***). As a result the estimated TOC curve indicated the best adjustment in relation to the measured TOC data. Even the estimation obtained at the level of *Heather Formation* is more accurate, visually compared with the previous cases. Additionally, in this case the estimations for the *Cretaceous* section are more reasonable since values of the curve are not below zero as in the previous case (Case1), on the contrary the TOC from log curve in the Upper *Kyrre* and *Jorsalfare Formations* indicated a significant presence of organic content.

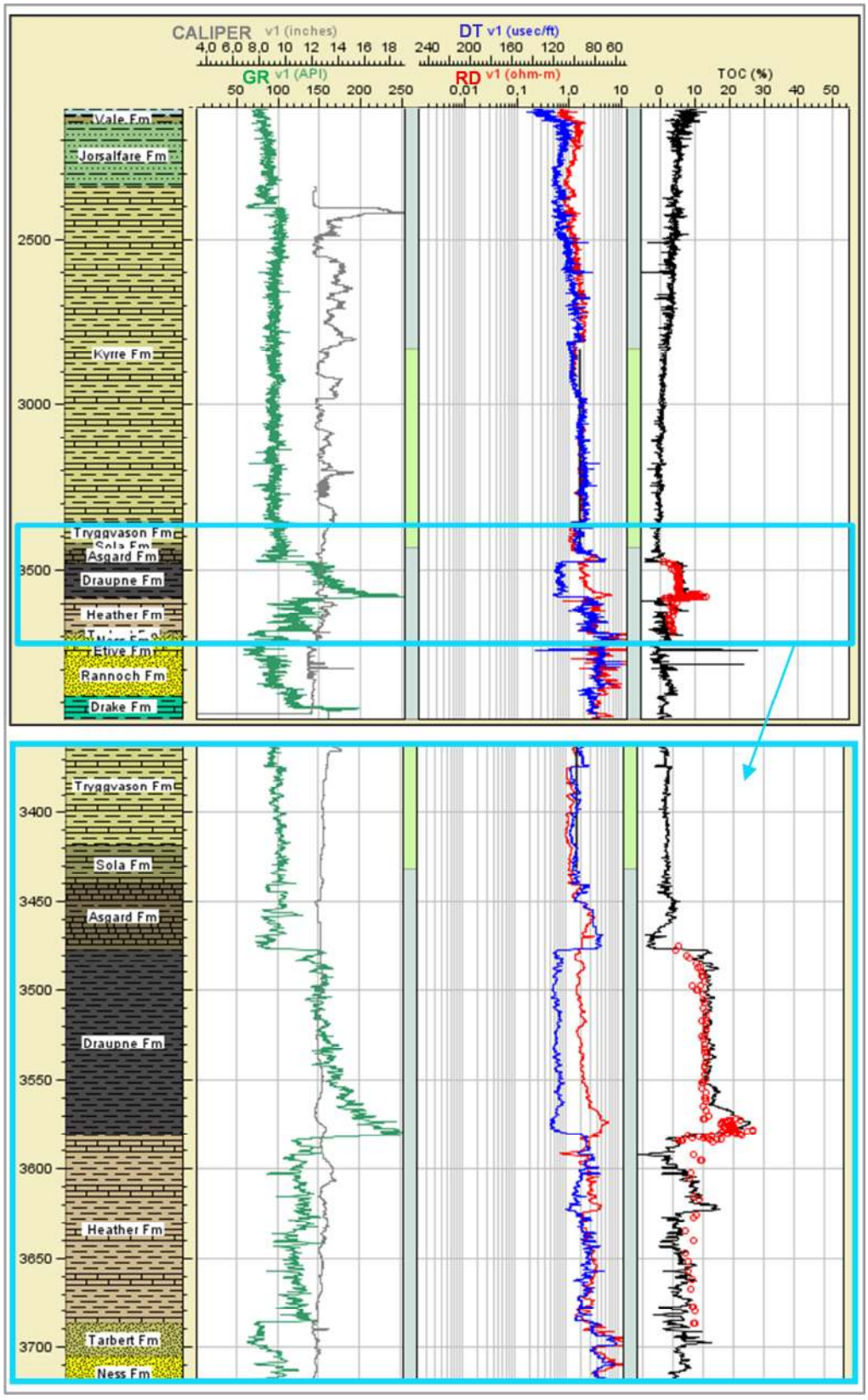

Fig. 43: Result of TOC curve from logs obtained in case 2. The best approach in the Jurassic section (Blue box) is achieved using a baseline in the lower Cretaceous interval. Note that in this case, an important estimation of organic content is obtained in the Upper *Cretaceous* section (*Jorsalfare Formation* and Upper *Kyrre Formation*).

Software Limitations

LOM values were calculated by the software using the %Ro data, but no report is provided by this tool to have the exact LOM values used.

The ***Fig 44*** illustrated the selection of points from the TOC log curve to obtain TOC numeric values. The idea was to obtain values at the exact same depth of the calibration data (172 values) to make them comparable. With this in mind, around 100 points were obtained in each case but not the total amount used for calibration neither at same depth. Intervals with high density of calibration points is one of the causes for this inaccuracy, since it is difficult to select the appropriate points that correlated in depth, and moreover changing the magnification scale can cause a wrong depth selection (***Figs 44, 45***). Calibration values far away from the TOC log curve are also source of error for the comparison (***Fig 45***).

Another important observation is that erratic points outside of the curve during the selection lead to unrealistic values in the table (even negative values). Another disadvantage is that the extracted values from the estimated curve are stored in a table and they are not updated if posterior adjustments are performed. If this is the case a completed new manual selection should be done to extract new TOC numerical values.

Only one well was tested using this tool since it was necessary to build a 1D basin model prior to do the estimation, which is time consuming and was not the purposes of this study.

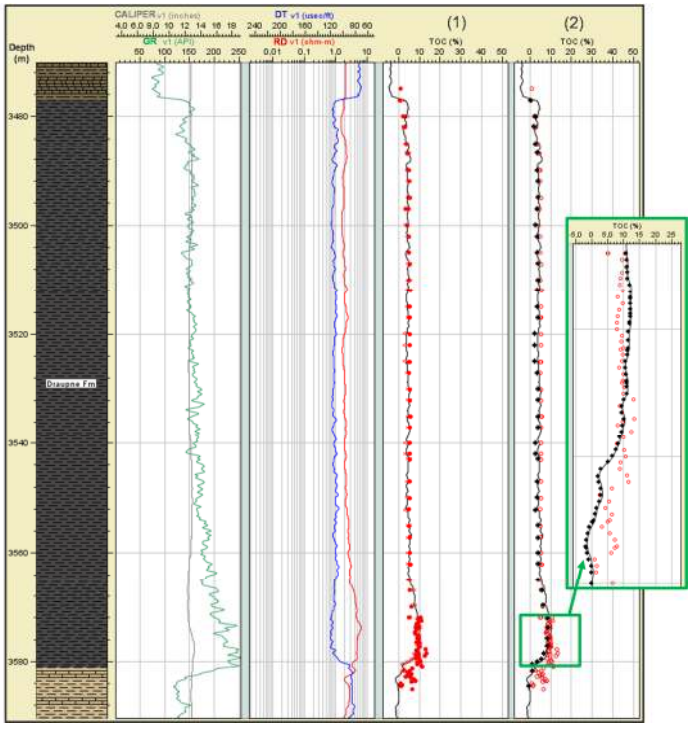

Fig. 44: Point selection from the TOC log curve to obtain TOC numeric values at the Jurassic level. Track (1) Toc log curve (in black) and calibration point (red circles). Track (2) manual point selection (black diamonds). The magnification of the green box shows the difficulty to obtain values from the curve at the same depth in intervals with high density calibration data.

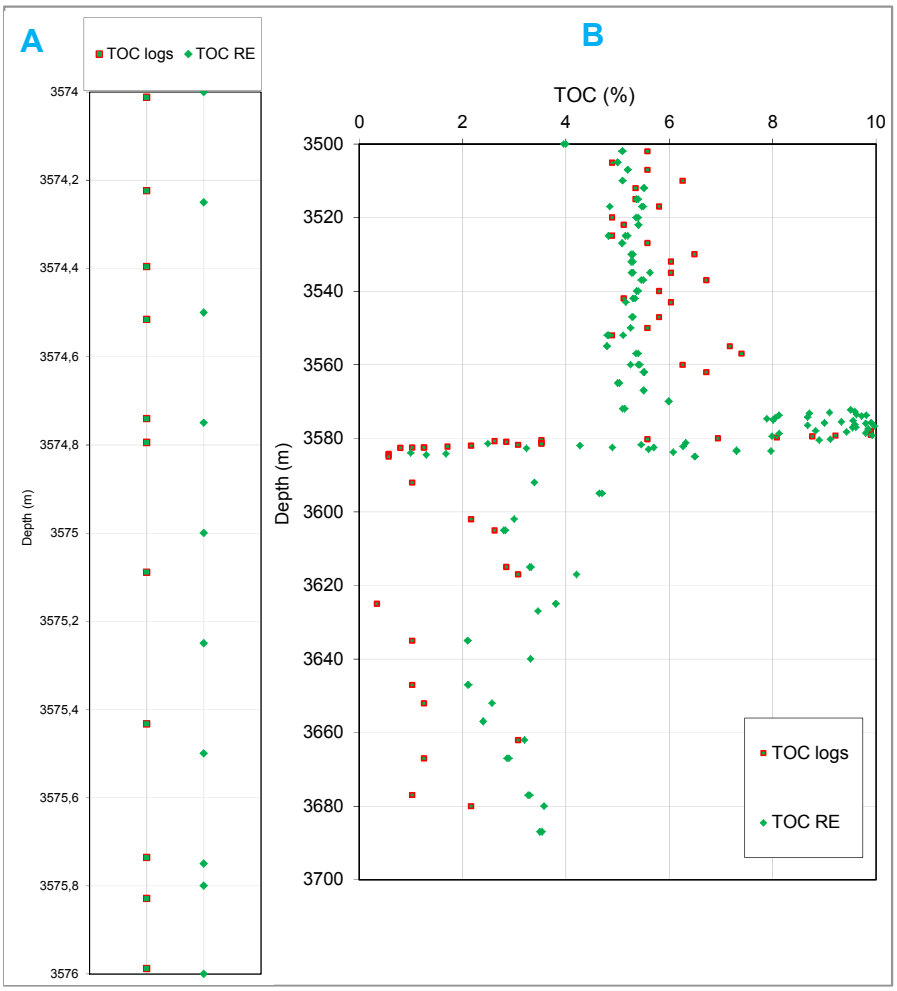

Fig. 45: Comparison between measured values of TOC (TOC RE) and values manually selected from TOC logs (TOC Logs) at the *Jurassic* Level. (A) A detail interval was choose to illustrating the mismatch regarding to different depths (B) plot of amplify scale of TOC against depth shows the dispersion of both set of data.

4.2 Permedia MPath version 4.18.1 (Landmark Software and Services, Halliburton).

The same data for the well NO 34/8-6 was evaluated using this tool and also the well NO 7120/12-1 was included in the evaluation. The main difference using this tool was the possibility to subdivide the interval to define independent baselines in the section to be evaluated. A brief statistical analysis was also obtained in order to compare the measured and estimated TOC values. Results are summarized as follow:

Well NO 34/8-6

The study interval was subdivided into zones to define different values of baselines for each section. ***Table 1*** summarizes values of baselines for each interval (horizontal break). Additionally, a Gamma Ray cutoff of 80 API was included in order to calculate values of TOC only in shale intervals (Gamma Ray values over 80 API).

Fig 46 shows this example in which 6 horizontal breaks allowed to define independent baselines. The estimated TOC curve decreased in the Cretaceous interval with respect to the previous cases. Reference values of measured TOC for *Kyrre Formation* from two different wells were incorporated with the purpose of evaluates the estimation at the Cretaceous interval and according to this data there is a good fit of the estimated TOC curve.

A very similar fit of the estimation and the calibration values for the Jurassic section was obtained with more deviation at *Heather Formation* than in the case 2 using *BasinMod* (***Fig 47***), even though different baselines values were chosen from the previous examples (***Fig 47***). It was also observed that at the lowest *Draupne Formation* the estimated curve produced a maximum zone of TOC that approximates in behavior, but still is much inferior, to the measured data (***Figs 47***).

After the estimation, it was found that the reduction of transit time baseline values with depth and increments of the resistivity baseline value with depth, give better results than *case 2* using *BasinMod*, in the whole section. (***Table 1***, ***Fig 47***).

Table 1: Summary of baselines values at each horizontal break used in TOC estimation from logs, Well NO 34/6-8.

Horiz. Break	*DT baseline*	*RD baseline*
1	115	0,8
2	105	1,2
3	100	1,3
4	90	1,5
5	86	1,9
6	82	2,2

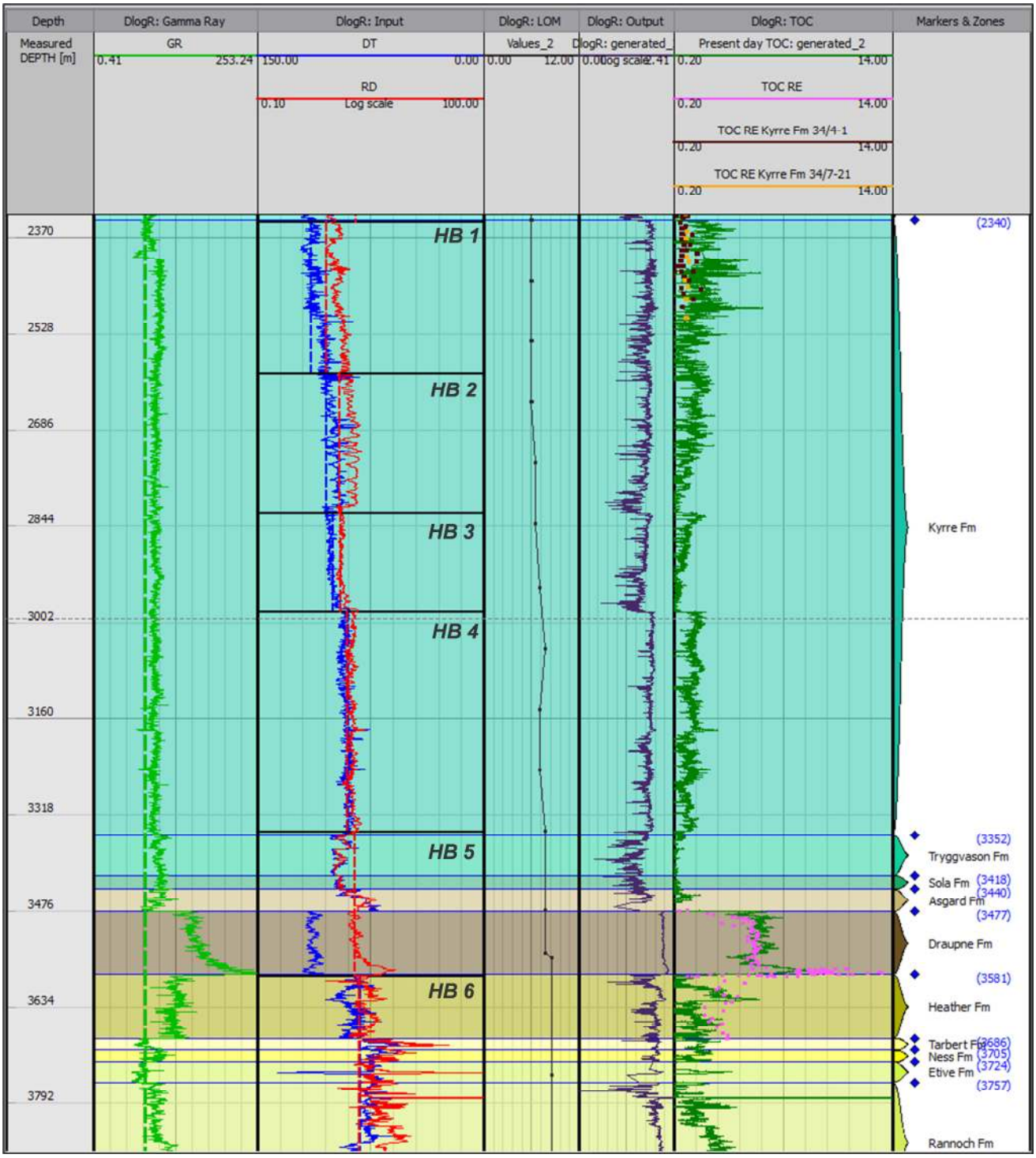

Fig. 46: Results of TOC from logs using horizontal breaks (HB) in *Permedia*, well data NO 34/8-6. Tracks from left to right: Measure depth (m), caliper (In), Gamma Ray (API, cutoff in green dash line) Transit time (DT µs/ft) and Resistivity (RD Ohm.m) with its baselines (dahs lines), LOM from %Ro, Delta Log R ($\Delta \log R = \log_{10}(R/R_{baseline}) + 0.02 * (\Delta t - \Delta t_{baseline})$), TOC log curve (%wt, in green) with calibration values (brown, orange and pink dots), and Formations. Note that the baselines were adjusted with and small increment for the case of the Resistivity and reduction for the case of the Transit time curve.

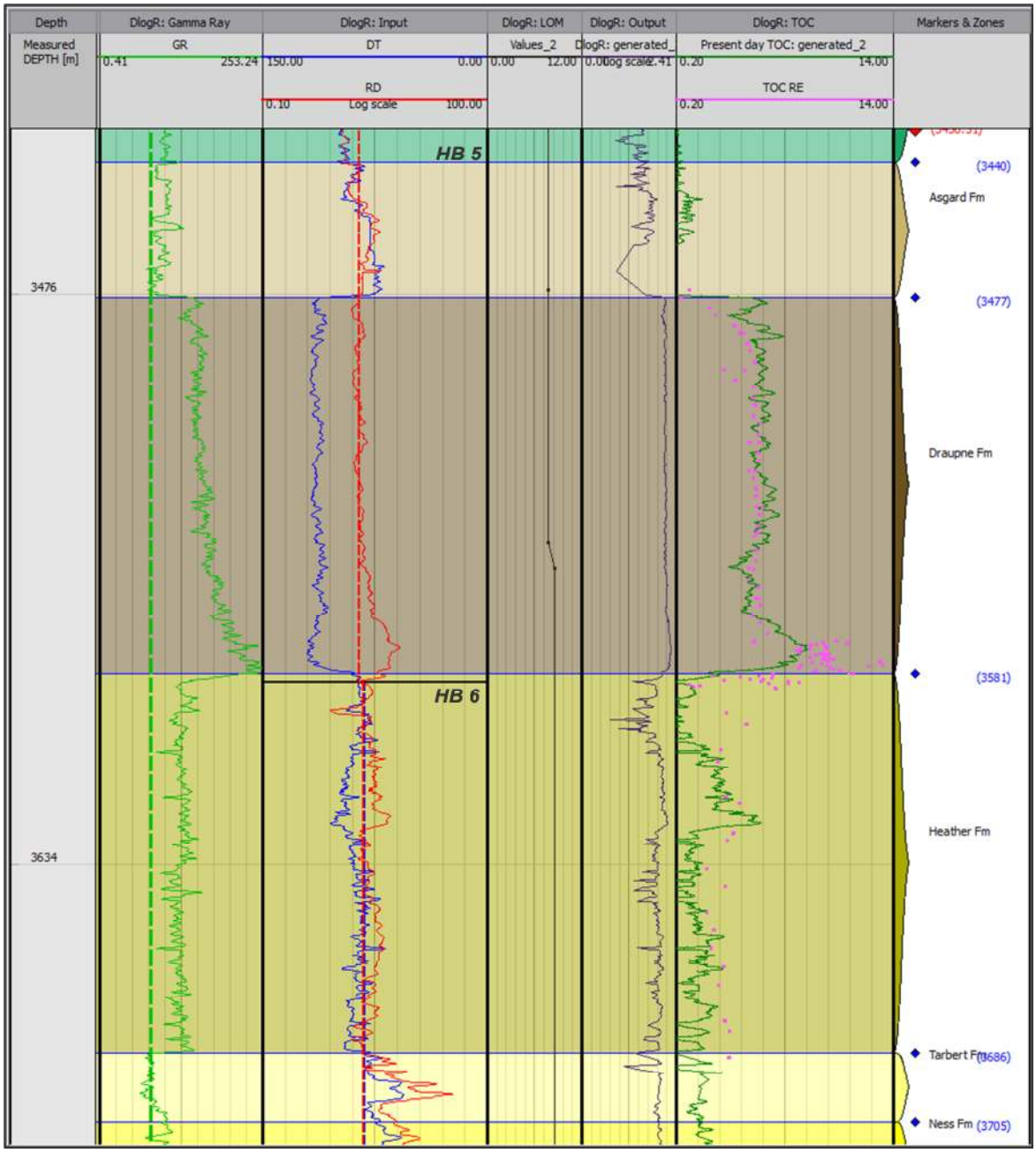

Fig. 47: Result of TOC curve from logs obtained in the Jurassic section of well NO 34/8-6, using horizontal breaks (HB) and different baselines values.

A gross exploratory data analysis was done to compare estimated values versus calibration values at the *Jurassic* interval (since calibration data for this well was only available in this interval). The summary of the exploratory data analysis such us minimum, maximum and mean suggest that both sets of data do not converge effectively as the visual results indicate (***Fig 48***). However, a similar frequency distribution was observed of both set of data at the *Jurassic* level, whereas the absolute frequencies are not comparable since estimation data have much more samples than calibration (***Fig 48***). On the other hand it is important to note the fact that in both sets of data a bimodal distribution was observed and also the cumulative frequency curve indicates that both distributions produced

the same rate of increment around values of 4% of TOC (*Fig 48*). Additionally, both distributions decreased when values of TOC are about 6%. It is well known that a better comparison can be done using relative frequencies instead of absolute frequencies but it was a limitation of the tool.

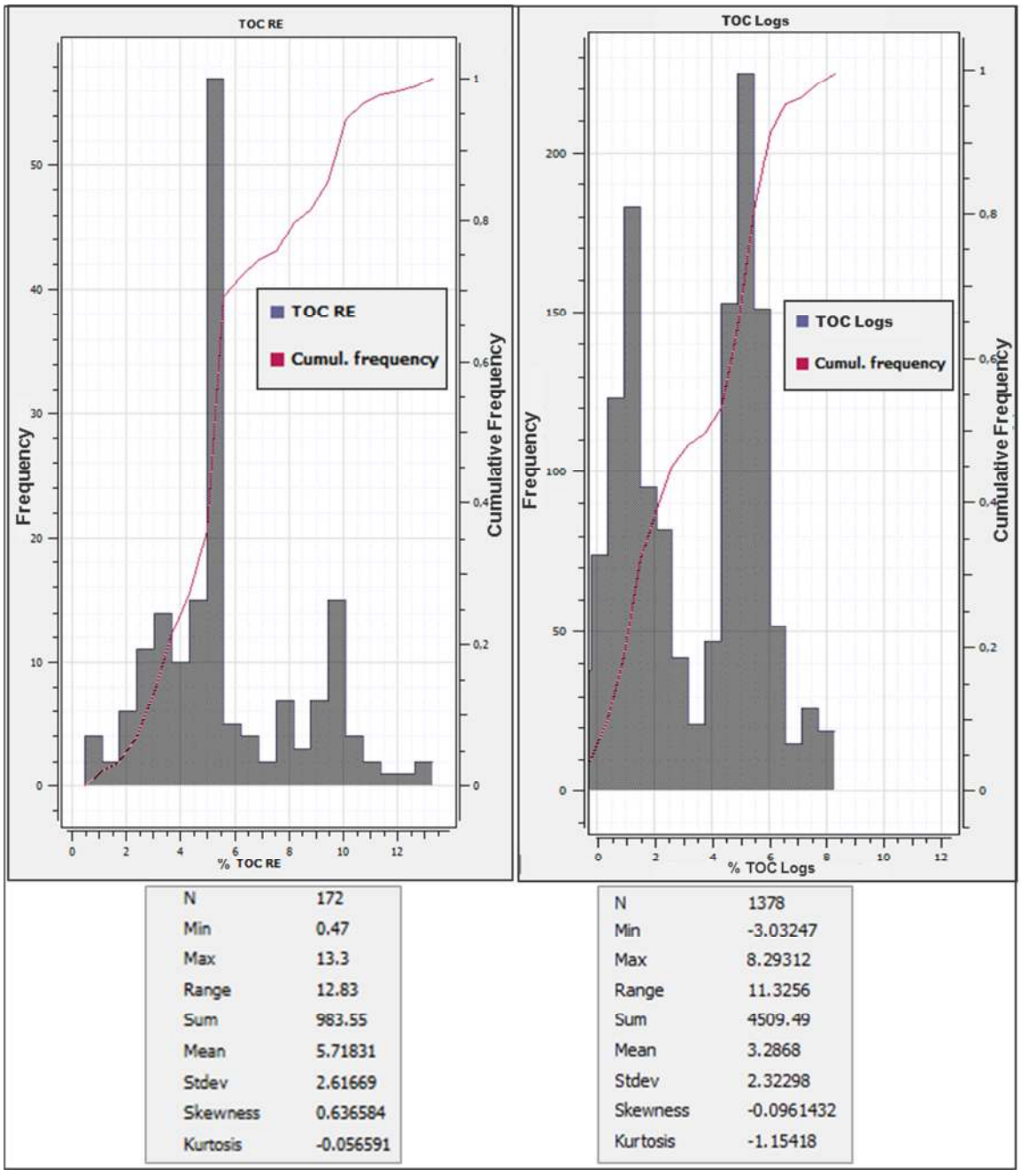

Fig. 48: Comparison of frequency distribution for TOC RE and TOC from logs in well NO 34/8-6, both showing bimodal distributions at the Jurassic level. At the bottom of each histogram are the results of exploratory data analysis.

Well NO 34/8-6

The data from the well 7120/12-1 was also evaluated in the same manner as the well 34/8-6. Since the study section includes a thick interval of 2732 m with variation in lithology, texture and also organic matter content, it was necessary to subdivide the section into 12 zones in order to make a more accurate estimation (***Fig 49***). Baselines values for each section are summarized in ***Table 2***. The cutoff for the Gamma Ray was established at 55 API in the whole section.

According to the log response, 2 main zones can be distinguished (***Fig 49***). The first one defined as *Zone A* (from 750 m to approximately 2000m) in the Cretaceous - Upper Jurassic interval is characterized by a more homogeneous Gamma Ray, Transit time and resistivity response. The Gamma Ray trend is deviated to the right reaching values over 250, which ends in an abrupt break. The values TOC measured also follow the same trend. A second zone or *Zone B* was recognized in the interval below 2000 m characterized by an almost continuous vertical and heterogeneous trend. Even values of TOC measured are more dispersed in this zone with significant variation in organic content (0,1-50%) at close depth.

It was found that tuning the baselines by using horizon breaks like in the case before (reduction of transit time baseline values and increments of the resistivity baseline value, with depth), the *zone A* results in a good visual approximation. In this interval the estimated curve has a similar shape described by the TOC values except for the lower section of *Kolmule Formation* in which the estimation was inferior to the measured data, mainly due to the Gamma Ray cutoff (not shale found to perform the calculation, ***Fig 50***).

Unlike *Zone A*, estimations of TOC for *zone B* were not accurate enough (***Fig 51***). Maximum values of TOC estimated reach values of 10%, while measured data have maximum values of more than 20%, at least in the lower *Jurassic* and upper *Cretaceous* section. On the contrary, the TOC log for *Snadd Formation* was mainly overestimated in the interval between 2600-2800m in comparison with calibration data.

Table 2: Summary of baselines values at each horizontal break used in TOC estimation from logs, Well NO 7120/12-1.

Horiz. Break	*DT baseline*	*RD baseline*
1	130	2
2	125	2
3	120	2
4	90	3,5
5	80	5
6	65	7
7	63	10
8	81	2,5
9	80	2,7
10	78	3,6
11	72	3,7
12	70	6

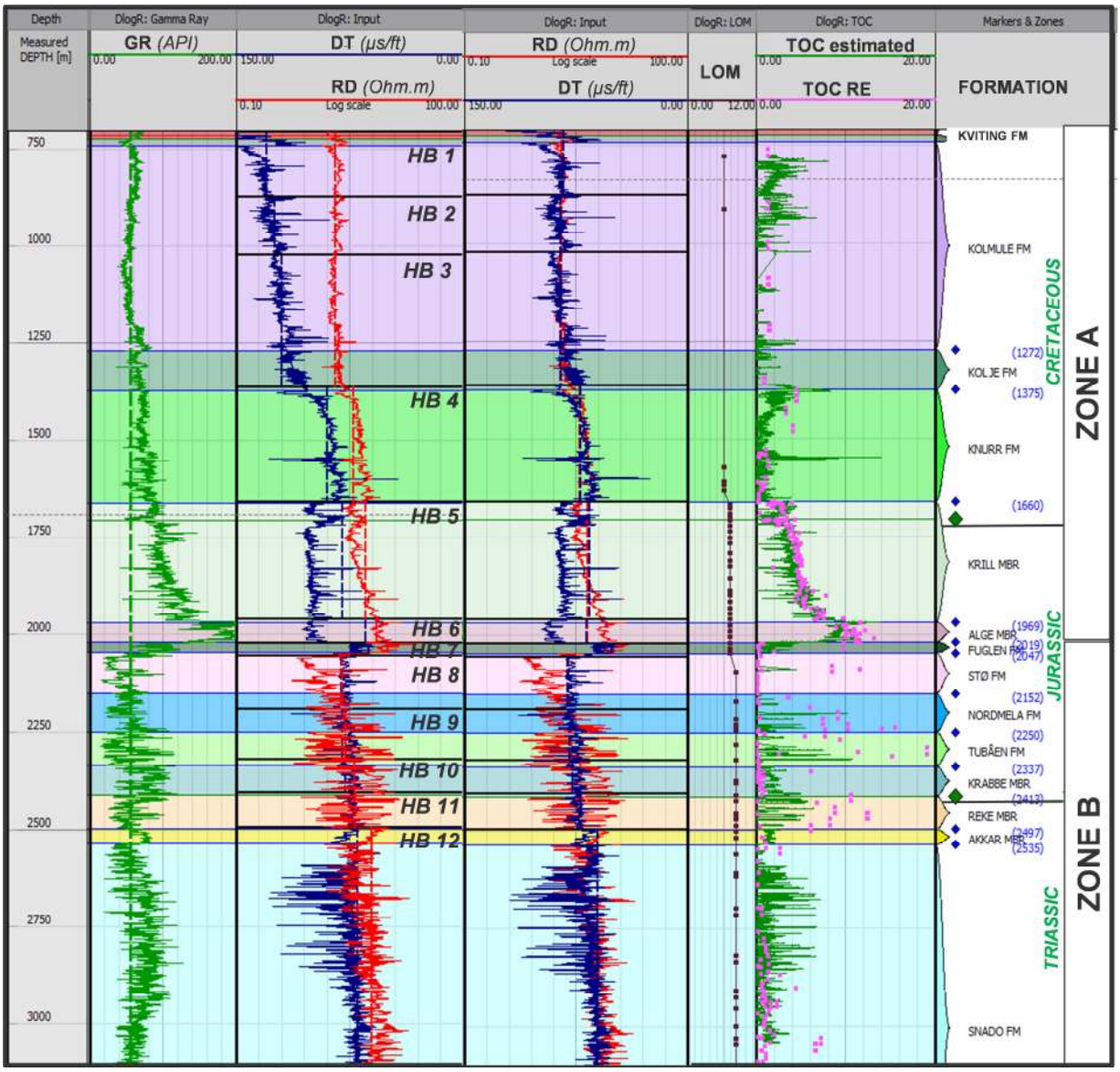

Fig. 49: Results of TOC from logs using *Permedia MPath software*, well data NO 7120/12-1. Tracks from left to right: Measure depth, Gamma Ray (cutoff IN green dash line) Transit time (DT) and Resistivity (RD) (baselines in dash lines) non shifted and shifted, LOM from %Ro, TOC log curve (in green) with calibration values (pink dots), and Formations. Note that on the left, the DT and RD logs are scaled for estimations and on the right track both logs are shifted for each horizontal break (HB) to visualize the delta log separation, in consequence, the values of the baseline do not correspond to the upper scale in the track for Zone A.

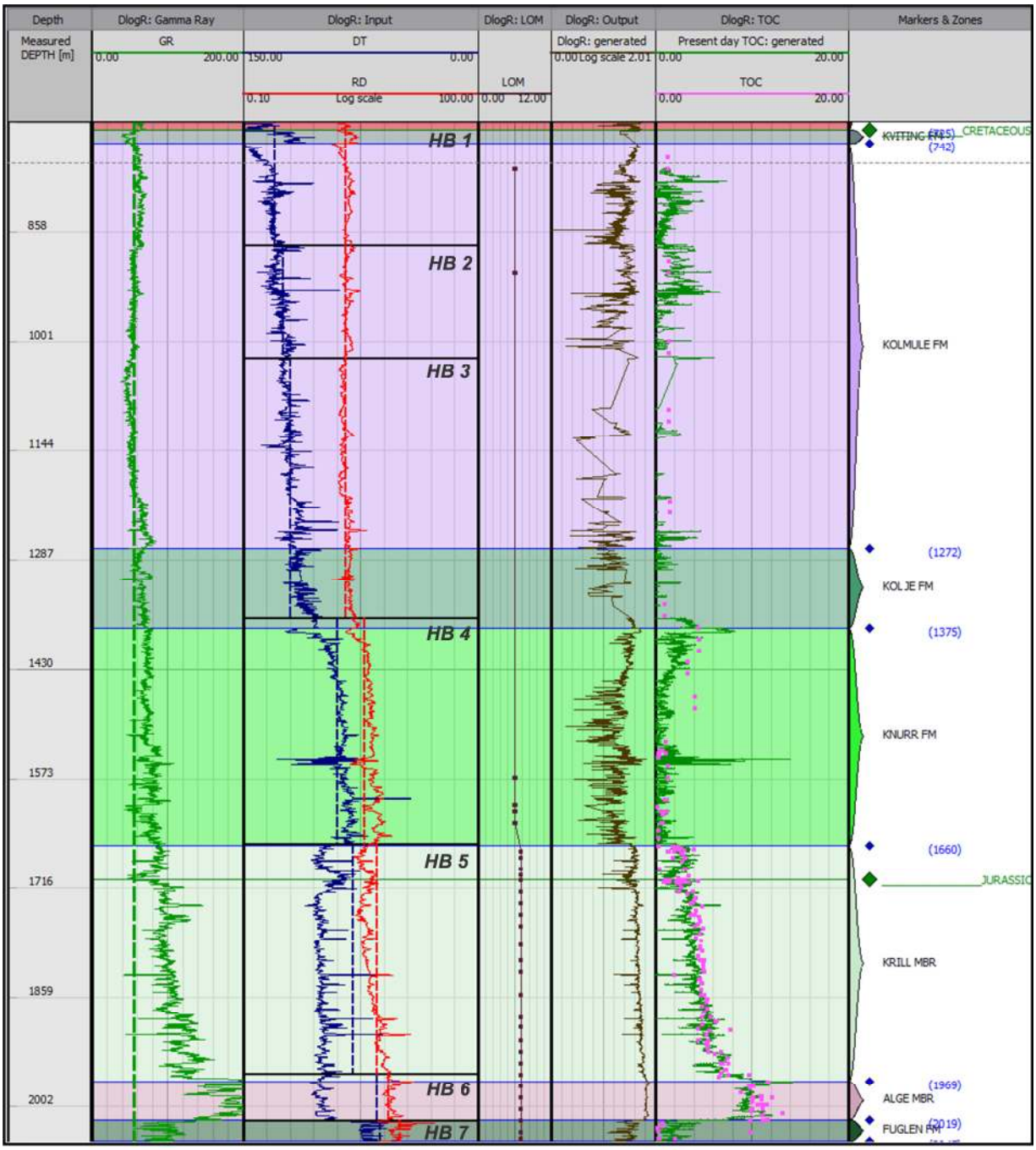

Fig. 50: Results of TOC from logs using *Permedia MPath software*, well data NO 7120/12-1. Calculations of TOC log in *Zone A* using horizontal breaks (HB) with independent baselines values by interval. Note that the baselines were adjusted in such a way that for Resistivity it increments with depth and for Transit time decreases with depth.

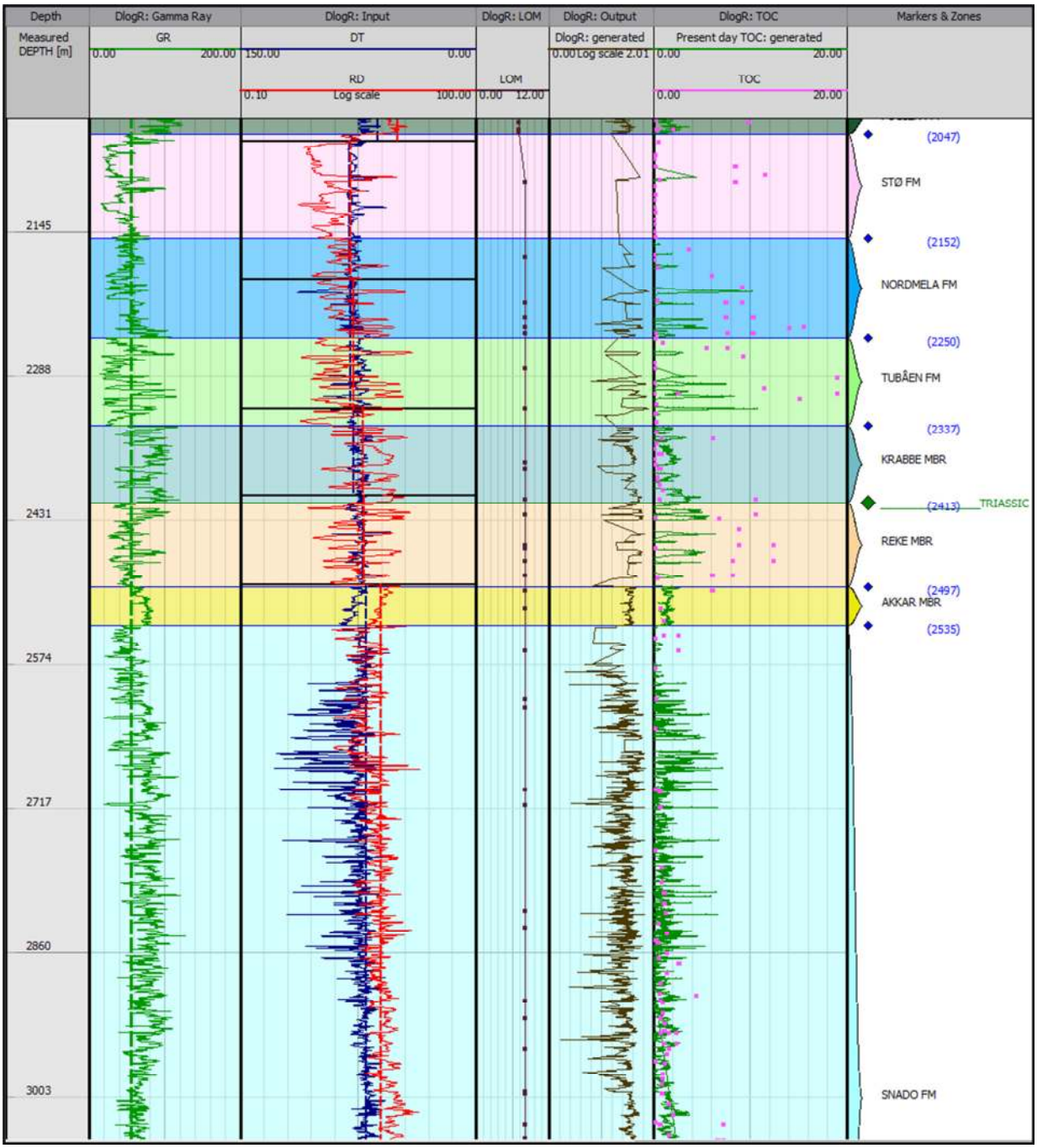

Fig. 51: Results of TOC from logs using *Permedia MPath software*, well data NO 7120/12-1. Calculation of TOC log in *Zone B* using horizontal breaks (HB) with independent baselines values by interval. Note that the baselines were adjusted with an increment in Resistivity and reduction in Transit time with depth.

According to the statistical analysis, there is some resemblance in the absolute frequency distributions for both TOC measured (TOC RE) and estimated, especially in the range between 0% to 10%, where TOC values have higher frequencies (***Fig 52***). Looking at the histograms it is evident that underestimation exist since measured values reach TOC values up to 50% while maximum estimated values are about 15% in TOC. As a consequence, the exploratory data analysis shows wide differences (***Fig 52***).

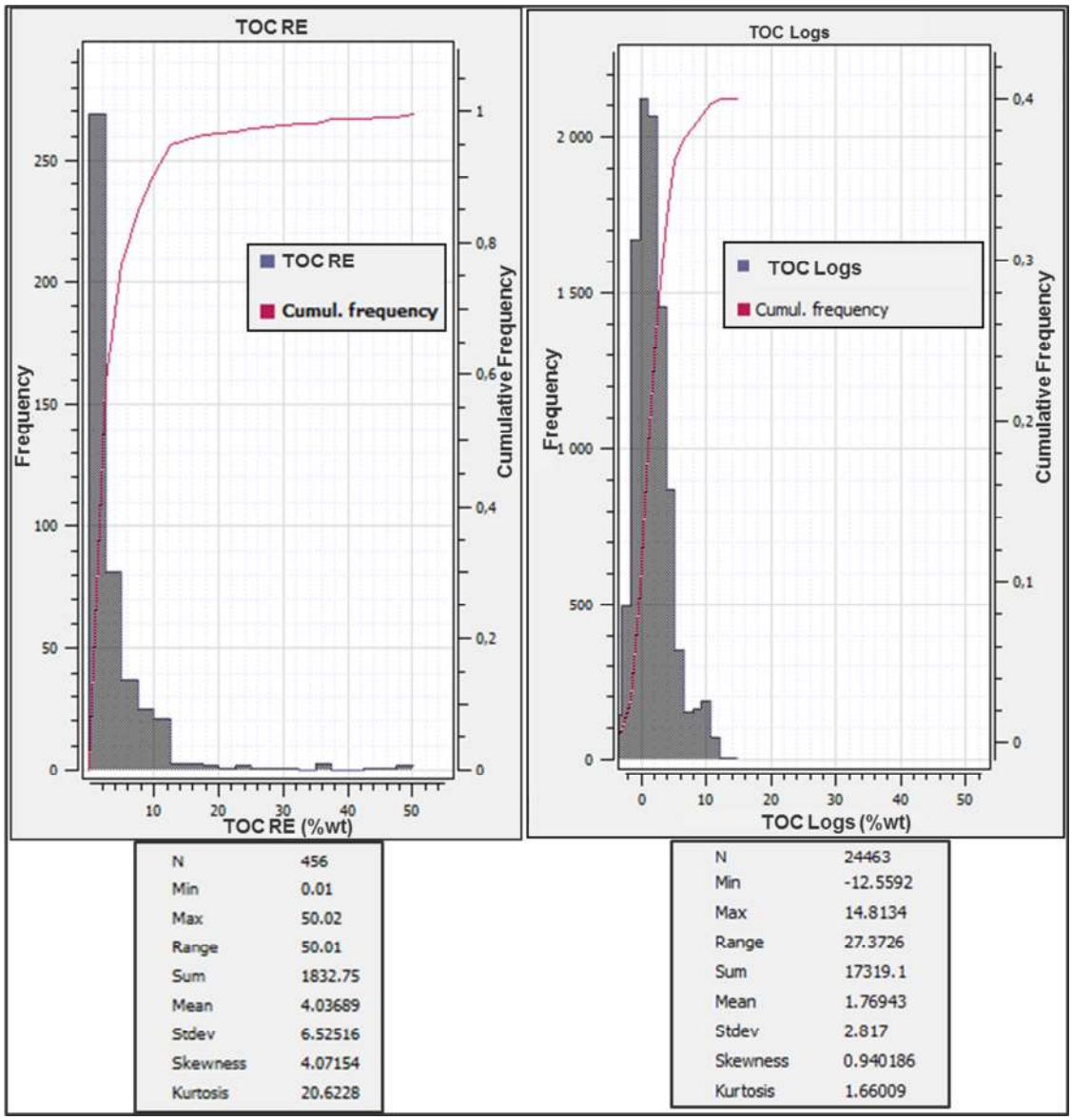

Fig. 52: Comparison of absolute frequency distribution for TOC RE and TOC from logs in the well NO 7120/12-1, showing different distributions. At the bottom of each histogram are the summary results of exploratory data analysis which also indicated differences in both set of data (max, mean, range, etc).

Advantages and limitations of the Software

As opposed to the previous tool, values of baselines were introduced instead of a visual shift, which imply more control on the parameters behind the estimation. Due to the good log display capability and resolution of this tool, it was possible to observe in more detail the results and also it allows a better manipulation of the data.
A gross exploratory data analysis was possible since all the values of the curve were automatically expressed as numerical values. It is well known that a better comparison can be done using relative frequencies instead of absolute frequencies but it was a limitation of the tool. Apart from this, the tool was not able to generate a simple linear regression or calculate regression coefficients.

General Observation of Delta Log R Technique

Until this point, it have been showed several examples using different tools based on Delta Log R technique. Previous examples has demonstrated that definition of interval for baseline Resistivity and Transit time curves is not an obvious task, and it is one of the main sensible parameter in the determination of TOC. In the case of intervals where there is not calibration data the accuracy is unknown.

It was also found that subdividing the interval evaluated and within those subintervals, increasing values of baselines for Resistivity and decreasing values for transit time baselines, both gradually with depth, results in a better approximation of TOC estimated.

After all observation and previous results in which the definition of baselines demonstrated to have important implications using this technique, it brings the idea of the use of trend lines instead of constants values by intervals such as it was proposed. The reason and bases of this approach will be exposed in the *Discussion* section.

4.3 New Trend Technique (Microsoft Excel, Microsoft Office Professional Plus 2010)

Results Well NO 34/8-6

As it was explain in the Methodology section, the first step was the calculation of the baselines. To do that a Gamma Ray range was established to create a “new filter GR” only for shales with low organic content. Using this “filter GR” as a references, the Resistivity and Transit time logs were filter as well, based on the depths of GR filter , thus generating a Resistivity and transit time logs only for shales intervals. Those values allows to calculate a trend line of non- source rock shales for resistivity and sonic in the interval to be evaluated. Therefore trend lines calculated by this procedure can be used as baselines for delta log R technique (*Passey* et. al., 1990).

This well was study at the same Cretaceous-Jurassic interval as in the previous cases. For this section the Gamma Ray was filtered to obtain only values between 80-90 API corresponding to shale with

low organic matter content. Based on this shale-GR, transit time and resistivity logs were filtered to finally calculate the trend lines (***Fig 53***). For each value of depth in the logs, a baseline value was calculated using the equation from the trend line. The values of the baselines were introduced in *Norsk Hydro Spreadsheet* to estimate the TOC.

The study section was divided into 5 intervals, to define the maturity values (LOM; ***Table 3***). The Gamma Ray cutoff (different from the GR Shale) was settled at 70 API (TOC estimation were not calculated for values of GR lower than 70 API).

Table 3: Summary of the intervals and parameter defined in TOC estimation for the well NO 34/8-6 using trend baselines.

INTERVAL	TOP	BASE	Clean GR	BASELINES		%Ro	LOM	
				DT_b	R_b		Suggested	Final
1	2300	2700	70	trend	trend	0,43	6,0	6
2	2700	3000	70	trend	trend	0,48	6,6	7
3	3000	3300	70	trend	trend	0,51	7,0	7
4	3300	3600	70	trend	trend	0,56	7,6	8
5	3600	3900	70	trend	trend	0,59	7,9	8

The results for this approach are shown in ***Figs. 53***, ***54*** and ***55***. According to these results TOC was estimated for the upper Cretaceous with some possible overestimation, whereas in the lower Cretaceous organic content was absent. A very good approximation was accomplished at the Jurassic with respect to the calibration values (***Fig. 55***).

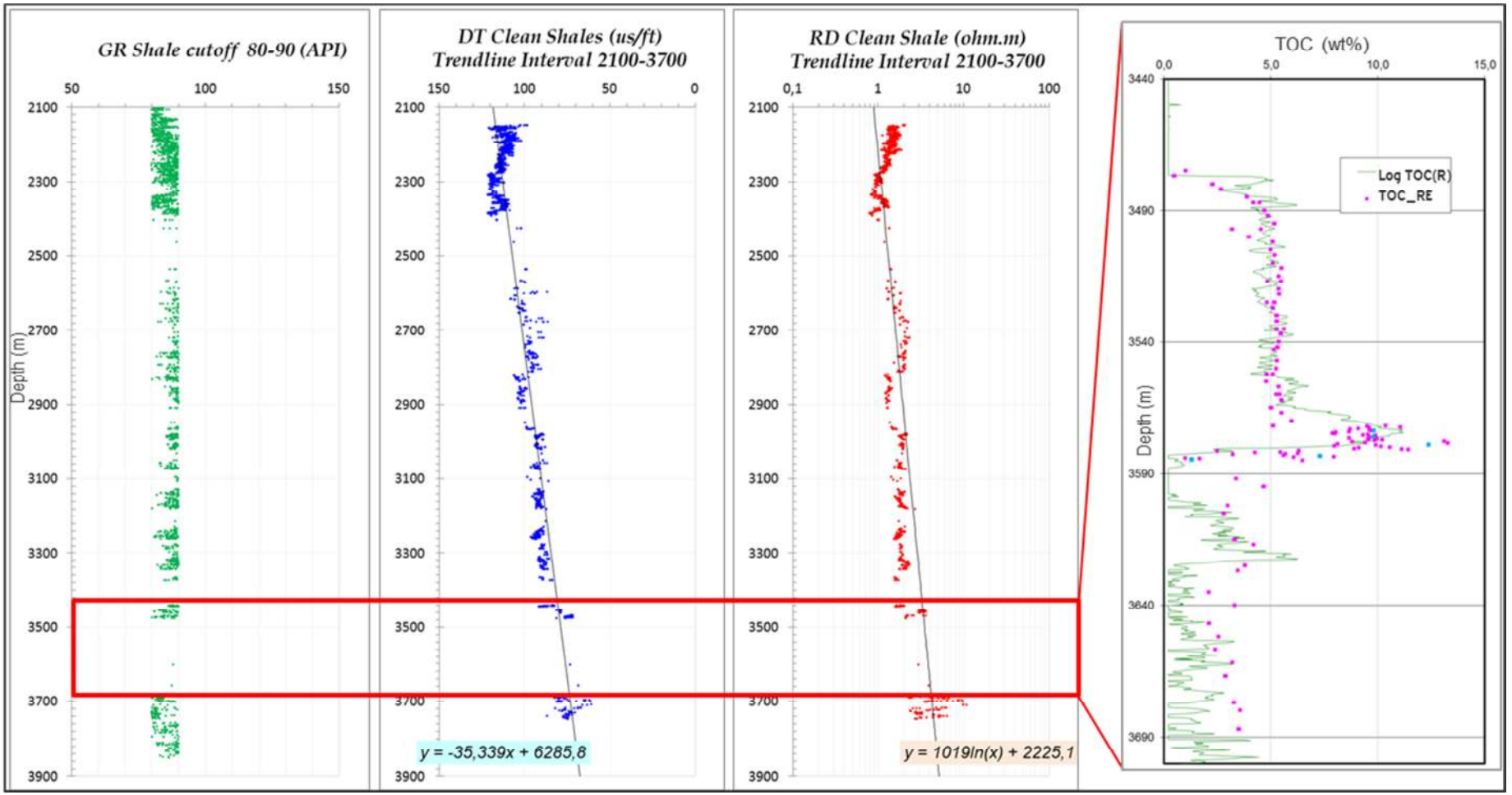

Fig. 53: Trend line definition for interval study in the Well NO 34/8-6, showing Gamma Ray values filtering for shale in a range between 80-90 API and trend baselines for Resistivity and Transit time corresponding to shales defined by the GR. Last track show the calibration results in the Jurassic section using these baselines.

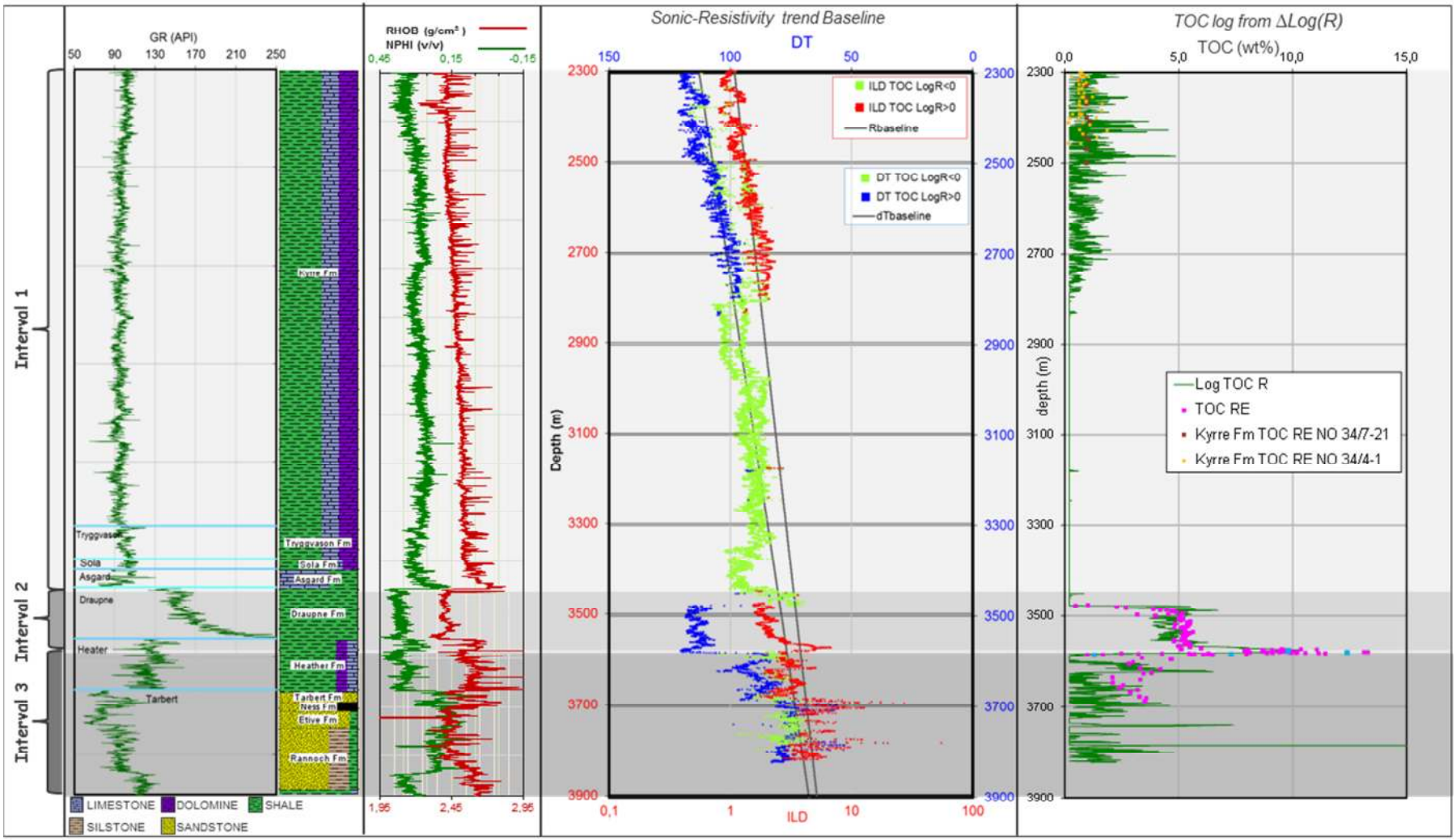

Fig. 54: Results of TOC Calculation using trend lines as baselines. Track 4 (from left to right) shows the result of Transit Time and Resistivity trend obtain from the mentioned logs only for shale values (representing by all the points in the plot) and delta log separation. Values in green indicated that the delta log R used in Passey equation was lower than zero hence TOC was not estimated (for R and DT), points in red are the values of Resistivity were the delta log R was over zero thus TOC values were estimated and the same for blue dots indicated values of Transit time relevant for the TOC estimation or delta log R more than zero.

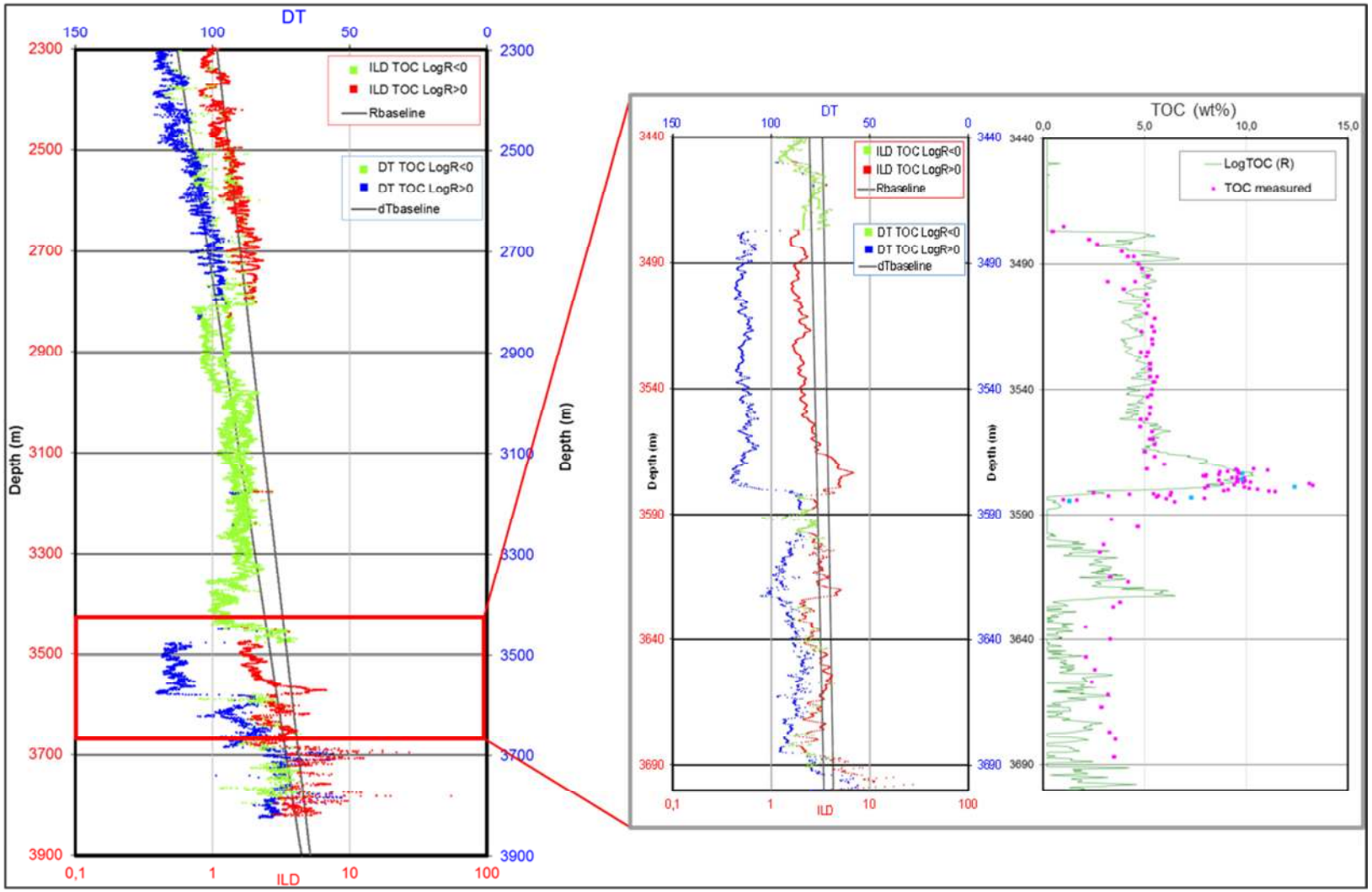

Fig. 55: Results of TOC Calculation using trend lines as baselines. Detail from the previous figure (***Fig. 54***) to show the accuracy obtain at the Jurassic level in comparison with the calibration values.

Since all the values were calculated for each depth in the logs, it was possible to extract the values of TOC estimated at exact the same depths of the calibration data to make a comparison. A correlation exits between both sets of data indicated by the linear correlation and the significant coefficient of correlation value (*r=0,70* and *p>0,05*, ***Figs. 56***).

The differences between both sets of data were determined in order to have a better idea of the accuracy of this method (***Figs. 56***). According to the differences calculated, the majority of the data set have differences of less than 1% in TOC (47% of the data) followed by less of 2% (that correspond to a 27% of the data set), it means that 74 % of the data set has differences less than 2% while the remainder 26% of the data evaluated have differences over 2% in TOC. Values with differences below 2% have a very significant correlation (*r=0,94*, *p<0,05*), this brings up the questions of where are major differences, where are they located and the possible reasons.

With this in mind, it was found that main differences were located in the lower *Draupne Formation* where maximum values of TOC measured are reported (refer also in section 4.2) and also in Heater Formation but with less frequency (***Figs. 57***).

The exploratory data analysis suggest that both sets of data are similar (mean, median, range, maximum are very near) in comparison to the previous approximations (***Fig 58***). Furthermore, a similar relative and cumulative frequency distribution were observed of both sets of data at the *Jurassic* level (***Fig 58***). The relative frequency shows a bimodal distribution in both cases, such as it was also describe in section 4.2 for this section.

In order to analyses the results in detail, the *Jurassic* section was subdivided into three subintervals according to the differences in estimated and measured TOC. According to values for quartiles, maximum and minimum, using boxplots, results for the upper part of *Draupne Formation* are very similar (***Fig 59***). On the other hand the differences observed in the lower part of this formation are more related to the maximum and minimum, while quartiles and median are almost analogous. Unlike *Draupne Formation*, the boxplots for *Heather Formations* indicated a poor relation between measured and estimated values (***Fig 59***).

In the same manner, frequencies were recalculated for each subinterval, in which very similar relative and cumulative distribution were observed for *Draupne Formation* but not for *Heater Formation* (***Fig 60***).

Finally the Quantile-Quantile plot of the percentiles, comparing the distribution of TOC measured and estimated, shows departure from the y=x curve for lower values than approximately 4% of TOC and over 10% of TOC, which indicated different distributions for values outside of the range of 4% to 10% of TOC (***Fig 61***).

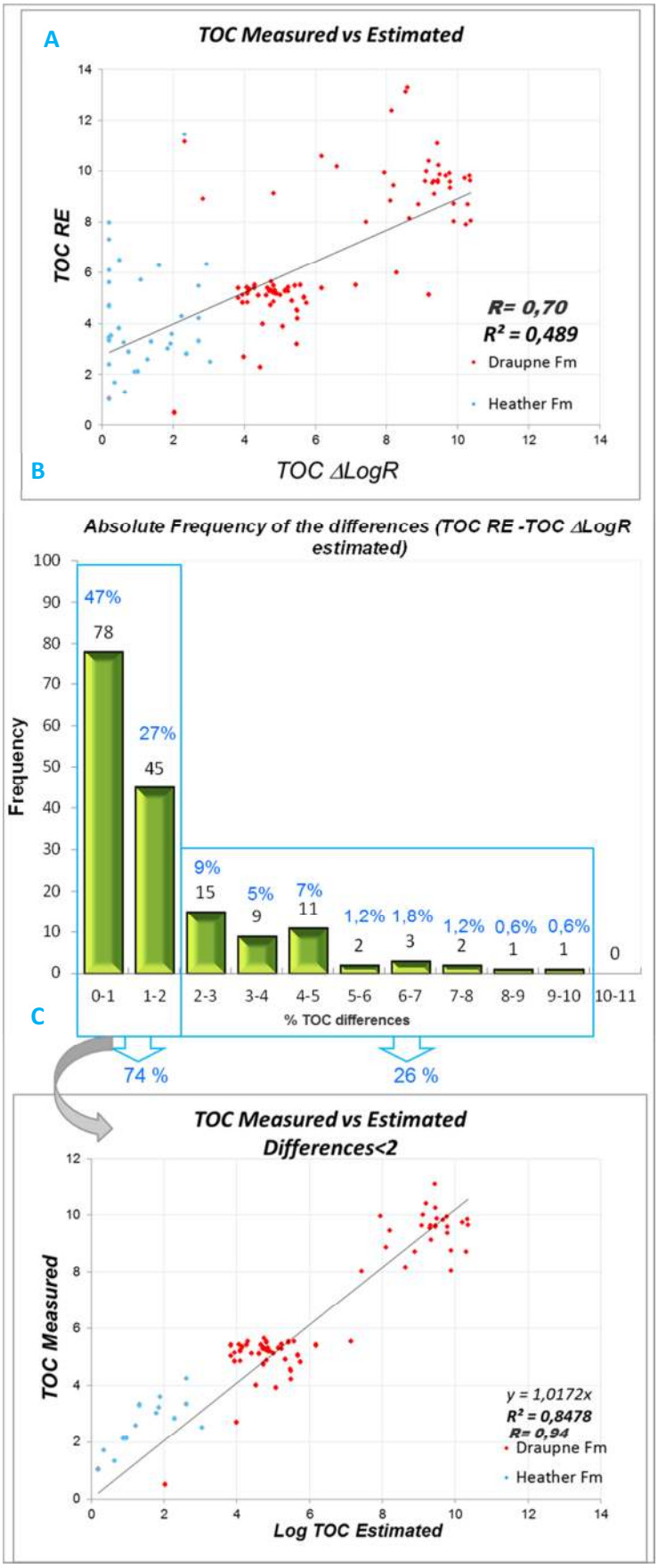

Fig. 56: **A.** Results of linear correlation between TOC estimation and TOC measured from Rock Eval. **B.** Histogram of the absolute frequencies of the differences between TOC estimated and measured. **C.** Linear correlation of the differences (TOC RE and TOC measured)

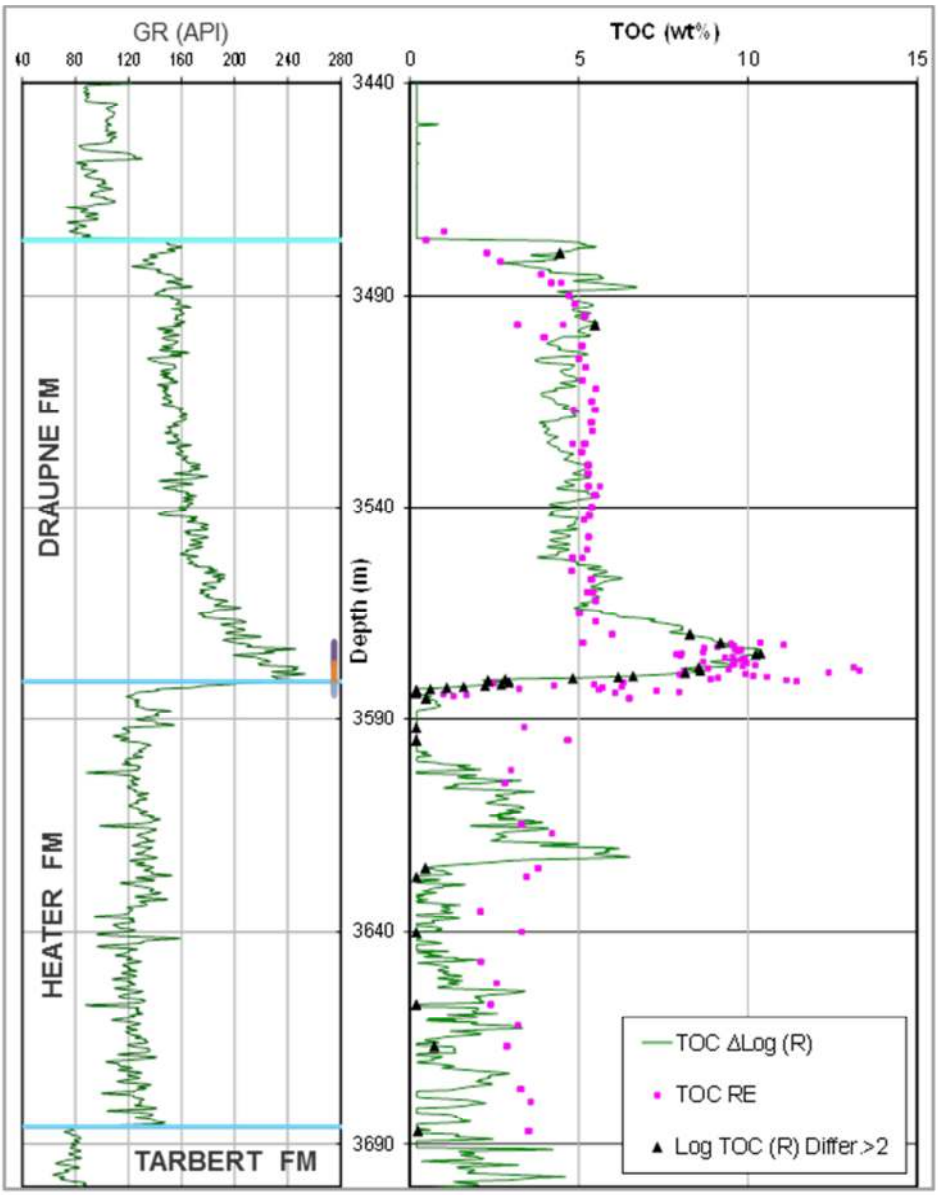

Fig. 57: Calibration between TOC measured and estimated showing positions in which the differences were more than 2% of TOC (black triangles), in the well NO 34/8-6.

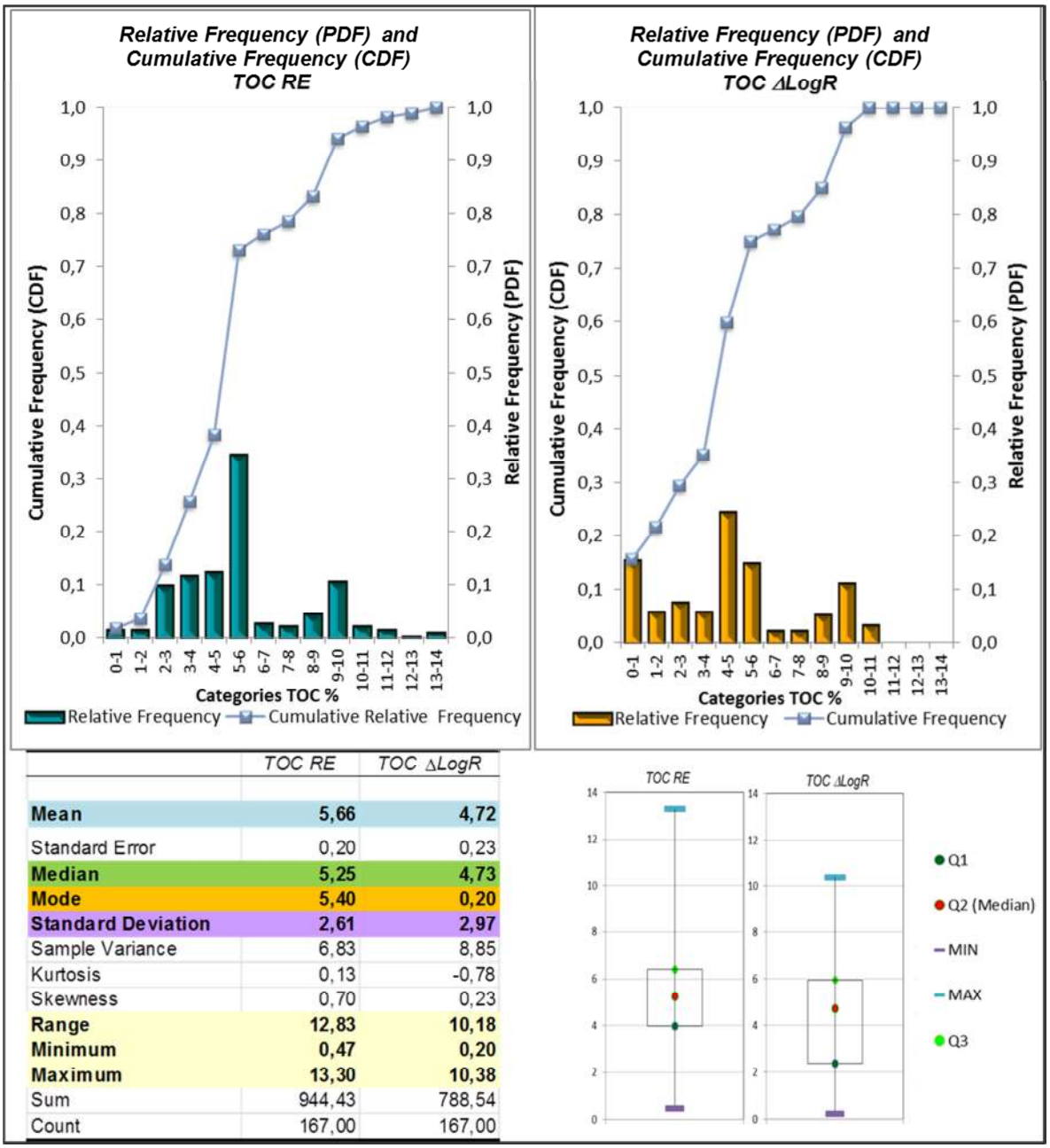

	TOC RE	TOC ΔLogR
Mean	**5,66**	**4,72**
Standard Error	0,20	0,23
Median	**5,25**	**4,73**
Mode	**5,40**	**0,20**
Standard Deviation	**2,61**	**2,97**
Sample Variance	6,83	8,85
Kurtosis	0,13	-0,78
Skewness	0,70	0,23
Range	**12,83**	**10,18**
Minimum	**0,47**	**0,20**
Maximum	**13,30**	**10,38**
Sum	944,43	788,54
Count	167,00	167,00

Fig. 58: Comparison of relative and cumulative frequency distribution for TOC RE and TOC from logs in the well NO 34/8-6, showing similar bimodal distribution. At the bottom to the left, the summary results of exploratory data analysis also indicate similarities in both set of data. At the right bottom, boxplots represents quartiles (Q1, Q2 and Q3), maximum and minimum values for visual comparison.

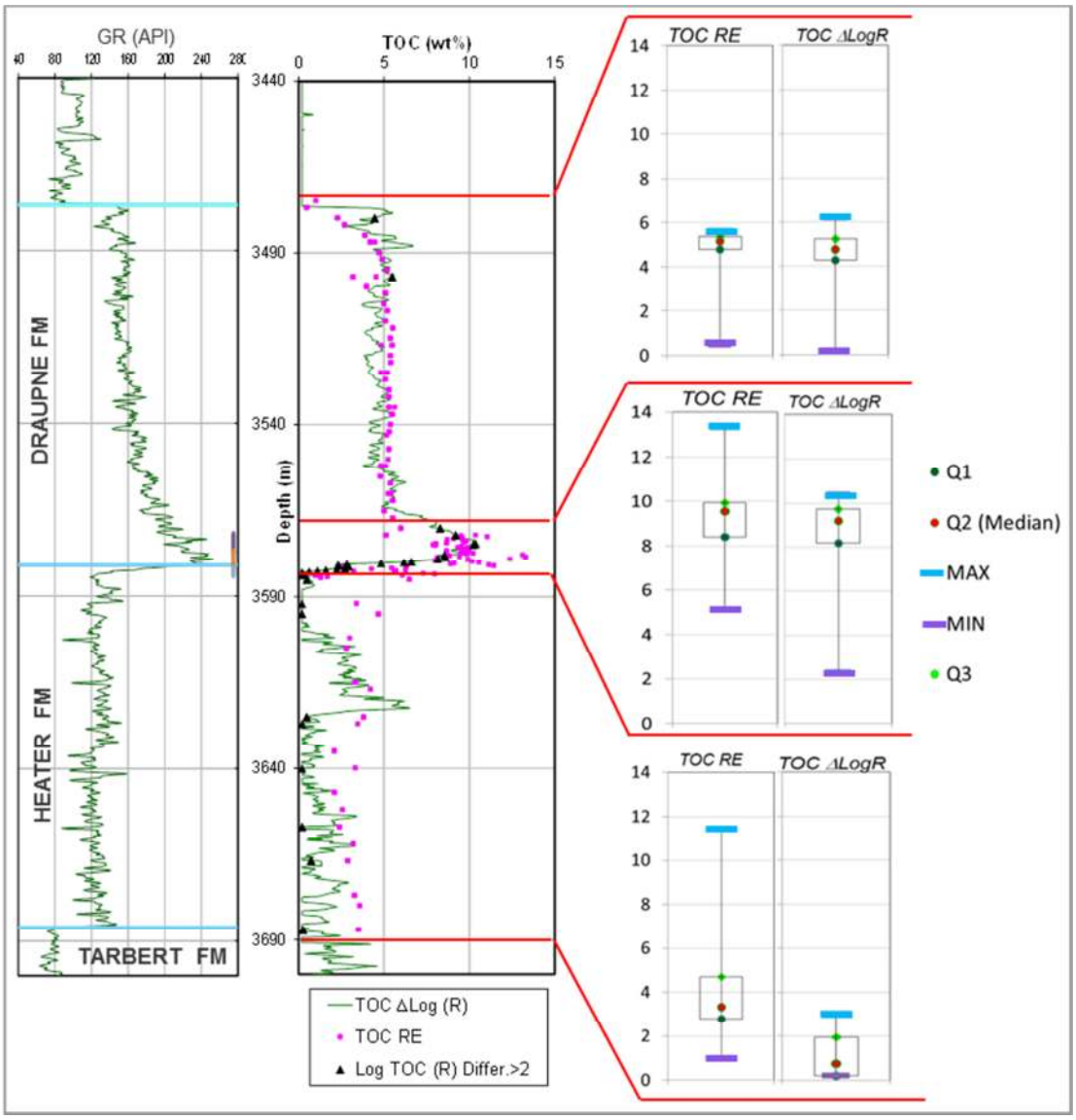

Fig. 59: Comparison boxplots representing quartiles (Q1, Q2 and Q3), maximum and minimum values for subintervals in the Jurassic section, well NO 34/8-6.

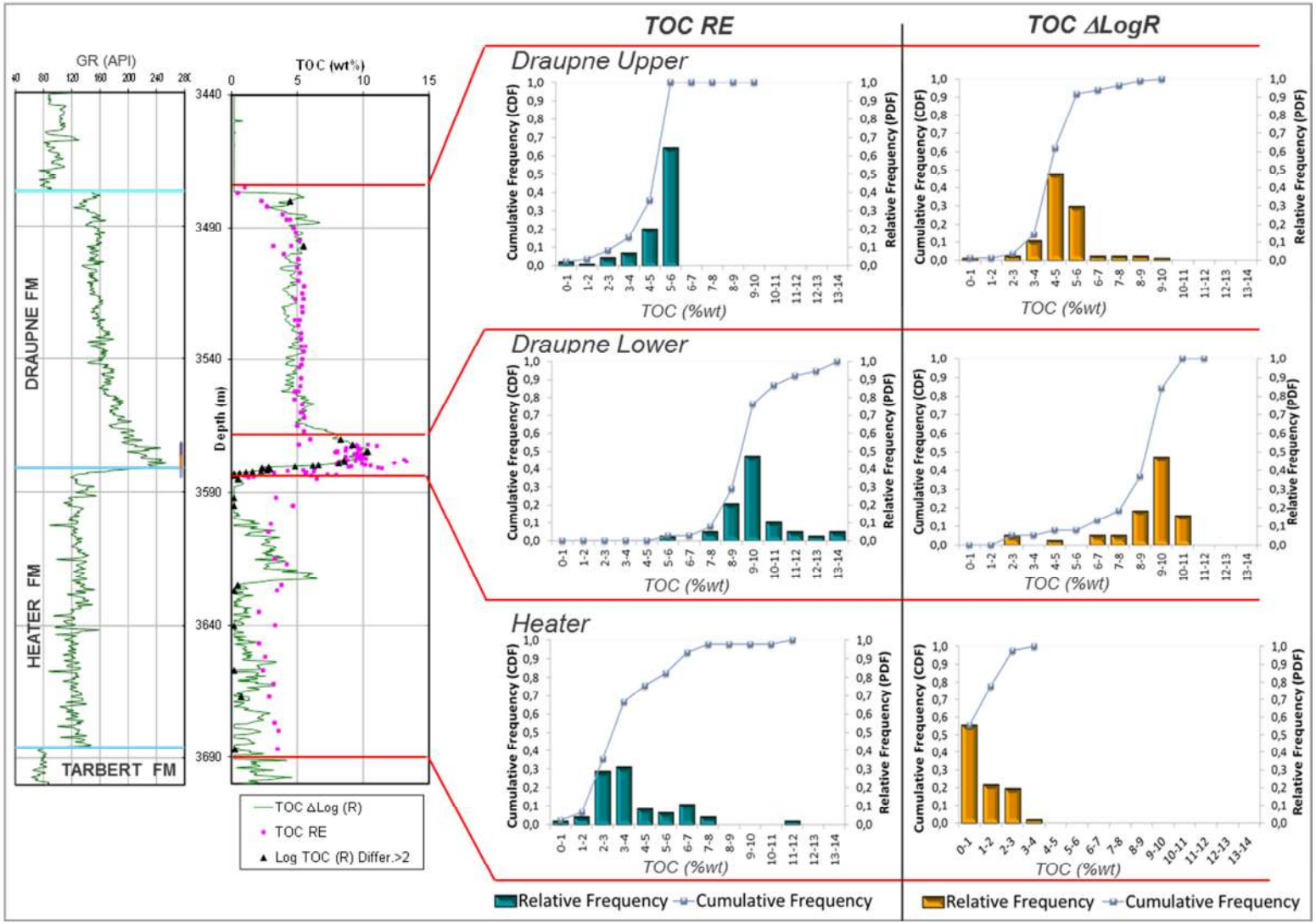

Fig. 60: Comparison of relative and cumulative frequency distribution for TOC RE and TOC from logs in subintervals at the Jurassic level in the well NO 34/8-6.

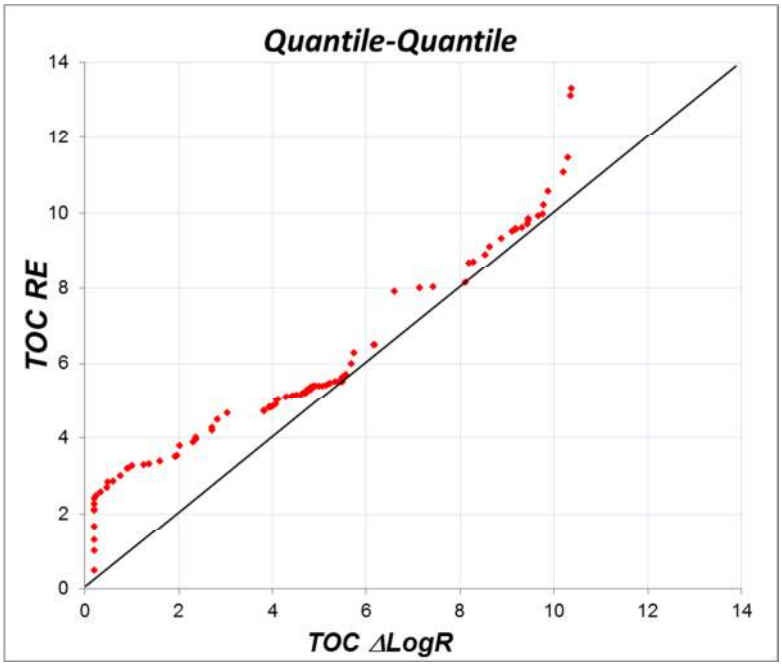

Fig. 61: Quantile-Quantile plot of percentiles comparing the distribution of TOC measured and estimated in well 34/8-6. Departure of values from the y=x curve indicates different distributions.

Results Well NO 7120/12-1

Using the trend technique, this well was studied at the same *Cretaceous-Jurassic-Triassic* interval as in the previous cases. For this section the Gamma Ray was filtered to obtain only values between 80-90 API considering to correspond with shale with low organic matter content. Based on this shale-GR, values of transit time and resistivity were extracted for the same shales follow by the trend lines calculation as it was explained in the previous well. In this case due to the fact that the study section includes a thick interval, two main trends were defined: one at the *Cretaceous-Jurassic* interval and a second interval at the *Triassic* section.

Since it was a requirement in the spreadsheet format, it was necessary to created three intervals for maturity values (LOM) (***Table 4***). The Gamma Ray cutoff (different from the GR Shale) was settled at 60 API (TOC estimation were not calculated for values of GR lower than 60 API).

Table 4: Summary of the intervals and parameter defined in TOC estimation for the well NO 7120/12-1 using trend baselines.

INTERVAL	TOP	BASE	Clean GR	BASELINES		%Ro	LOM	
				DT_b	R_b		Suggested	Final
1	25	1666,7	60	trend	trend	1,23	9,2	6
2	1666,7	2095	60	trend	trend	0,49	6,7	7
3	2095	3043,00	60	trend	trend	0,53	7,3	8

Results of trend baselines and calibration for interval 1 and 2 are summarized in ***Fig 62, 63*** and ***64.*** In the first interval, for section between 700m and 1500m, the estimated curve does not proper fit calibration values. Within this section the interval between approximately 1000 to 1200 m was not calculated due to the Gamma Ray values were below the cutoff for estimation (less than 60 API), in other words this interval (not calculated) is mostly composed of sandstones beds. Measured values maybe are related to thin shales layers out of the resolution of logs. The second part of the interval 1, below 1500 have a very good approach, estimated curve in this interval show a good approximation very similar to previous results (*Section4.2*).

Approximations in interval 2 were very different to calibration values, such as in previous cases. As it was explained in section ***4.2*** the heterogeneity related to the logs and TOC measured values in this interval is very difficult to reproduce. The differences in resolution between measured data in cores compared with logs may have something to do with these results. It can be observed that again at some sections TOC was not estimated because of the Gamma Ray cutoff or simply because not delta log separation was obtained according to the baselines (***Fig 63*** and ***64***).

The statistical analysis was also carried out in this well. A weak correlation between measured and estimated values was found for the entire section study (*r=0,47; p<0,05*, ***Fig 65A***). Separating the section by age and according to correlation coefficients, the *Jurassic* interval also indicated a weak correlation (*r=0,38; p<0,05*) while *Cretaceous* and *Triassic* intervals show a very weak correlation (r<0,30) (***Fig 65B, C, D***).

Frequencies distributions for the whole data set for both calibration and estimated values are shown in ***Fig 66***. A very similar unimodal distribution was obtained in both cases with the largest amount of data falling in the range between 0-15% of TOC. Main differences observed in the statistic summary and boxplots are related to higher values (TOC over 40%) that are reported in the measured data within the *Triassic* interval and may be related to coals from *Nordmela* and *Fruholmen Formations* (***Fig 66***).

According to the boxplots (***Fig 67***), major differences are related to the *Cretaceous* and *Triassic* interval, such as is expected base on previous observations, while in the *Jurassic* section minimum and quartiles are very similar except for the maximum which is related to the possible coals mentioned above (***Fig 67***).

The same statistical behavior by age sequence was observed in the frequencies distributions (***Fig 68***). The frequencies distributions showed that again, *Triassic* and *Jurassic* intervals do not converge when comparing relative and cumulative frequencies of TOC values, while the estimated values of TOC from logs in the *Jurassic* section reproduce a very similar distribution except for the maximum values reported from Rock Eval data.

The Quantile-Quantile plot of percentiles comparing the distribution of TOC measured and estimated shows that lower values than approximately 4% of TOC indicated a different in spread and likely the previous case values over 10% of TOC have a departure from the y=x curve indicated different distributions (***Fig 69***).

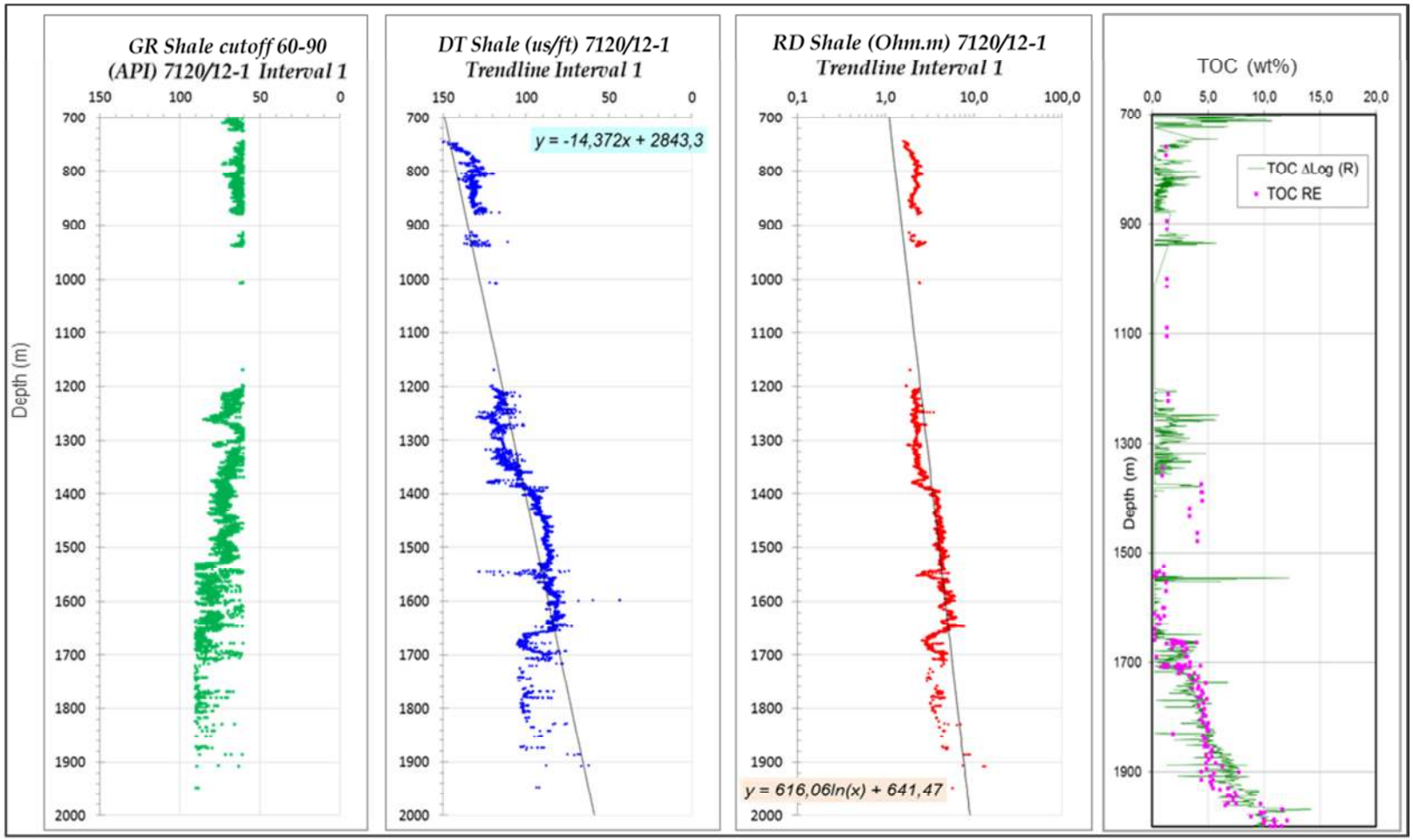

Fig. 62: Trend line definition for interval 1 in the Well NO 7120/12-1, showing Gamma Ray values filtering for shale in a range between 60-90 API and trend baselines for Resistivity and Transit time corresponding to shales defined by the GR. Last track show the calibration results in the Cretaceous -Jurassic section using these baselines.

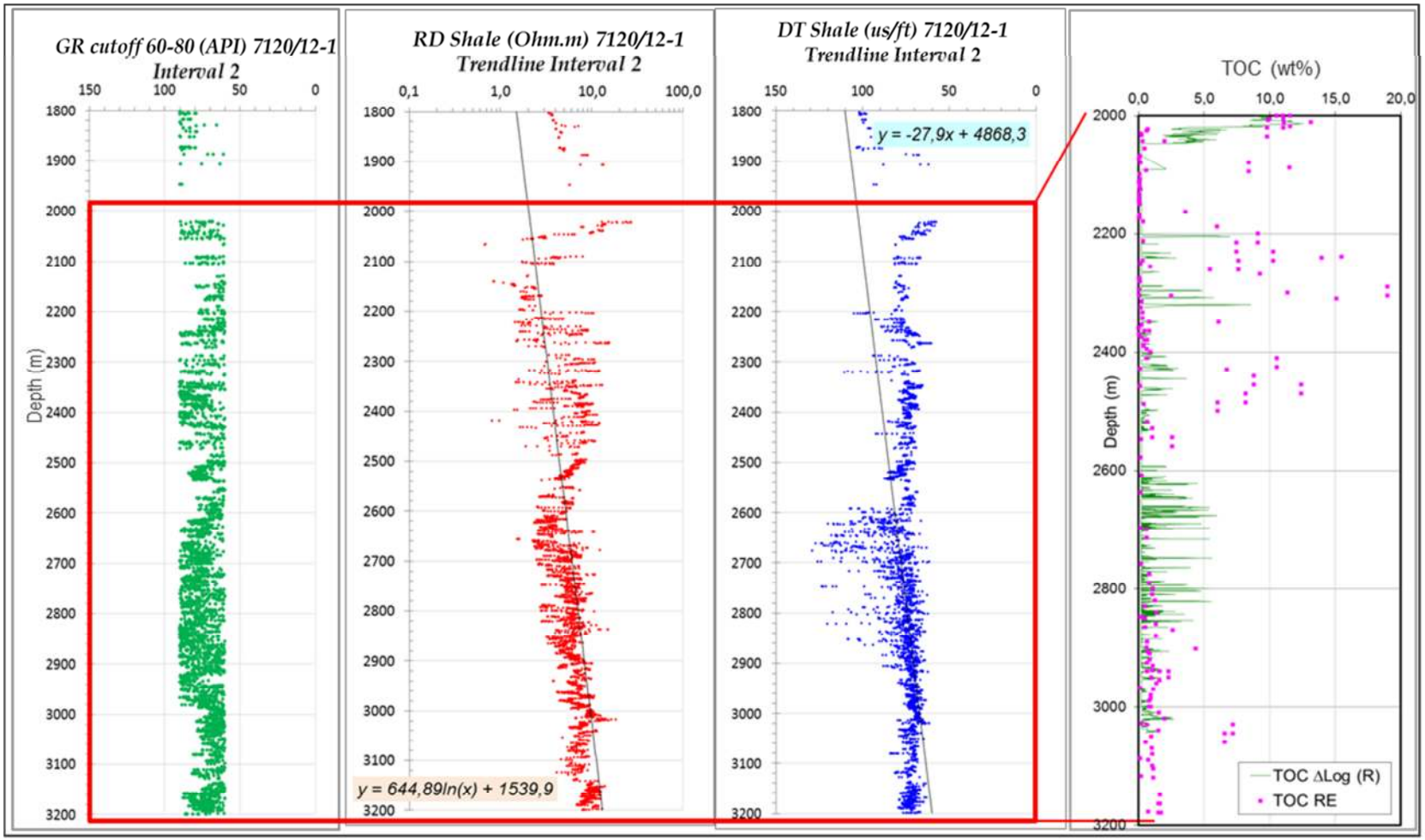

Fig. 63: Trend line definition for interval 2 in the Well NO 7120/12-1, showing Gamma Ray values filtering for shale in a range between 60-90 API and trend baselines for Resistivity and Transit time corresponding to shales defined by the GR. Last track show the calibration results in the Triassic section using these baselines.

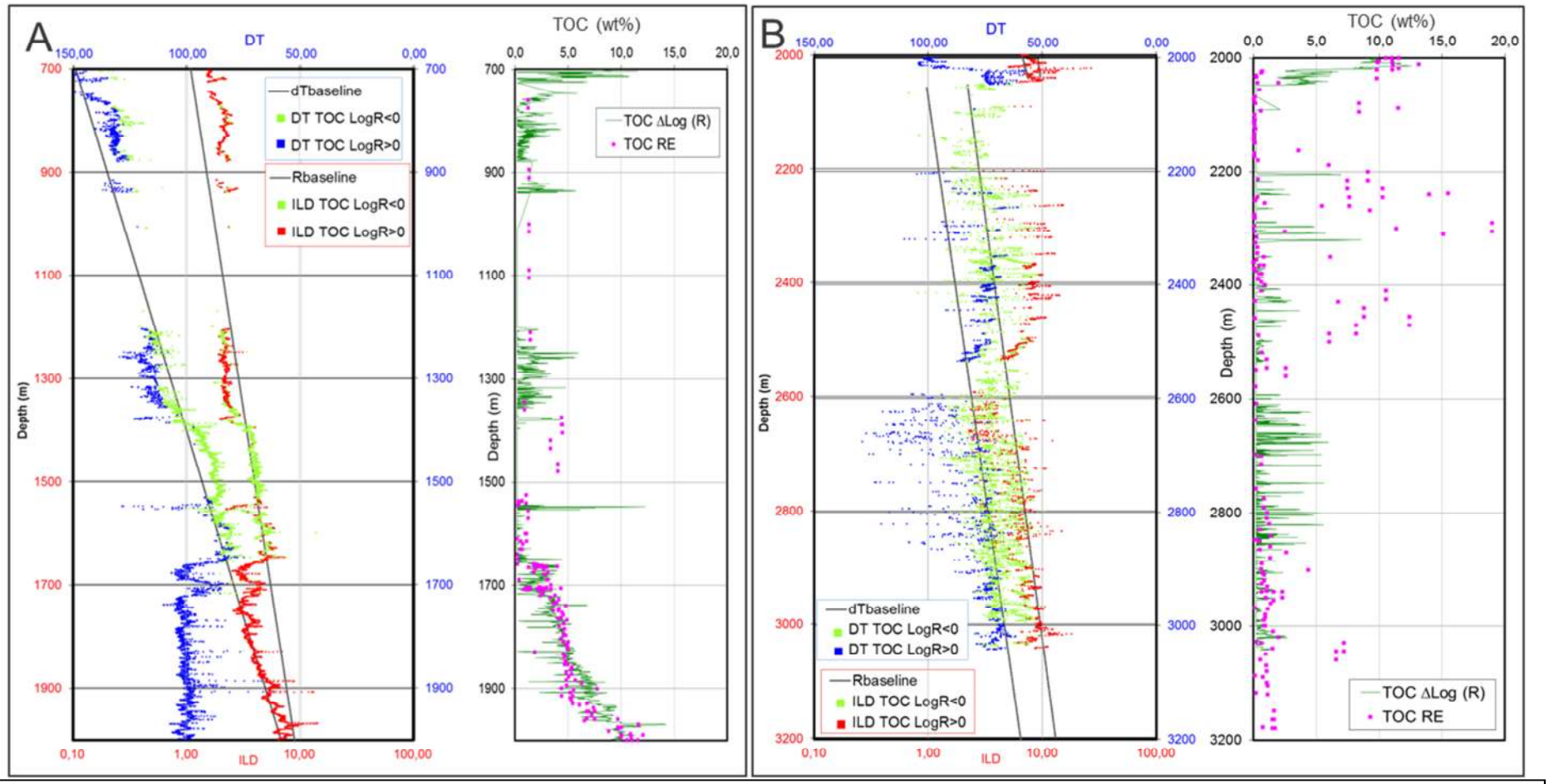

Fig. 64: Results of TOC Calculation using trend lines as baselines, well NO 7120/12-1. Result of Transit Time and Resistivity trend obtain from the mentioned logs only for shale values (representing by all the points in the plot) and delta log separation. Values in green indicated that the delta log R used in Passey et al. equation was lower than zero hence TOC was not estimated (for R and DT), points in red are the values of Resistivity were the delta log R was over zero thus TOC values were estimated and the same for blue dots indicated values of Transit time relevant for the TOC estimation or delta log R more than zero. **A.** Interval 1 showing the estimation and calibration. **B.** Interval 2 with estimation and its respective calibration.

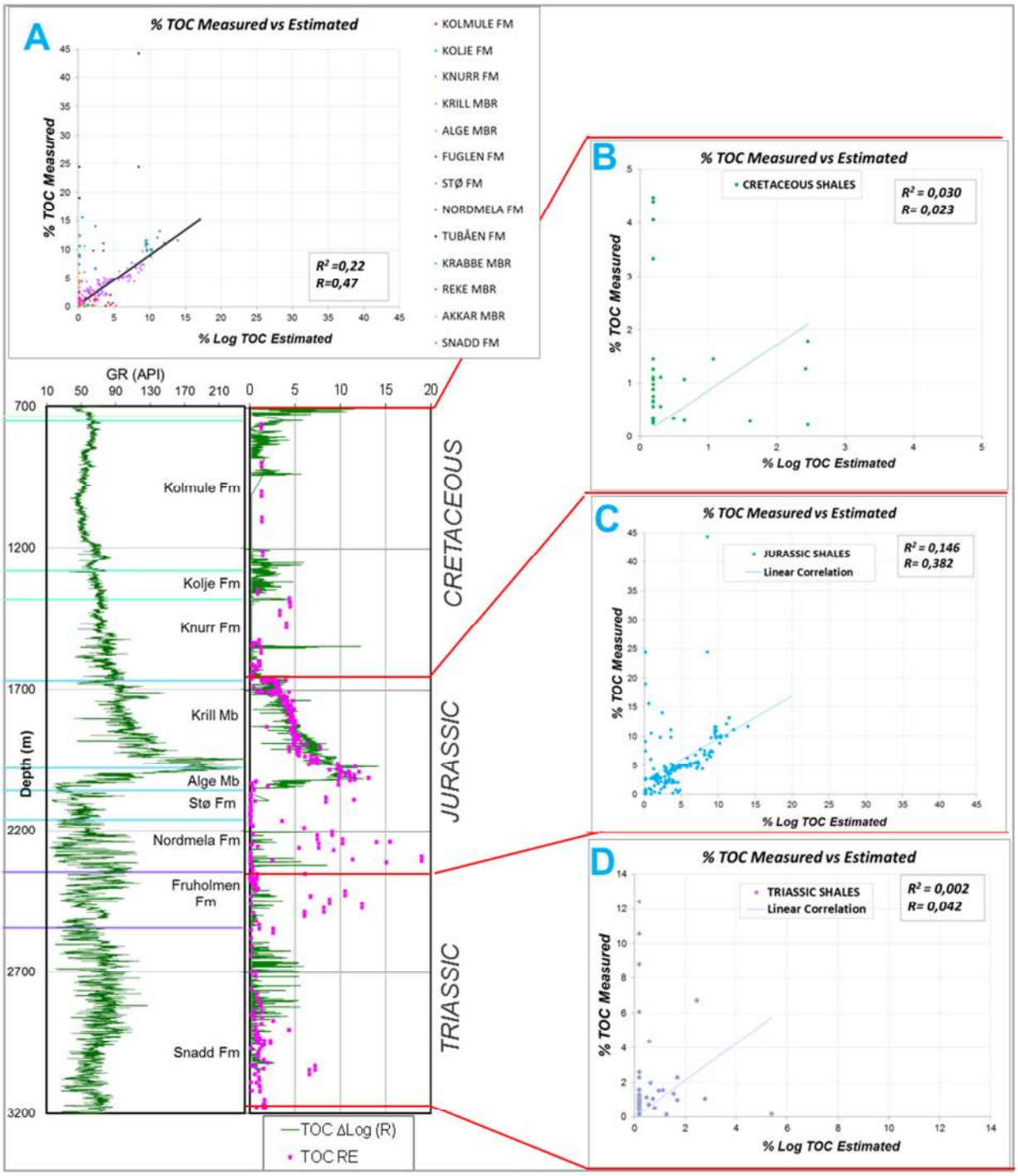

Fig. 65: Results of linear correlation between TOC estimation and TOC measured from Rock Eval, for the entire interval (**A**) and for Cretaceous (**B**), Jurassic (**C**) and Triassic (**D**) intervals, in the well NO 7120/12-1.

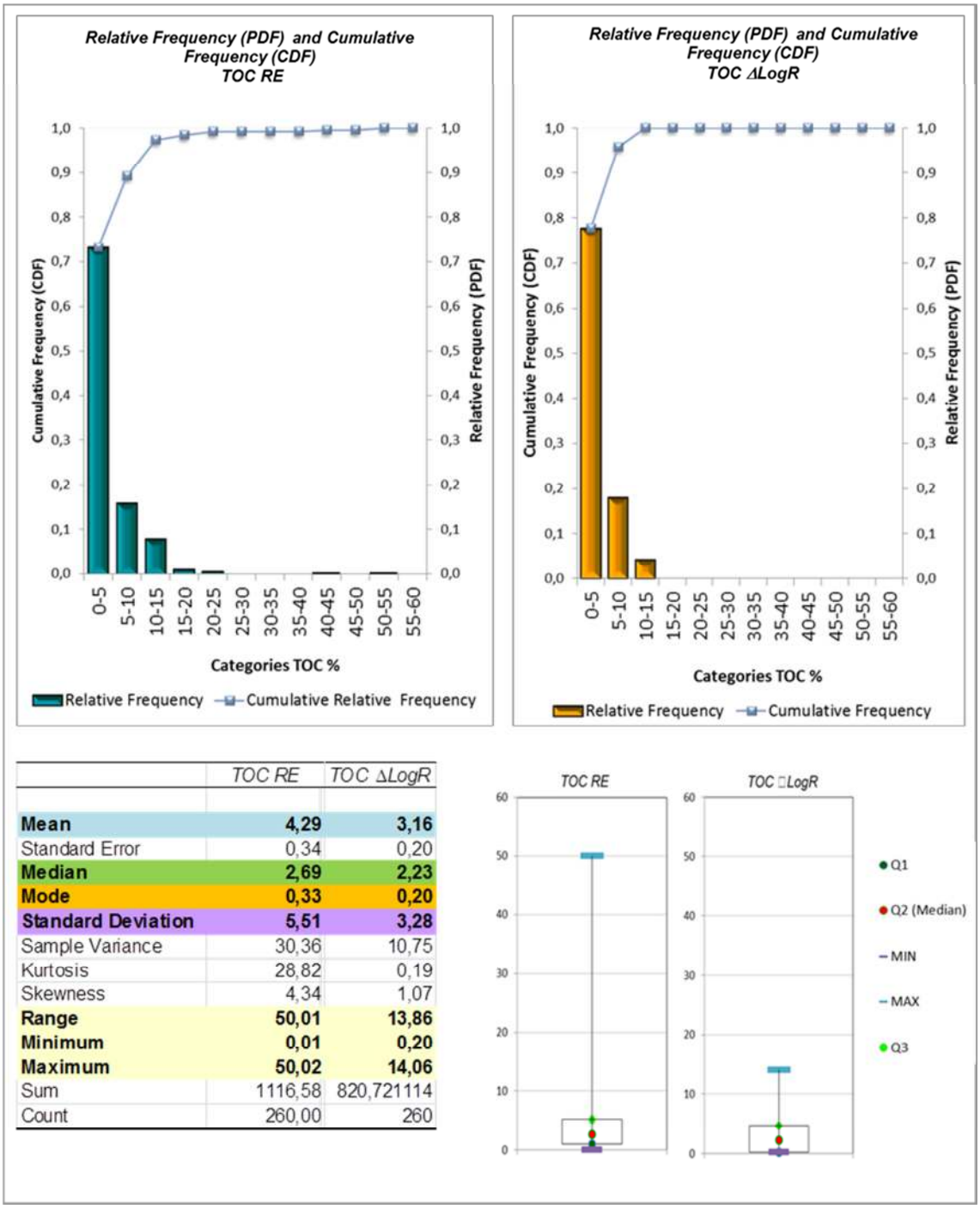

	TOC RE	TOC ΔLogR
Mean	**4,29**	**3,16**
Standard Error	0,34	0,20
Median	**2,69**	**2,23**
Mode	**0,33**	**0,20**
Standard Deviation	**5,51**	**3,28**
Sample Variance	30,36	10,75
Kurtosis	28,82	0,19
Skewness	4,34	1,07
Range	**50,01**	**13,86**
Minimum	**0,01**	**0,20**
Maximum	**50,02**	**14,06**
Sum	1116,58	820,721114
Count	260,00	260

Fig. 66: Comparison of relative and cumulative frequencies distribution for TOC RE and TOC from logs in the well NO 34/8-6, showing similar distributions. At the bottom to the left, the summary results of exploratory data analysis. At the right bottom, boxplots representing quartiles (Q1, Q2 and Q3), maximum and minimum values for visual comparison.

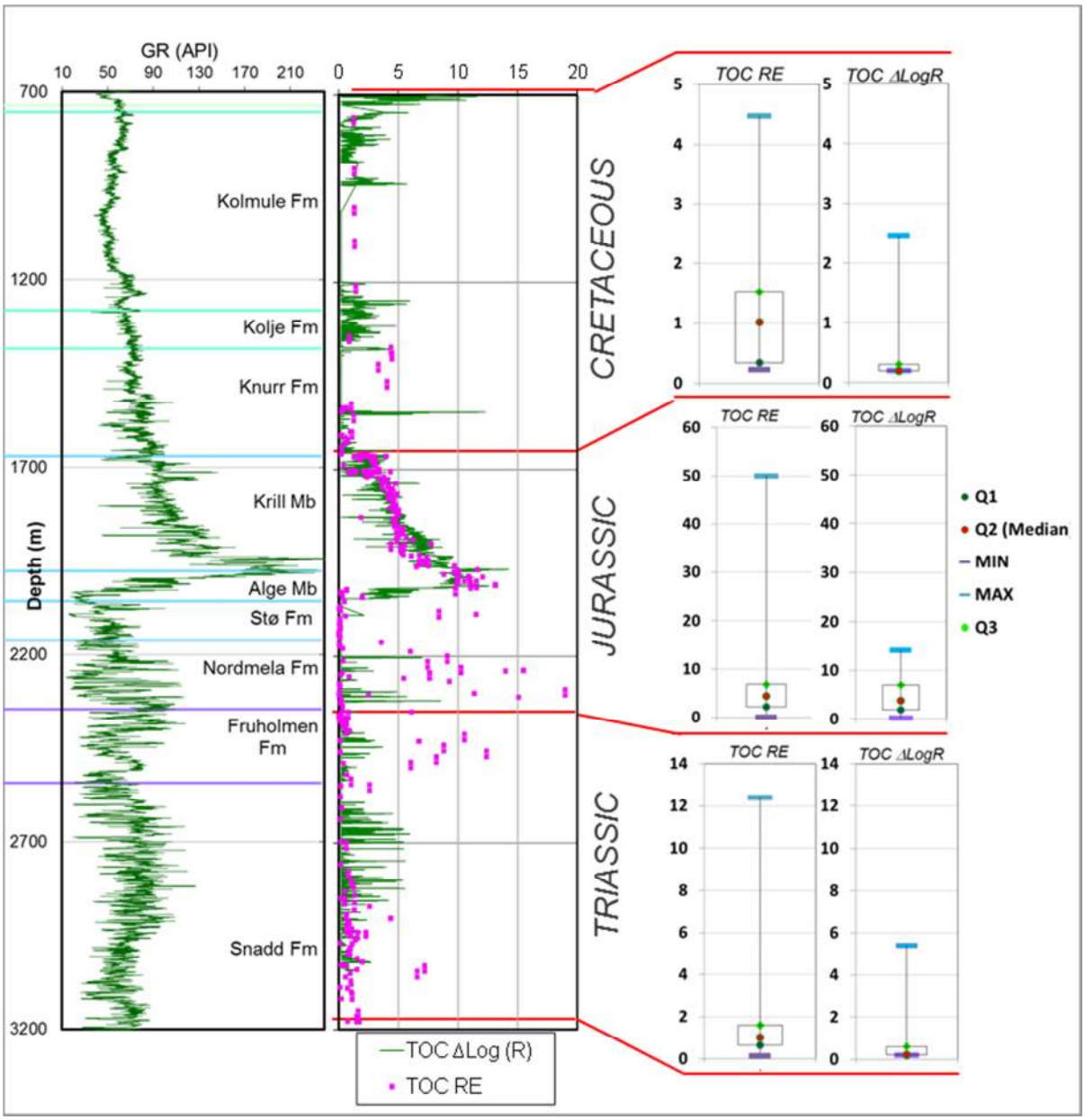

Fig. 67: Comparison of boxplots representing quartiles (Q1, Q2 and Q3), maximum and minimum values for the Cretaceous, Jurassic and Triassic intervals, in the well NO 7120/12-1.

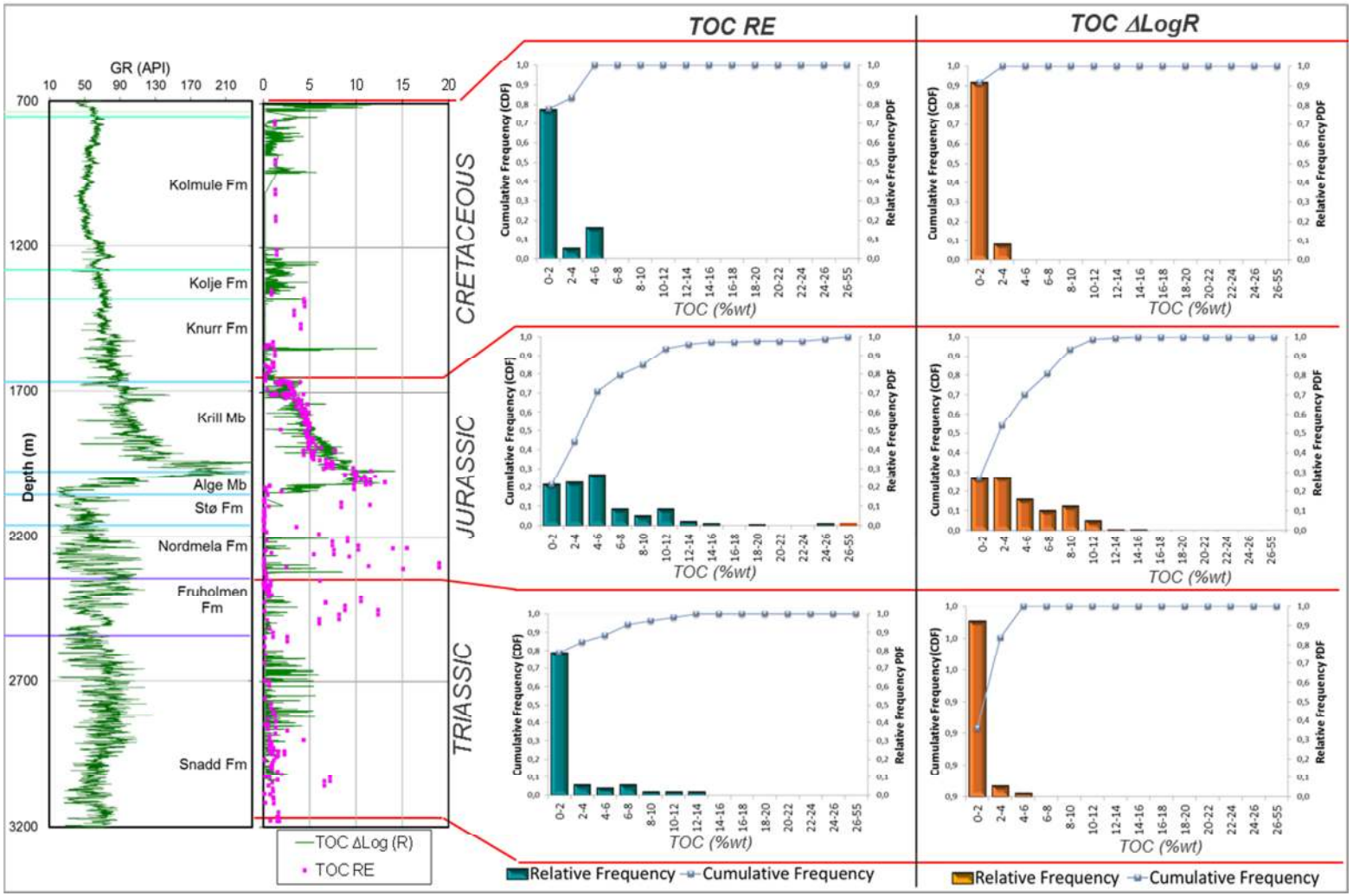

Fig. 68: Comparison of relative and cumulative frequency distribution for TOC RE and TOC from logs for the Cretaceous, Jurassic and Triassic intervals, in the well NO 7120/12-1.

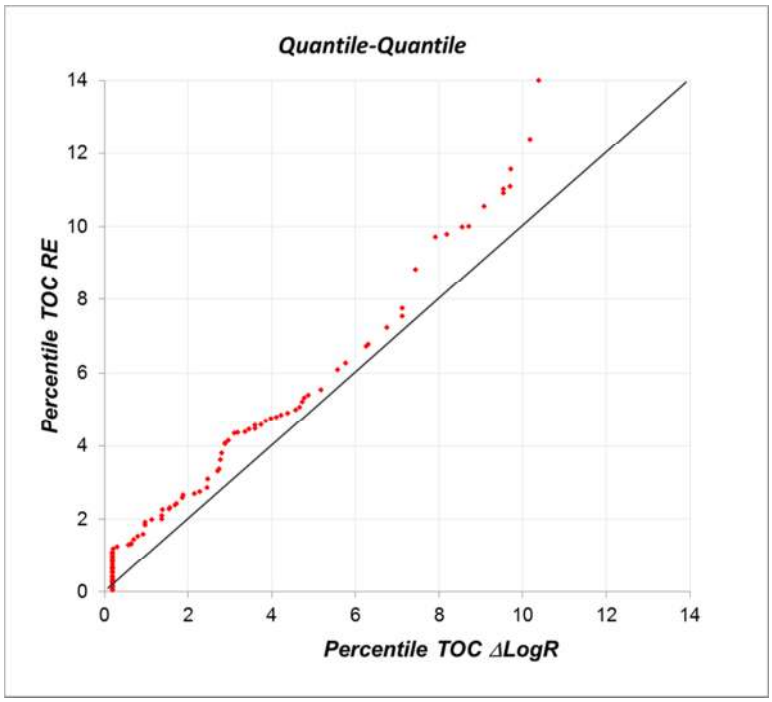

Fig. 69: Quantile-Quantile plot of percentiles comparing the distribution of TOC measured and estimated in the well NO 7120/12-1. Departure of values from the y=x curve indicated different distributions.

Advantages and limitations of the Software and Procedure

Main advantage using this tool (*In-house spreadsheet solution*) is related to the flexibility in the manipulation of the data which implied a complete manual procedure that allowed to a deeply evaluation of the methodology and to test new insights that were not possible in the previous tool described.

With regards to the trend baseline approximations, it has reasonable solid bases to define values of baselines and avoids subjective and long procedures.

4.4 Multiple Linear Regression Model (MLR)

With the purpose of determining the best predictor of TOC from log response, a multiple stepwise regression was carried out as was described in the methodology section. As independent variables the response of Gamma Ray, Resistivity and Transit time logs were included in the analysis. These responses were directly compared with the values of TOC measured from *Rock Eval* (or dependent variable). Only data from the well 34/8-6 was included in this analysis. The variables (Gamma Ray, Transit time and Resistivity logs) were selected using the forward selection with an F to enter of 4.00 and an F to remove equal to 3.99 ($p<0.05$).

The multiple regression analysis showed that 62% of the variation of TOC RE is explained by the variation in GR, DT and R, represented by the multiple coefficient of determination adjusted (adjusted R^2, ***Table 5***). The relationship of each of the variables with TOC RE was calculated using a simple regression (***Fig 70***) indicating a positive correlation in each case. The gamma Ray log indicated a strong correlation with TOC values (*r=0,75, p<0,05*) compared to Transit time and Resistivity logs that showed lower dependency (*r≈0,5*) (***Fig 70***).

Table 5: Determination coefficients of the Regression Model

R	R^2	Adjusted R^2	F	p	Standard Error of the estimate
0,7967	0,6347	0,6238	58,487	0,0000	1,1143

In this model, the t-statistic test for values of the partial regression coefficient standardized (B) showed that the variation of TOC RE was significant and positive related with the variation of all variables considered (***Table 6***) and produce the following prediction equation:

$$\boldsymbol{TOC} = -5{,}39 + 0{,}02\boldsymbol{GR} + 0{,}78\boldsymbol{R} + 0{,}047\boldsymbol{DT}$$

Table 6: Regression Model for dependence variable: TOC RE. Beta: partial regression coefficient; B: partial regression coefficient standardized; t: statistic test; p-level: level of significance of t-test.

	Beta	Std.Err.	B	Std.Err.	t	p-level
Intercept			-5,39682	1,266864	-4,25999	0,000046
GR (API)	0,353085	0,132945	0,02089	0,007864	2,65588	0,009194
R (ohm.m)	0,418434	0,098025	0,78859	0,184740	4,26863	0,000044
DT (us/ft)	0,338669	0,125273	0,04650	0,017200	2,70344	0,008053

Using this equation to predict the TOC values from logs reproduce the same trend curve of TOC, although values are possible to be overestimated in some intervals. ***Figs 71*** and ***72*** show the results for the two wells studied, same approximation was observed using well data from different basins: *Visund* in the North Sea and *Trom I* in the Barents Sea. Major values obtained with the Regression Model corresponds to intervals with high values of TOC, in spite of in both cases the values of TOC were overestimated compared to measured TOC from Rock Eval. However, in general term a good approximation was obtain using a method statistically based completely different from empirical techniques, furthermore results in heterogeneous intervals are better reproduce like *Heather Formation* in the well NO 34/8-6 and the Triassic section in the well NO 7120/12-1(***Figs 71, 72***).

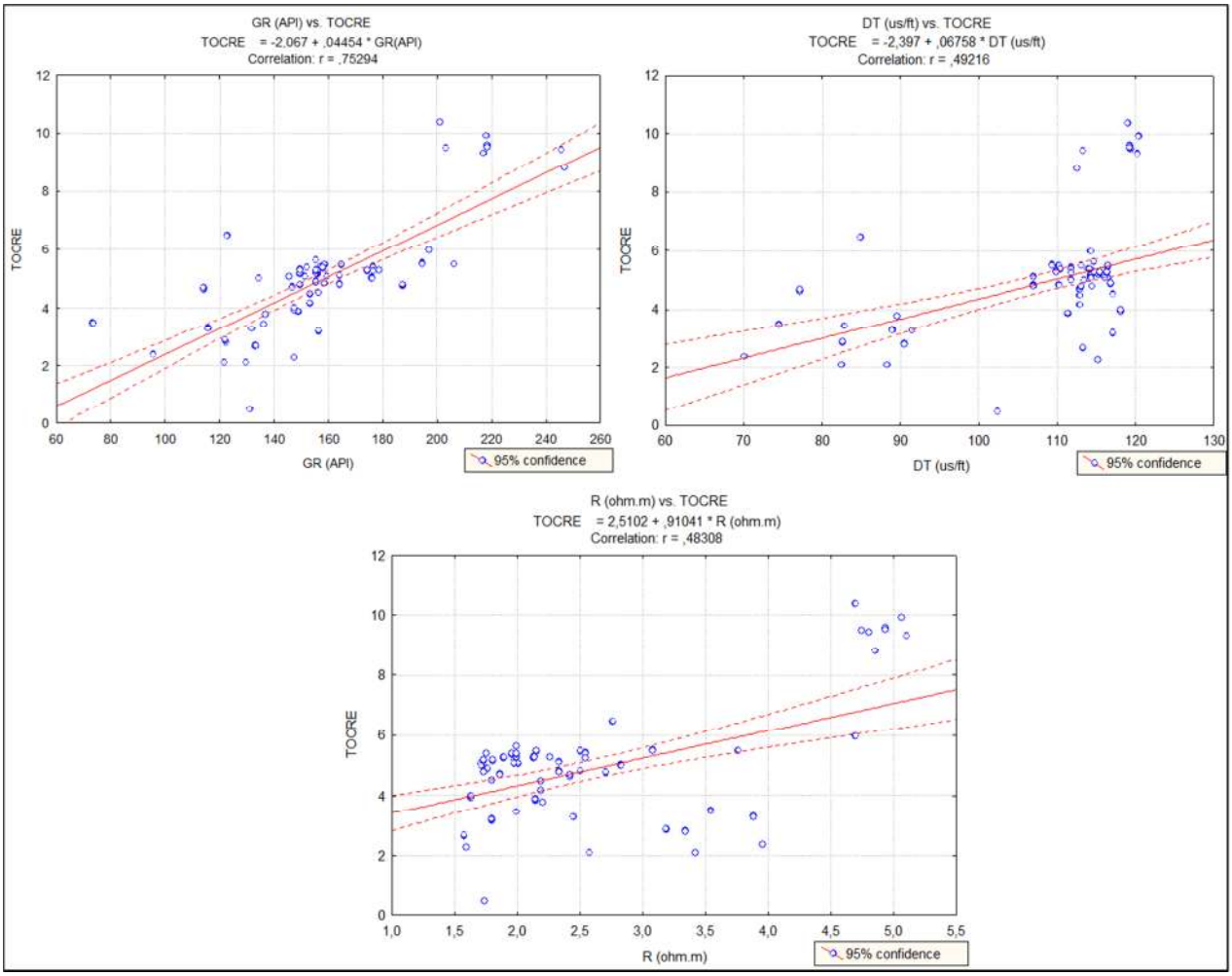

Fig. 70: Scatter plot of linear regression for each independent variable (Gamma Ray, Resistivity and Transit Time) against TOC RE showing the confident interval and the correlation coefficient.

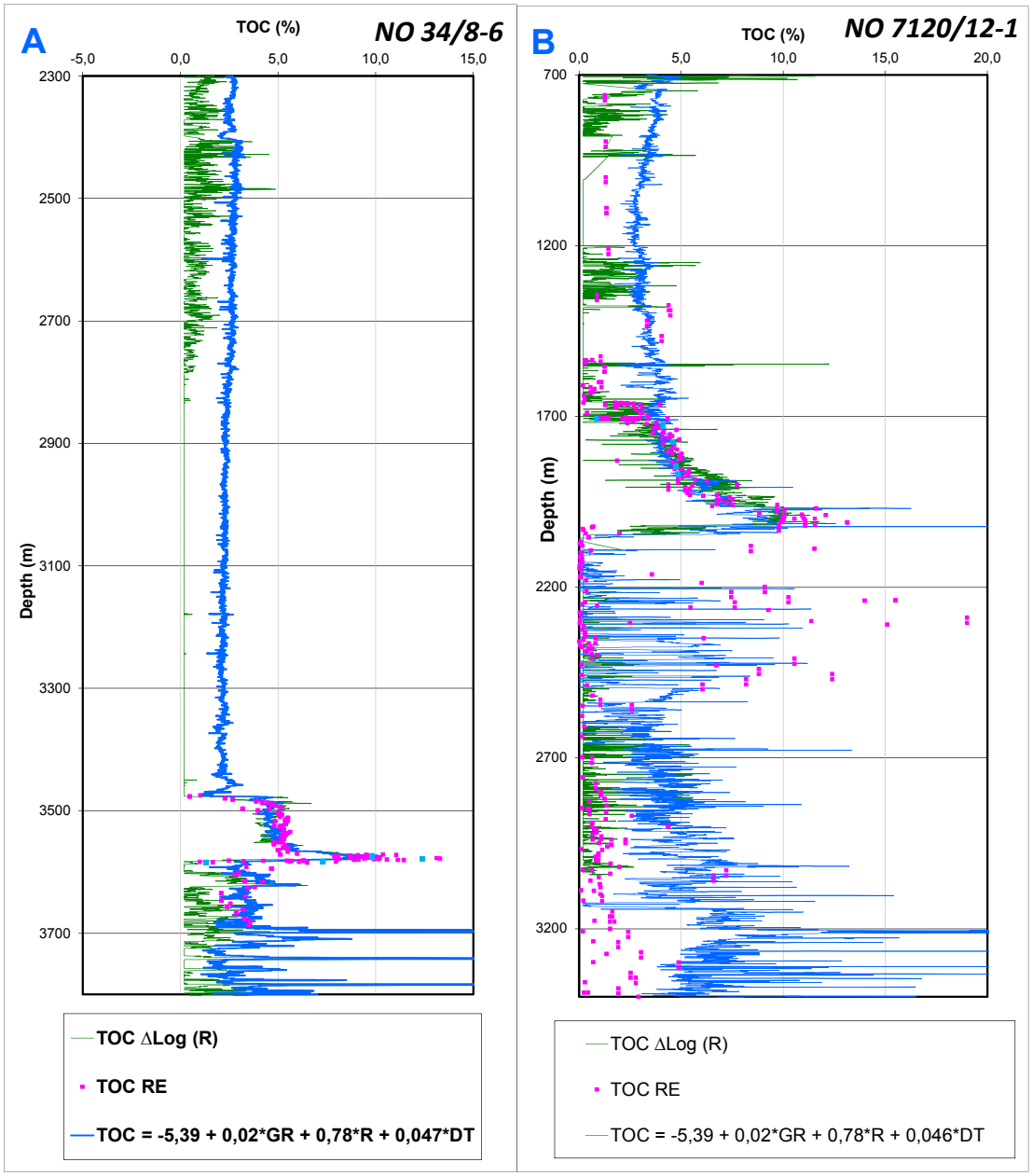

Fig. 71: Comparison of the results of Delta log R and Multiple Regression models as TOC predictors. In Green TOC curve from Delta Log R, in blue TOC values from Multiple Regression Model, in pink TOC measured values from Rock Eval. **A.** Data from the well NO 34/8-6, Visund area, North Sea. **B.** Data from well NO 7120/12/1, Troms I area, Barents Sea.

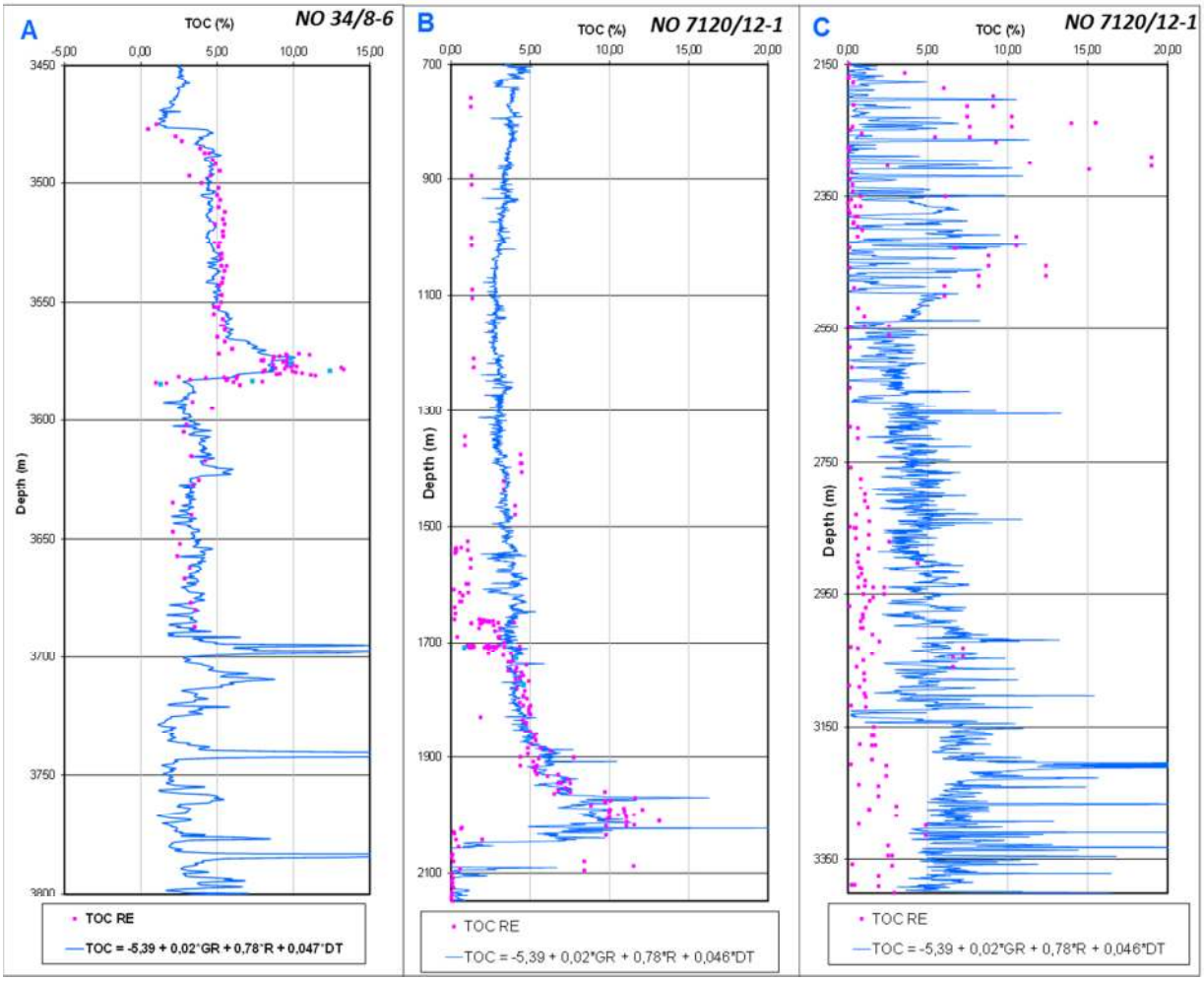

Fig. 72: Results of Multiple Regression models as TOC predictors. In blue TOC values from Multiple Regression Model, in pink TOC measured values from Rock Eval. **A.** Data from the well NO 34/8-6, Visund area, North Sea. **B.** and **C.** Data from well NO 7120/12/1, Troms I area, Barents Sea, for the *Cretaceous-Jurassic* and *Triassic* intervals respectively.

5. Discussion

About Δ Log R method (Paseey, et. al., 1990) and tools

In this study two wells were used for the testing of different tools based on $\Delta \ Log \ R$ method. The results obtained using this approach indicated that depending on the tool and the parameter used, the degree of accuracy can vary substantially. Δ Log R method cannot be applied directly as it claims; it requires a previous knowledge of the data to define appropriate parameters such as intervals and baselines values.

This method imply the use of data values that in large degree will depend on interpretation more than on hard data, which may increase the uncertainty and error related to the estimation. The procedure to define intervals and the selection of appropriate baselines is vague and very subjective and since it is possible to used multiple combinations of variables such as intervals range, baselines for resistivity-transit time and LOM, can lead to many possible estimations which without calibration values results in unknown accuracy. For example in the *Cretaceous* interval in *Kyrre Formation* of the well NO 34/8-6, where not values for calibration exist and more than 2 different estimations were possible.

It was shown that the definition of baseline intervals and baseline values are the parameters that yield most uncertainty. Definition of baselines required a very detailed lithological description to identify real non-source rocks intervals, however an exact value is not obvious since within an baseline interval there are variation in the log response and small variation of values of baselines have important influence in the results of TOC estimation using this method (***Fig 73***).

Moreover the method basically depends on shales with not organic content to predict rich ones, which sometimes it not easy to determine in in the interval to be evaluated where not data is available or in intervals where no poor shales in organic content are present. Apart from this, the background level of TOC can deviated from the value of 0,8% proposed by the authors, depending on the shale used for baselines values. Furthermore the concept that a baseline condition exist when the transit time and resistivity overlie each other in a significant depth of range (*Passey et. al., 1990*) is not clear. Baselines with different depth range were also tested and it was proven that an interval of about 10m in which both curve overlie works better than a baseline chosen from an interval range of 100m (***Fig. A2*** *Appendices*). Regarding to the results it seem that the use of baselines very close to the intervals to be evaluated lead a better approach (*Section 4.2)*

It was also showed that in heterogeneous log intervals this method is not a good predictor ((***Figs 51, 74***). Good predictions were observed mainly in thick shale package with values of TOC over 5%, for example in *Draupne Formation* in the well NO 34/8-6 and *Hekkingen Formation* in the well 7120/12-1 (***Figs 46, 47*** *Section 4,2*).

Additionally more error is introduced when values of maturity are converted to LOM values.

All the tools tested in this study are based in $\Delta\ Log\ R$ method, the differences amount them are related to the freedom of manipulating the data and the degree of manual control on the variables and parameters used. It was demonstrated that tools with better well log display are more appropriated to predict TOC using $\Delta\ Log\ R$ method. It is also very important that the tool allows to obtain the estimation results in numerical values in order to make statistical comparison to have an idea of the precision and accuracy of the results.

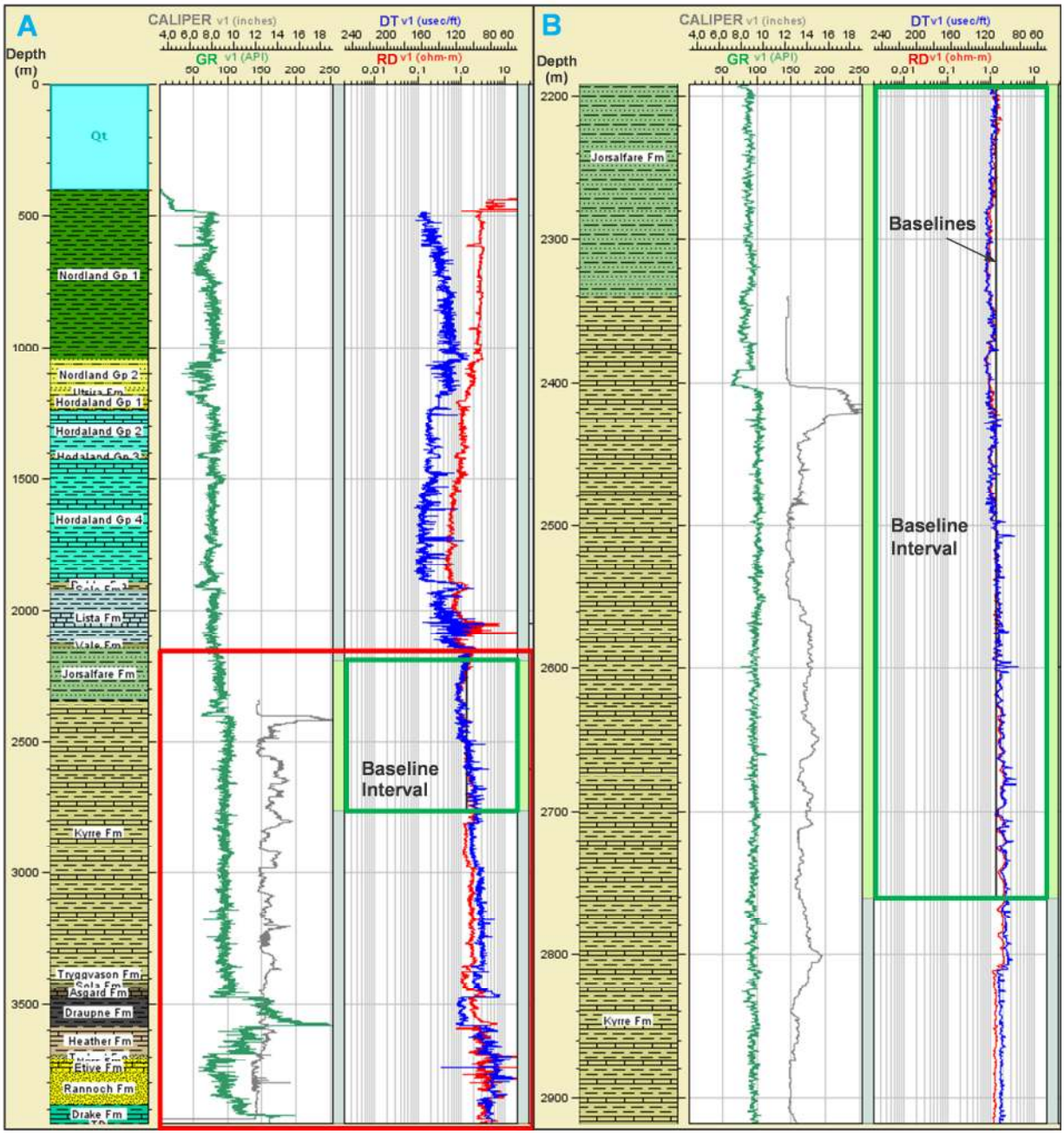

Fig. 73: Case 1 TOC calculations using a baseline in the upper Cretaceous using *BasinMod*. **A**. Well logs used in the estimation, interval of study (red box) and interval of baselines (green box) **B**. Zoom in of the interval baseline showing the constant baseline values taking by the software. Note that there is an uncertainty related to the location of the baselines since the log response has variations.

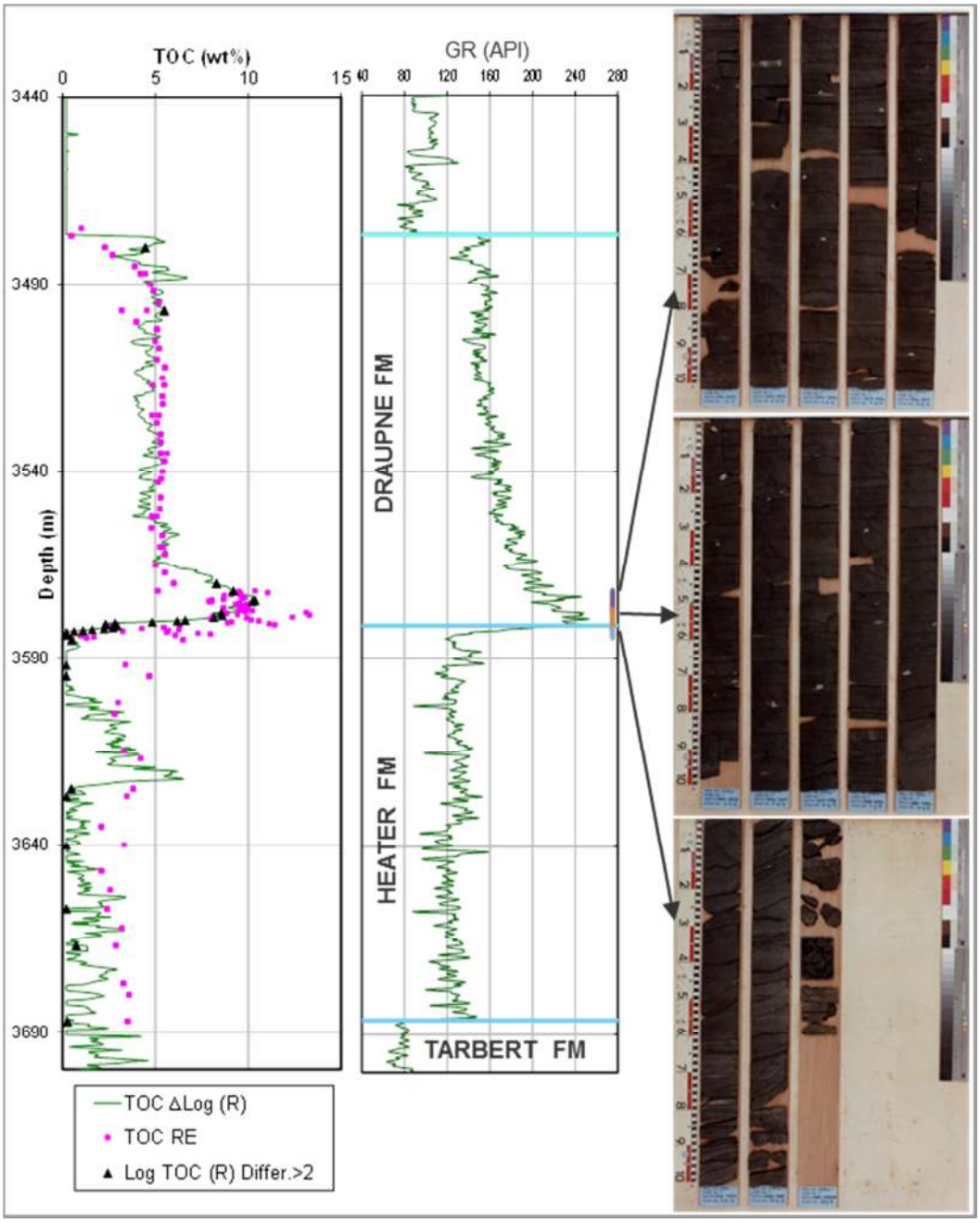

Fig. 74: TOC estimation in the well NO 34/8-6 at the level of the Jurassic section, showing that major differences (black triangles) with respect to calibration data were found in heterogeneous intervals from the lower part of *Draupne Fm*. and *Heater Fm*. The core present in this section describes this variation in lithology.

Basically $\Delta\ Log\ R$ method is the results of the comparison between the resistivity and the transit time log response for shales with no organic content and shales rich in organic content, its differences result in the estimation of TOC.

Hence, the comparison is done through the definition of baselines which have the purpose of predict the log behavior of non-source rocks in order to recognize source rock when such behaviors changes. In other words when the $\Delta\ Log\ R$ separation occurs. Having this in mind, the best way of defining baselines is to predict its behavior with depth instead of defining different constant values by intervals without any bases.

The example in ***Fig 75*** illustrates this idea from an evaluation done in the well NO 34/8-6, using as a calculation tool the spreadsheet (***Figs. A1, A2, A3*** *Appendices*). Comparing two sets of baselines chosen for the evaluation bring the question if those baselines really describe the behavior of non-source rock shale with depth.

Based in: 1) transit time decreases with depth due to compaction that causes reduction in porosity (except in overpressure zones) 2) that resistivity values increases with depth also because of compaction and causing a porosity reduction with resultant extrusion of saline connate water (*Hottmann & Johnson*,*1965 ; Issler, 1992; Mcgregor, 1965;* ***Figs 76, 77***); best it is reasonable to think in trend of shales instead of constant baselines as it is proposed by the *Δ Log R* method. *Passey et. al*., (*1980*), agrees with this observation mentioning that gradual baseline shifts are necessary to account for compaction with depth.

Added to that, the previous results in section *Section 4.2* also demonstrates that discretizing the interval evaluated plus a gradual increment in values of resistivity baseline with depth and reduction of transit time also with depth, resulted in a better approach of TOC.

Additionally, taking into account that baselines should be the log response of poor organic content shales, is necessary not only estimated trend for shales but first extract shale with high TOC content in order to exclude them from the trend calculation. This was done using a Gamma Ray range as a reference of intervals that correspond to most probable zones with clean shales.

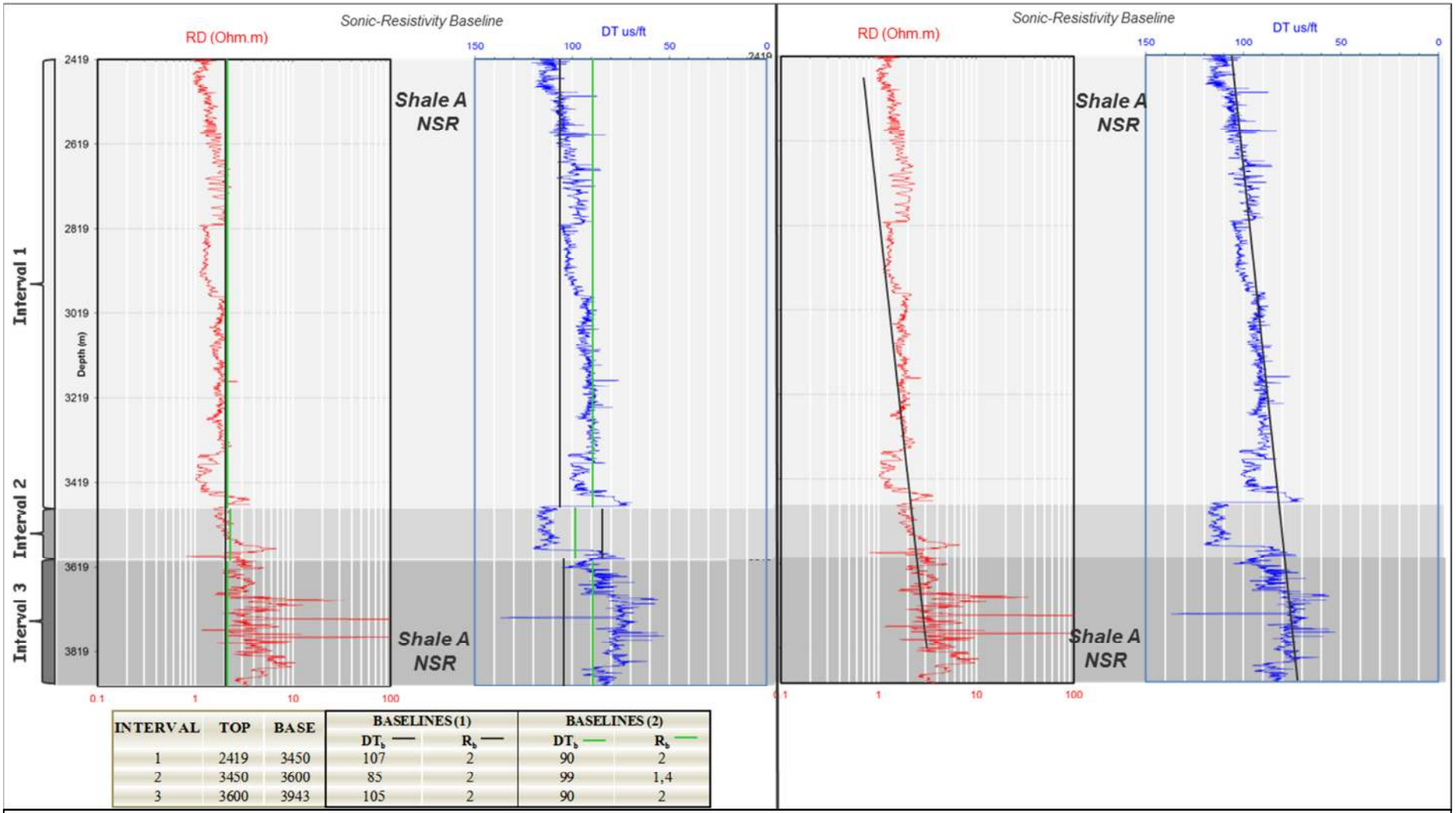

INTERVAL	TOP	BASE	BASELINES (1)		BASELINES (2)	
			DT_b —	R_b —	DT_b —	R_b —
1	2419	3450	107	2	90	2
2	3450	3600	85	2	99	1,4
3	3600	3943	105	2	90	2

Fig. 75: On the right, comparison of 2 set of transit time and resistivity baselines used in the TOC estimation in the well NO 34/8-6. In black set of baseline 1 and in green set of baselines 2, values summarized in the table. The question that arise looking at this baselines is: will be the log response of a non-source rock (NSR) shale ***A*** located in the upper part of this interval similar to the same shale located in the lower part?. A more reasonable solution can be the use of a trend line such as is illustrated on the left of this figure.

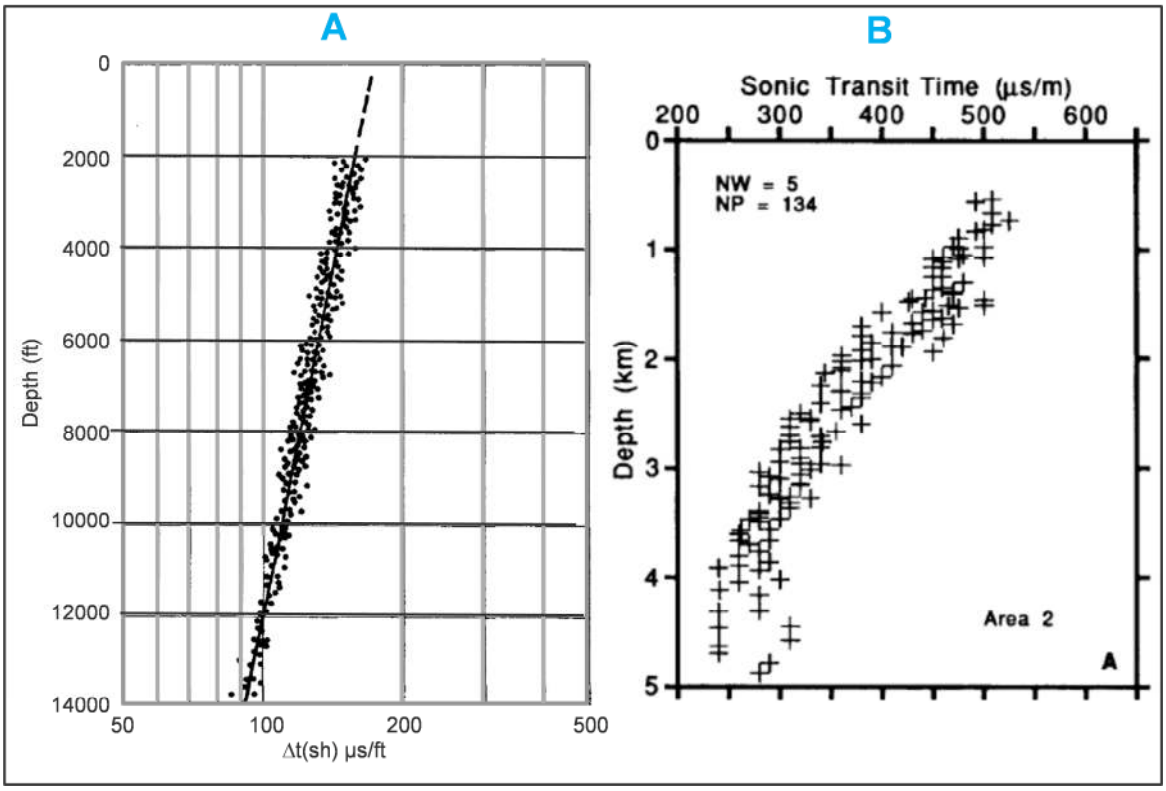

Fig. 76: **A.** Shale travel time vs. Depth for Miocene and Oligocene shales, Upper Texas and Southern Louisiana Gulf Coast (*Hottmann & Johnson, 1965*). **B.** Average shale sonic transit time vs. depth in Beaufort-Mackenzie Basin, Northern Canada (*Issler, 1992*).

In general terms and according to the statistical results the use of this methodology produces a better approximation in homogeneous shale intervals than in heterogeneous facies, similar to the regular $\Delta \, Log \, R$ method, however trend baseline approximations are obtained directly instead of the try and error procedure, in other words the definition of baselines using trends implies a more clear and reasonable practice.

Another important point is that statistical analysis should be carried out parallel to TOC estimations to evaluate the accuracy of the results. Results from quantile-quantile plots (***Figs. 69, 77***) indicates that the best accuracy of TOC determination is in the range between 4 and 10%, in other words, beds with organic content lower than 4 % and major than 10 % are not well estimated.

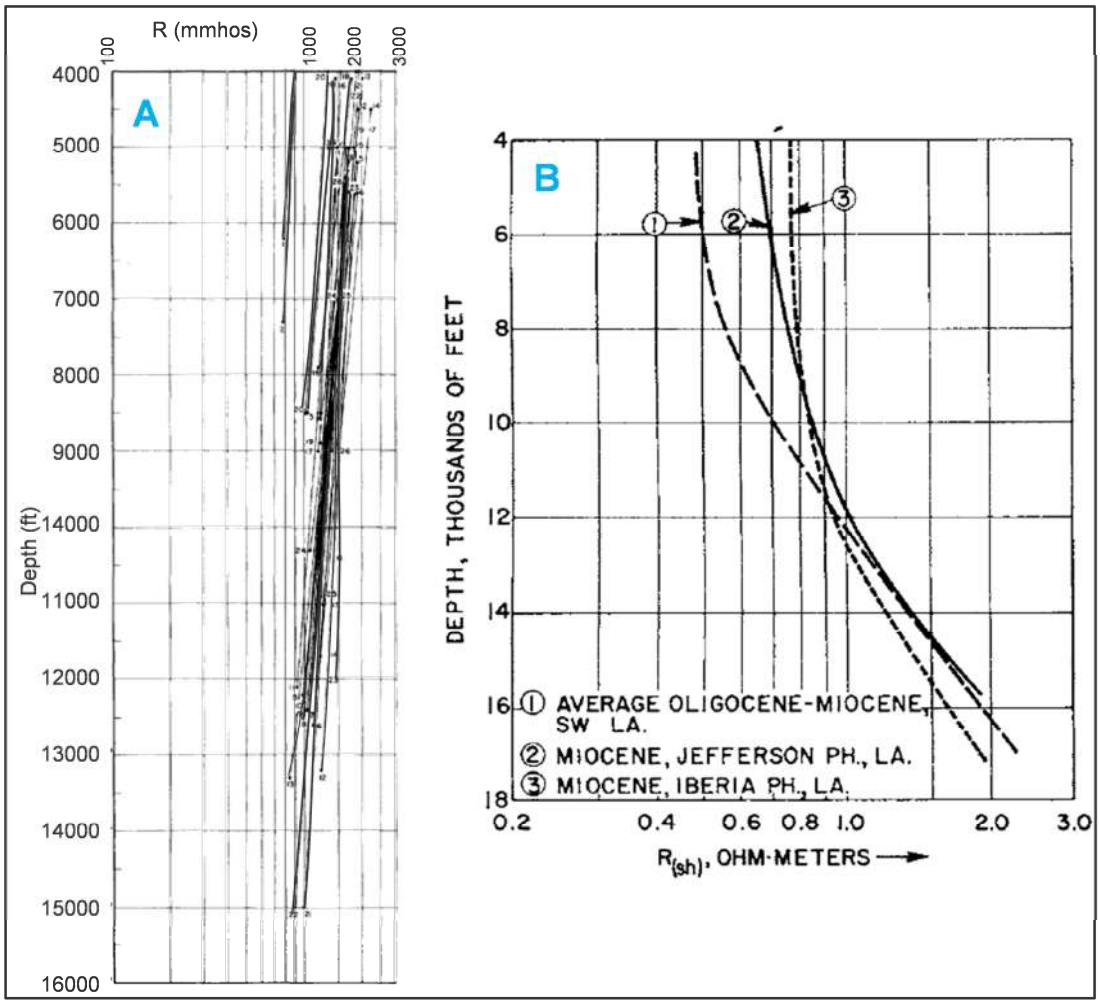

Fig. 77: **A.** Conductivity in clean shales in 26 wells in 5 offshore areas and 4 onshore fields from West Cameron to south Timbalier areas (*Mcgregor, 1965*) **B.** Shale travel time vs. Depth for Miocene and Oligocene shales, Upper Texas and Southern Louisiana Gulf Coast (*Hottmann & Johnson, 1965*).

Well data implications

After the evaluation done in this study, some considerations regarding to the nature of the data can explain the results obtained. The first thing to take into account is the fact that the well data used in this study consist of wireline logs recorded about 20 years ago. Even though not major problems were found respect to the quality of the data, it was observed that a possible mismatch in depth related to the cable tension and elasticity could explain part of the important differences between measured and estimated TOC values in the well NO 34/8-6 since bots set of data were in measured depth. ***Fig 78***, shows that shifting in the curve about 2,5 m can lead to a much better fit.

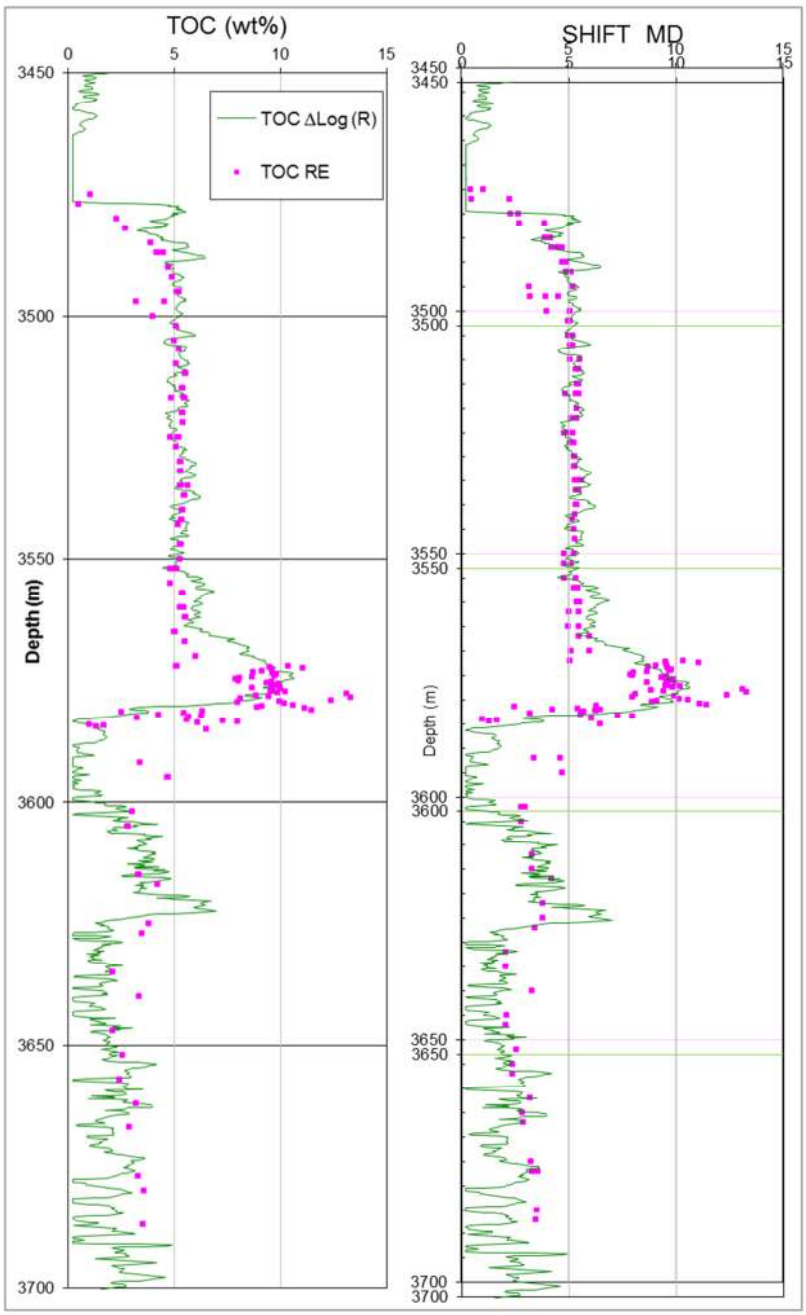

Fig. 78: Possible depth mismatch between log data and calibration values due to cable tension and elasticity in wireline logging tools. On the right the initial results, on the left a fit after a shifting of 2,5 m between both set of data.

Another point related to the data is the fact that TOC and maturity data come from different sources as it was mentioned in the methodology (conventional core, sidewall and ditch cutting) and also different labs, thus the error associated with these samples is uncertain. It implies that estimations of TOC could be a good approach even though does not fit calibration data.

Sometimes the vertical resolution in the cores compared with logs is another source of disagreement in the results. In some cases core data can have a high density of samples in one interval that allows to have results from thin beds that log data is not able to reproduce.

About the Multiple Regression Model

Using log data from one well only, it was possible to generated and equation that related values of Gamma Ray, Resistivity and Transit time to predict Total Organic Carbon. On top of that, this equation not only reproduced TOC values from the same well data used to create the equation as it was expected, but also from a well located in a different geological setting (NO 7120/12-1 in the Barents Sea).

In spite of the fact that possible overestimation can occur, using this equation, it is important to know that this tool could predict in a very direct way most important source rocks in the wells studies. Additionally, the use of this equation do not required long procedures and definition of parameters depending on the well data; it only needs the raw log data from Gamma Ray, Resistivity and Transit time.

A better accuracy of this approach can be achieved by including additional variables in the regression model that are influenced by the presence of organic content, such as the Density or Neutron logs that could help to improve the predictions.

This equation can also be improved including more data values of TOC measured by depth which can enhance the mean and the variance in the model, since in this case it was necessary to group some values of TOC close in depth to proper apply the regression. Additionally, it is important to highlight that measured TOC values are derived from different types of samples (like conventional core, sidewall cuttings and ditch cuttings) and there is an uncertainty related to the quality of the data. It is also clear that the dispersion of TOC measured values in some intervals can represent a difficulty for the predictive model.

An important future step is to test this procedure in different geological settings. Not only testing the equation with different wells data but also thinking in the possibility of created this kind of model according to type of organic matter or facies of source rock.

Finally, it should be stressed that this approach represent an insight to derivate new models using statistical tools that allows a directly determination of TOC from logs with a better control of variables and avoiding bias procedures. There is still a long way to explore using predictive models to extract geochemical information for well logs.

6. Conclusion

The main purposed of this project was to predict Total Organic Carbon from well logs. After an exhaustive analysis using different tools and methods the main conclusions are summarized as follow:

- It was proven that the delta log R technique is an indirect empirical approximation able to quantify Total Organic Carbon only in the presence of calibration data, otherwise can lead in uncertain results.

- The main source of uncertainty in the delta log R technique is related to the definition of baselines for the transit time and resistivity curve.

- For the data set evaluated in this study, the delta log R technique was able to make a good approach only in homogeneous shale package; in heterogeneous intervals the estimation was very poor. Additionally, better accuracy was obtained in ranges between 4 to 10 % of TOC, values outside of this range are poorly estimated.

- The use of trend shales to define baselines implies a more appropriate practice in the application of delta log R technique.

- The multiple linear regression method is a powerful tool to generate a model from well log data able to predict Total Organic Carbon from well logs with a simplified procedure.

- The multiple linear regression model can be improved by including additional variables that are influenced by the presence of organic content, such as the Density or Neutron logs.

- Estimations of Total Organic Carbon from well logs should be combined with statistical analysis to evaluate the degree of accuracy of the results.

7. References

A

Alyousuf, T., Algharbi W., Algeer R. and Samsudin A. (2011). *Source rock characterization of the Hanifa and Tuwaig Mountain formations in the Arabian Basin, based on Rock-Eval pyrolisis and the modified Delta Log R method*. SPE/DGS Saudi Arabia Section Technical Symposium and Exhibition, Al-Khobar, Saudi Arabia, 15-18 May 2011.

Abrahão, D. (1989). *Well-log evaluation of lacustrine source rocks of the Lagoa Feia formation, lower Cretaceous, Campos Basin, offshore Brasil*. SPWLA Thirtieth Annual Logging Symposium, June 11-14, 1989.

Acharya, M. N., Al-Awadi M. A., AL-Ajmi A. A., and Al-Eidan A. J. (2009). *Characterization of kerogen reservoirs by organic richness from well logs: a new approach for gas condensate reservoir in Najmah formation, North Kuwait.* SPE/EAGE Reservoir Characterizaton and Simulation Conference, Abu Dhabi, UEA, 19-21 October 2009.

Aly, S. A., Ali H. A. M., Abou Ashour N. M. H., and El-Gezeiry M. M. (2003*). Resistivity, radioactivity and porosity logs as tools to evaluate the organic content of Abu Roash "F" and "G" members, North Western Desert, Egypt.* Egyptian Geophysical Society 1(1): 129-137.

Abou Shagar, S. (2006). *Source rock evaluation of some intervals in the Gulf of Suez area, Egypt*. Egyptian journal of aquatic research 32(1):1687-4285.

Autric, A., and Dumesnil P. (1985). *Resistivity, radioactivity and sonic transit time logs to evaluate the organic content of low permeability rocks*. The Log Analyst 26(3): 36-45.

B

Bardsley, S.R., and Algermissen S.T. (1963). *Evaluating oil shale by log analysis*. Journal of Petroleum Technology 15(1): 81-84.

Biswas, S. K., Ariketi R., and Behera B. K. (2011). *Analyzing Applicability of Lopatin's Method and Estimation of Total Organic Carbon Content (TOC) through Conventional Log Responses: A case study of Mumbai Offshore Basin, Western India.* 2011 International Conference on Environment and BioScience, IPCBEE vol.21, IACSIT Press, Singapore.

B.S. Cooper, P.C. Barnard (1984). *Source Rocks and Oils of the Central and Northern North Sea AAPG Special Volumes.* Volume M 35: Petroleum Geochemistry and Basin Evaluation, Pages 303 - 314

Bardsley, S. R., and Algermissen, S. T., 1963 *Evaluating oil shale by log analysis.* Journal of Petroleum Tech., v. 15 no. 1, p.81-84

C

Carpentier, B., Huc A.Y., and Bessereau G. (1991). *Wireline Logging and Source Rocks - Estimation of Organic Carbon Content by the CARBOLBG@ Method.* The Log Analyst, May-June 279-297.

Christoffel, D. A., and Kayal J. R. (1989). *Coal Quality from Geophysical Logs: Southland Lignite Region, New Zealand.* The Log Analyst 30(5): 343-352.

Cluff, B. (2011). *Practical use of core data for shale petrophysics: a petrophysicists perspective.* SPWLA 2011 Annual Symposium, Colorado Springs, Short course1: Laboratory measurements of shale gas cores.

D

Dalland, A., Worsley, D. and Ofstad, K. (1988). *A lithostratigraphic scheme for the Mesozoic and Cenozoic succession offshore mid- and northern Norway.* NPD-Bulletin No. 4, 65 pp.

Du Rochet, J., (1981). *Stress fields, a key to oil migration*. AAPG Bulletin, V. 65, p. 74-85

E

Ehrenberg, S. N., and Svånå T. A. (2001). *Use of spectral gamma-ray signature to interpret stratigraphic surfaces in carbonate strata: An example from the Finnmark carbonate platform (Carboniferous–Permian)*. Barents Sea. AAPG Bulletin 85: 295-308.

F

Fertl, W. H., and Rieke III H. H. (1980). *Gamma ray spectral evaluation techniques identify fractured shale reservoirs and source rocks characteristics.* Journal of Petroleum Technology 32(11): 2053-2062.

Fertl, W. H., and Chiligar G. V. (1988). *Total Organic carbon content determination from well logs*. SPE Formation Evaluation 3(2): 407-419

Flower, J. G. (1983). *Use of sonic-shear-wave/resistivity overlay as a quick-look method for identifying potential pay zones in the Ohio (Devonian) Shale.* Journal of Petroleum Technology 35(3): 638-642.

G

Gonfalini, M. (1991). *Evaluation of the organic carbon content from geophysical well log interpretation in carbonate Triassic source rocks of the Streppenosa basin, Sicily (Italy)*. Source-Rock Geology. P. 105-112. 13th World Petroleum Congress, October 20 - 25, 1991, Buenos Aires, Brazil.

Gautier, Donald L., (2005). *Kimmeridgian Shales Total Petroleum System of the North Sea Graben Province.* U.S. Geological Survey Bulletin 2204-C, 24 p.

Gueininn K. J., Hulme N.A.C., Braham W. And Bayley H.W. (1993). *Project: Well 34/7-21 biostratigraphy of the interval 340m – 3,014m* (T.D.). Project Number 2941. Statoil ASA, Internal Report.

H

Hassan, M., Hossin A., and Combaz A. (1976). *Fundamentals of the differential gamma ray log, interpretation technique.* SPWLA 17th Annual Logging Symposium, 1976.

Herron, S. L., and Le Tendre L. (1990). *Wireline source-rock evaluation in the Paris basin: Chapter 5*. AAPG Special Volumes, Volume SG 30: Deposition of Organic Facies, Pages 57 - 71.

Herron, M. M., Grau J. A., Herron S. L., Kleinberg R. L., Machlus M., Reeder S.L., and Vissapragasa B. (2011). *Total organic carbon and formation evaluation with wireline logs in the Green River Oil Shale.* SPE Annual Technical Conference and Exhibiton, Denver, Colorado USA, 30 October -2 November 2011.

Herron, S. L. (1986). *A total organic carbon log for source rock evaluation*. SPWLA 27th Annual Logging Symposium, 1986.

Hottmann C. E and R.K. Johnson (1995) *Estimation of formation pressures from log-derived shale properties*. Journal of Petroleum Technology, v. 17, p. 717-722.

Habiger, R. M. (1985). *Determination of oil shale yield from well log data*. United States Patent Number 4,548,071. Phillips Petroleum Company, Bartlesville, Okla.

I

Issler, D.R. (1992) *A new aproach to shale compactation and strathigraphic restoration*. Beaufort-Mckenzie Basin and Mackenzie corridor, northern Canada. American Association of Petroleom Geologist. Bulletin, v. 76 p. 1170-1189.

K

Kamalia, M. R., Mirshadyb A. A. (2004). *Total organic carbon content determined from well logs using DLogR and Neuro Fuzzy techniques.* Journal of Petroleum Science and Engineering 45: 141– 148.

L

LaGesse, J. and Hurley N. (2008). *Predicting source rock quality using GR wireline response and Umaa vs. ρmaa crossplots in the Lewis Shale, Green River Basin, Wyoming.* SPE Annual Technical Conference and Exhibiton, Denver, Colorado USA, 21-24 September 2008.

Lang, W. H. (1994). *The Determination Of Thermal Maturity in Potential Source Rocks Using Interval Transit Time/interval Velocity.* The Log Analyst 35 (6): 47-59.

Lin, J. L. and Salisch H. A. (1993). *Determination from well logs of the total organic carbon content in potential source rocks.* Society of Petroleum Engineers. SPE Paper no. 27 627.

LeCompte, B. and Hursan G. (2010). *Quantifying source rock maturity from logs: how to get more than TOC from Delta Logs R.* SEP Annual Technical conference and Exhibition, Florence, Italy, 19-22 September 2010.

Leith, T.L., and Fallick A.E. (1997). *Organic geochemistry of cap-rock hydrocarbons, Snorre Field, Norwegian North Sea.*In R.C. Surdam, ed., Seals, traps, and the petroleum system: AAPG Memoir 67, p. 115–134.

Lashin, A., Lindner H., Abu Ashor N., El Dien M. S., and Zahra H. (2001). *Hydrocarbon Potentialities and Source Rock Recognition in the Area North of October Field-Gulf of Suez-Egypt*. Deutsche Geophysikalische Gesellschaft e.V. FKPE Hannover, Germany, P.6.

Lynn E. Eberly (2007). *Multiple linear regression Methods in Molecular Biology*. Volume 404, Topics in Biostatistics, Pages 165-187

Løseth, H., et al. (2011) *Can hydrocarbon source rocks be identified on seismic data?*. Geology December 2011 v. 39, no. 12, p. 1167-1170

M

Mallick, R. K. and Raju S. V. (1995). *Application of Wireline Logs in Characterization and Evaluation of Generation Potential of alaeocene-Lower Eocene Source Rocks in Parts of Upper Assam Basin, India.* The Log Analyst, May-June: 49-63.

Mcgregor, J.R. (1965). *Quantitative determination of reservoir pressures from conductivity log.* American Association of Petroleom Geologist. Bulletin, v. 49 p. 1502-1511.

Mendelzon, J.D., and Toksiöz M.N. (1985). *Source rock characterization using multivariate analisis of log data.* SPWLA Twenty-sixth Annual Logging Symposium, June 17-20, 198.

Meyer, B. L., and Nederlof M. H. (1984). *Identification of Source Rocks on Wireline Logs by Density/Resistivity and Sonic Transit Time/Resistivity Crossplots.* The American Association of Petroleum Geologists Bulletin 68 (2): 121-129.

Mott, L. V., and Drever J. I. (1983). *Origin of Uraniferous Phosphatic Beds in Wilkins Peak Member of Green River Formation, Wyoming.* The American Association of Petroleum Geologists Bulletin 57(1): 70-82.

Myers, K. J., And Jenkyns K. F. (1992). *Determining total organic carbon contents from well logs: an intercomparison of GST* data and a new density log method.* From Hurst, A., Griffiths, C. M. & Worthington, P. F. (eds), 1992. Geological Applications of Wireline Logs H. Geological Society Special Publication No. 65, pp. 369-376.

McKenzie, D. (1978). *Some remarks on the development of sedimentary basins.* Earth and Planetary Science Letters. Vol. 40, p. 25-32.

Meissner, C. D., (1978). *Petroleum geology of the Bakken Formation Williston Basin, North Dakota and Montana*. In D. Rehig, ed.: 1978 Williston Basin Symposium: Billings, Montana, Montana Geological Society, p. 207-227.

N

Nixon, R. P. (1973). *Oil Source Beds in Cretaceous Mowry Shale of Northwestern Interior United States*. The American Association of Petroleum Geologists Bulletin 57(1): 136-161.

Norwegian Petroleum Directorate ***NPD*** (2012), *Well Data Sheets* (WDS), [online]. Available from: http://www.npd.no/engelsk/cwi/pbl/en/index.htm

P

Passey, Q. R., Creaney S., Kulla J. B., Moretti F. J., and Strouds J. D. (1990). *A practical model for organic richness from porosity and resistivity logs.* The American Association of Petroleum Geologists Bulletin 74 (12): 1777-1794.

Passey, Q.R., Bohacs K.M., Esch W.L., Klimentidis R., and Sinha S. (2010). *From oil-prone source rock to gas-producing shale reservoir – geologic and petrophysical characterization of unconventional shale-gas reservoirs.* International Oil and Gas Conference and Exhibition in China, 8-10 June 2010, Beijing, China.

R

Russell, W. L. (1945). *Relation of radioactivity, organic content, and sedimentation.* Bulletin of The American Association Of Petroleum Geologists 29(10): 1470-1494

Rider, M. (2008). *The Geological interpretation of Well Logs.* Whittles Publishing 199. 2nd Edition.

S

Shayesteh, M. (2011). *Source rock analysis from well logs in the southern Dezful embayment.* The 2nd South Asain Geoscience Conference and Exhibition,GEOIndia2011, 12-14th Jan,2011,Gearter Noida,New Delhi,India.

Schmoker, J. W. and Hester T. C. (1990). *Formation Resistivity as an Indicator of Oil Generation - Bakken Formation of North Dakota and Woodford Shale of Oklahoma.* The Log Analyst 31(1): 1-9.

Schmoker, J.W. and Hester T. C. (1989). *Oil generation inferred from formation resistivity– Bakken formation, Williston basin, North Dakota.* SPWLA Thirtieth Annual Logging Symposium, June 11-14.

Swanson, V. E. (1960). *Oil yield and uranium content of black shales.* Geological surveys professional paper 356-A.

Schmoker, J. W. (1981). *Determination of Organic-Matter Content of Appalachian Devonian Shales from Gamma-Ray Logs.* AAPG Bulletin 65: 1285-1298.

Schmoker, J. W. (1979). *Determination of Organic Content of Appalachian Devonian Shales from Formation-Density Logs.* The American Association of Petroleum Geologists Bulletin 63(9): 1504-1537.

Schmoker, J.W., Timothy C. Hester. (1983). *Organic Carbon in Bakken Formation, United States Portion of Williston Basin.* AAPG Bulletin 67(12): 2165 – 2174.

Serra, O. (2008) *The well logging handbook.* Editions Technip, Paris.

Serra, O. (1984) *Fundamentals of Well-log Interpretation: The acquisition of logging data.* Elsevier Science Publishers B.V., Amsterdam. First Edition.

Stephen C. Ruppel and Jeffery Kane (2006). *The Mississippian Barnett Formation: A Source-Rock, Seal, And Reservoir Produced By Early Carboniferous Flooding Of The Texas.* Craton Bureau of Economic Geology, Jackson School of Geosciences, The University of Texas at Austin Austin,. TX. Available from: http://www.beg.utexas.edu/resprog/permianbasin/PBGSP_members/writ_synth/Mississippian_chapter.pdf

Steel, R. G. D. and Torrie, J. H., (1960). *Principles and Procedures of Statistics*. New York: McGraw-Hill, pp. 187, 287.

T

Tixier, M. P. and Curtis, M. R. (1967). *Oil shale yield predicted from well logs.* 7th World Petroleum Congress, April 2 - 9, 1967 , Mexico City, Mexico

W

Wadsworth, M. C., and McEwan J. (1993). *Geochemical interpretation of well 34/7-21 and 34/7-21A.* Saga Petroleum A.S. Memorandum Number: SL/93/628.

Y

Yang, H. Zhang W., Wu K., Li S., Peng P., Qin Y. (2010). *Uranium enrichment in lacustrine oil source rocks of the Chang 7 member of the Yanchang Formation, Erdos Basin, China*. Journal of Asian Earth Sciences 39: 285–293.

Z

Zhu, Z., Z., Liu H., and Li Y. (2003). *Logging Identification and Evaluation of Cambrian-Ordovician Source Rock In Tarim Basin*. Society of Exploration Geophysicists. SEG Annual Meeting, October 26 - 31, 2003, Dallas, Texas.

8. Appendices

Table A: *In-house spreadsheet* tested in the Well NO 34/8-6. Summary of the intervals and parameters used in TOC estimation from logs (Fig).

INTERVAL	TOP	BASE	Clean GR	BASELINES		Ave. %Ro	LOM	
				DT_b	R_b		Suggested	Final
1	2419	3450	70	107	2	0,49	6,6	7
1	2419	3450	70	90	2	0,49	6,6	7
2	3450	3600	70	90	2	0,57	7,6	8
2	3450	3600	70	99	1,4	0,57	7,6	8
2	3450	3600	70	85	2	0,57	7,6	8
3	3600	3943	70	90	2	0,58	7,8	8
3	3600	3943	70	107	2	0,58	7,8	8

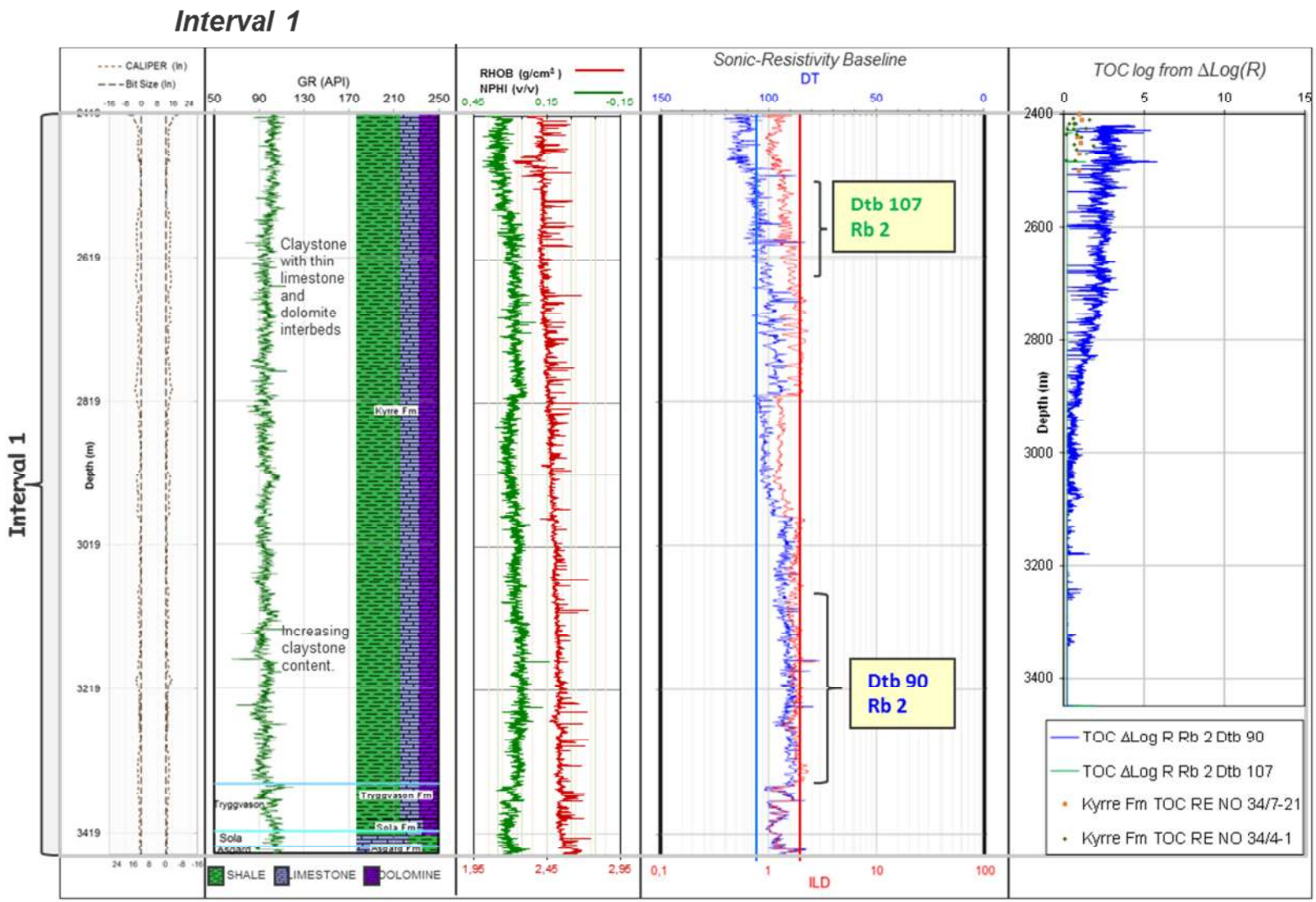

Fig. A1: TOC estimations using the In-house spreadsheet with data from the Well NO 34/8-6 in the interval 1, showing the results obtained using 2 different baselines intervals for Transit time (Dtb) and Resistivity (Rb) logs (values in yellow boxes). In the track of TOC from logs the two TOC estimation curves are compared.

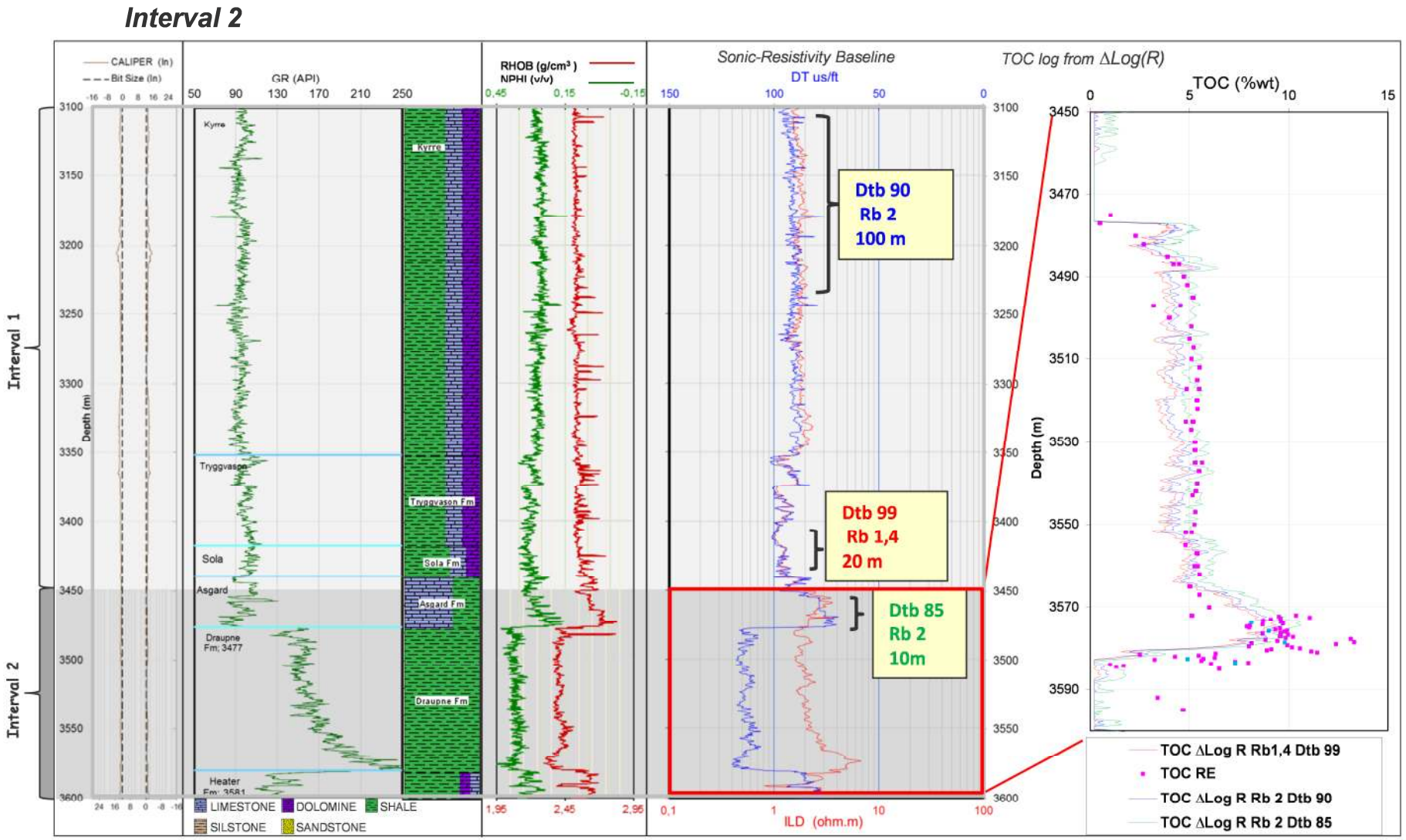

Fig. A2: TOC estimations using the In-house spreadsheet with data from the Well NO 34/8-6 in interval 2, showing the results obtained using 3 different baselines for Transit time (Dtb) and Resistivity (Rb) logs (values in yellow boxes) and also comparing the thickness of the baselines intervals. In the track of TOC from logs the three TOC estimation curves are compared.

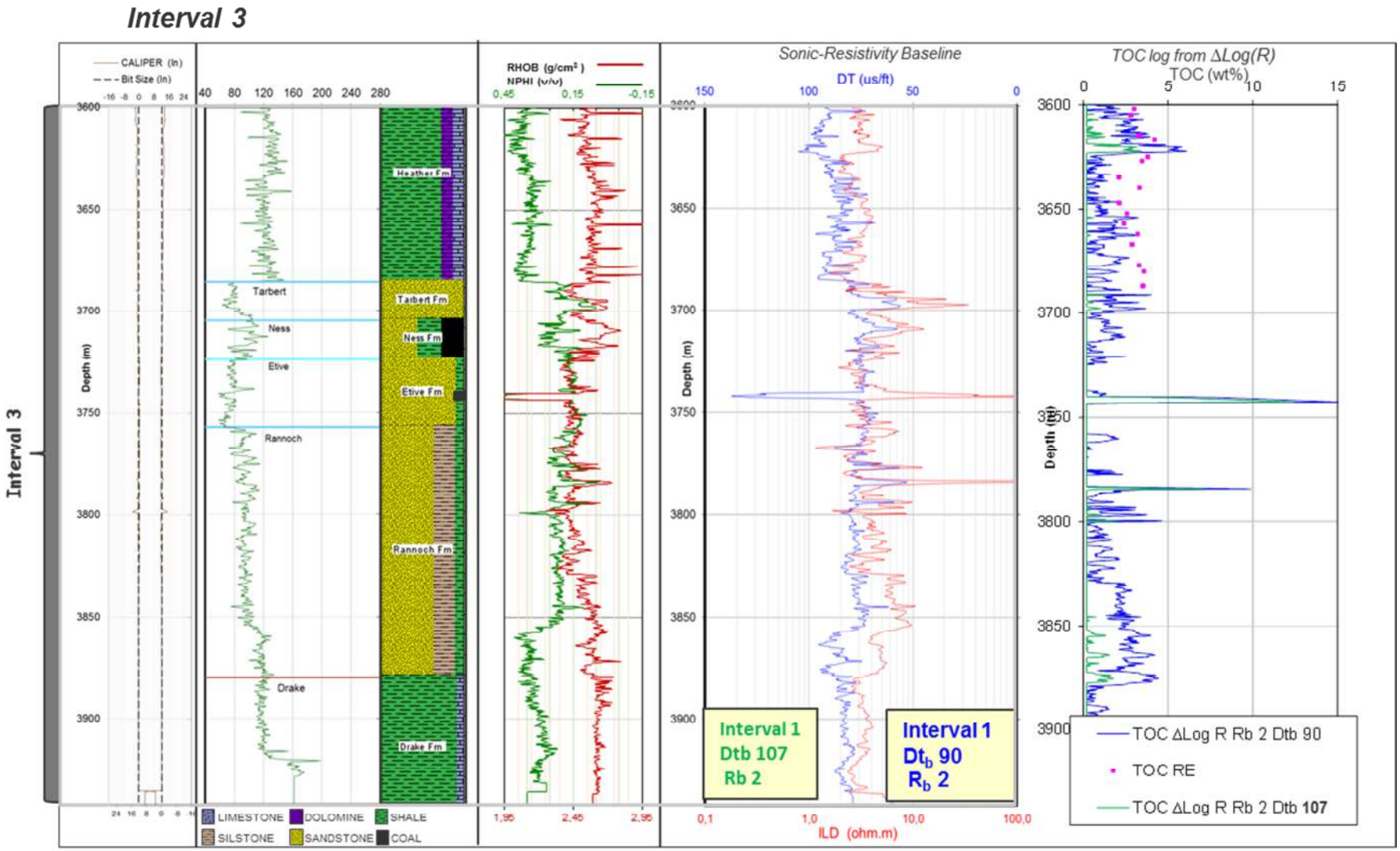

Fig. A3: TOC estimations using the In-house spreadsheet with data from the Well NO 34/8-6 in the interval 3, showing the results obtained using 3 different baselines for Transit time (Dtb) and Resistivity (Rb) logs (values in yellow boxes). In the track of TOC from logs the three TOC estimation curves are compared.